Universidade de Lisboa

Faculdade de Medicina de Lisboa

"Deciphering the role of αB-crystallin in Huntington's Disease"

Ana Cristina Osório Marinho Oliveira

Orientador: Prof. Doutor Tiago Fleming de Oliveira Outeiro

Co-orientadores: Prof. Doutor Steven Michael Finkbeiner

Prof. Doutor Paul Joseph Muchoswki

Doutoramento em Ciências Biomédicas

Neurociências

2017

Universidade de Lisboa
Faculdade de Medicina de Lisboa

"Deciphering the role of αB-crystallin in Huntington's Disease"

Ana Cristina Osório Marinho Oliveira

Orientador: Prof. Doutor Tiago Fleming de Oliveira Outeiro
Co-orientadores: Prof. Doutor Steven Michael Finkbeiner
Prof. Doutor Paul Joseph Muchoswki

Júri:

Presidente:

- Doutor José Luís Bliebernicht Ducla Soares, Professor Catedrático em regime de *tenure* e Vice-Presidente do Conselho Científico da Faculdade de Medicina da Universidade de Lisboa.

Vogais:

- Doutora Ana Cristina Rego, Professora Auxiliar com Agregação da Faculdade de Medicina da Universidade de Coimbra ;
- Doutora Patrícia Espinheira Sá Maciel, Professora Associada da Escola de Medicina da Universidade do Minho;
- Doutora Luísa Maria Vaqueiro Lopes, Especialista de Reconhecido Mérito e Competência, Investigadora, *Group Leader* do Instituto de Medicina Molecular da Faculdade de Medicina da Universidade de Lisboa;
- Doutor Joaquim José Coutinho Ferreira, Professor Associado Convidado da Faculdade de Medicina da Universidade de Lisboa;
- Doutor Tiago Fleming de Oliveira Outeiro, Professor Associado Convidado da Faculdade de Medicina da Universidade de Lisboa, (Orientador);
- Doutor Mário Miguel Coelho da Silva Rosa, Especialista de Reconhecido Mérito e Competência da Faculdade de Medicina da Universidade de Lisboa

2017

Todas as afirmações efectuadas no presente documento são da exclusiva responsabilidade do seu autor, não cabendo qualquer responsabilidade à Faculdade de Medicina de Lisboa pelos conteúdos nele apresentados.

Este projecto foi parcialmente financiado pela Bolsa de Doutoramento SFRH/BD/65942/2009 atribuída pela Fundação de Ciência e Tecnologia (FCT).

A impressão desta tese foi aprovada pelo Conselho Científico da Faculdade de Medicina de Lisboa na reunião de Outubro de 2016, e aprovada com Distinção e Louvor na Defesa de Provas de Doutoramento a dia 1 de Fevereiro de 2017.

Table of contents

Acknowledgements

In many ways I consider this section to be the most important part of my thesis, as so many people directly and indirectly have helped and supported me through my five years of graduate school. Much of this time, regardless of the specifics of one's project, is about learning to think like a scientist. While I have no doubt that I have grown tremendously as a scientist over the years, I strongly believe that I've grown even more as a human being. I have had the opportunity to work with incredible role models, to learn self-reliance and perseverance in the face of seemingly- constant failure, and to refine my ability to navigate a complex and often frustrating world without sacrificing my values or losing the pleasure I derive from simply being curious.

I must begin by thanking my supervisors, Tiago Outeiro, Paul Muchowski and Steven Finkbeiner for their support, guidance, confidence and for the opportunity to pursue a research project in your laboratory.

An enormous thank you to everyone I have met during this journey, and every single friend and labmate from my three distinct PhD laboratories as well as incredible people from neighboring labs I got the chance to meet and work with. You are all so special!

To my Science "outsider's" friends goes a special "Thank you" for making me realize how lucky I am to have you around and to put all my experiments, which includes many failures, and some interesting findings, into perspective. My "University Girls", my "Trivia team" and "Zumba team" were extreme- and uniquely important in this process.

I have had a great and special "partner in crime" for most part of this PhD, and I will be always grateful for the little surprises during crazy work weekends and long night shifts in the lab - a very special thank you goes to my favorite neighbor and my boyfriend Geno Moscetti. Thank you for your love, support and encouragment throughout my PhD.

I could not have done this without my amazing family, especially my parents and my brother, but also my great aunts and cousins. Your love and support throughout this process has been incredible. Thank you for your patience, holding your "saudades" during this time and more importantly, thank you for instilling the kind of values in me that led to this amazing opportunity! I dedicate this thesis to my beloved and unforgettable grandmothers, for being such a special inspiration during my whole life!

Abstract

Huntington's disease (HD) is caused by an expanded polyglutamine (polyQ) tract in the huntingtin (Htt) protein. The polyQ expansion increases the propensity of Htt to aggregate and accumulate, and manipulations that mitigate protein misfolding or facilitate the clearance of misfolded proteins are predicted to slow disease progression based on studies in HD models. αB-crystallin (αBc) or HspB5 is a well-characterized member of the small heat shock protein (sHsp) family that reduces mutant Htt (mHtt) aggregation and toxicity *in vitro* and in *Drosophila* models of HD. Here, we determined if overexpressing or diminishing αBc levels *in vivo* modulates aggregation and the onset and progression of disease in a full-length mouse model of HD known as the BACHD mice. Expression of sHsps in neurodegenerative disease predominantly occurs in non-neuronal cells, and in the brain, αBc is mainly found in astrocytes and oligodendrocytes. In Chapter 3, we show that directed αBc overexpression in astrocytes improves motor performance in rotarod and balance beam tests, and improves cognitive function in the BACHD mice. Improvement in behavioral deficits correlated with mitigation of neuropathological features commonly observed in HD. Interestingly, astrocytic αBc overexpression was neuroprotective against neuronal cell loss in BACHD brains, suggesting αBc might act in a non-cell-autonomous manner. At the protein level, αBc decreased the levels of soluble mHtt and decreased the size of mHtt inclusions in BACHD brain. These results support a model in which elevating astrocytic αBc confers neuroprotection through a putative non-cell-autonomous pathway that modulates mHtt aggregation and protein levels.

In Chapter 4, we attempted to elucidate the non-autonomous mechanism by which overexpressing astrocytic αBc confers neuroprotection in the progression of the disease of the BACHD mice. Several essential cellular pathways are impaired in neurological disorders such as HD. Among others, activation of caspase-3 pathways as well as formation of carbonyl species are oxidative stress hallmarks of HD pathology, and αBc has been reported to play a role in these mechanisms. Our studies, looking at mRNA and protein levels from BACHD mice as well as from primary cells (astrocytic and neuronal), found no significant differences in caspase-3 activation, and in expression of several HD markers, e.g., Glucose transporter 1 (Glut1), dopamine receptor 1 (DR1) and dopamine receptor 2 (DR2), brain-derived

neurotrophic factor (BDNF), in this disease context. Despite not finding a significant difference, when looking at the formation of protein carbonyls (derived from oxidative stress), we found a small trend towards a decrease of the levels of these species when αBc was over-expressed in astrocytes, both in brains and primary cultures of BACHD. These data may support the potential antioxidant effect of αBc in the context of HD pathology.

In Chapter 5, we hypothesized that αBc deficiency would accelerate HD disease severity and progression, as previously observed in a mouse model of Alzheimer's Disease (AD). We tested this hypothesis by crossing mice null for αBc (and HspB2) to BACHD mice and monitoring behavioral and neuropathological symptoms of HD during disease progression. Our study showed that genetic deficiency of αBc (and HspB2) did not aggravate disease progression.

Taken together, the results presented in this thesis provide novel insight into the role of αBc and its function on essential cellular pathways in the context of HD. This work also supports the emerging significance of non-neuronal cells in chronic diseases such as HD suggesting adaptive and differential responses that might contribute to and/or provide a route to therapy of distinct aspects of neurodegeneration. Ultimately, this knowledge aims to promote and highlight the impact and role of sHsps, specifically αBc, in HD and related disorders in order to help the development of promising therapeutics for these devastating diseases.

Resumo

A doença de Huntington (HD) é causada por uma expansão de poliglutamina (polyQ) na proteína huntingtina (Htt). A expansão de polyQ aumenta a propensão da Htt para se agregar e acumular, e manipulações que mitiguem a mal-formação proteica ou que facilitem a degradação destas proteínas mal-conformadas são capazes de abrandar a progressão da doença em modelos de HD. αB-cristalina (αBc) ou HspB5 é uma proteína bem caracterizada membro da família das "small heat shock protein" (sHsp) que reduz a agregação e toxicidade da huntingtina mutante (mHtt) em estudos *in vitro* e em modelos Drosophila de HD. Aqui, determinámos se a sobre-expressão ou diminuição dos níveis da αBc *in vivo* foi capaz de modelar a agregação e atrasar o aparecimento e a progressão da doença num modelo de longo comprimento genético de HD, os ratinhos BACHD. A expressão de sHsps em doenças neurodegenerativas ocorre predominantemente em células não-neuronais, e no cérebro, a αBc é principalmente encontrada em astrócitos e oligodendrócitos. No capítulo 3, demonstrámos que a sobre-expressão da αBc dirigida em astrócitos melhorou a performance motora nos testes de Rotarod e Balancim "Balance Beam" e melhorou a função cognitiva dos ratinhos BACHD. A melhora dos déficits de comportamento esteve relacionado com a mitigação de características neuropatológicas muito comuns observadas em HD. Interessantemente, a sobre-expressão astrocítica da αBc foi neuroprotectora contra a perda neuronal nos cérebros dos BACHD, sugerindo que αBc talvez esteja a actuar de uma forma celular não autónoma. Ao nível proteico, a αBc diminuíu os níveis de mHtt solúvel e diminuíu o tamanho das inclusoes de mHtt nos cérebros dos BACHD. Estes resultados apoiam um modelo no qual elevar a αBc astrocítica confere neuroprotecção através de um potencial mecanismo celular não-autónomo que modela os agregados e os níveis proteicos solúveis da mHtt.

No capítulo 4, tentámos elucidar o mecanismo celular não autónomo pelo qual a sobre-exressão da αBc confere neuroprotecção na progressão da doença dos ratinhos BACHD. Vários mecanismos celulares essenciais estão debilitados em doenças neurológicas como a HD. Entre muitos, a activação das vias da caspase-3, transporte e sinalização de glutamato e stress oxidativo são marcas moleculares comuns na patologia da HD, e a αBc tem um papel nestes mecanismos. Os nossos estudos baseados no mRNA e níveis proteicos dos BACHD e também em células primárias (astrócitos e neurónios), não mostraram uma

diferença significativa na activação da caspase-3, e na expressão do transportador-1 do glutamato neste contexto. No entanto, quando investigámos a formação de grupos proteicos carbonilo (derivados do stresse oxidativo), encontrámos uma pequena tendência para a diminuicão destas espécies de carbonil na presença da sobre-expressão astrocítica da αBc, tanto nos cérebros como nas culturas primárias dos BACHD. Estes dados apoiam o potencial efeito antioxidante da αBc no contexto da patologia de HD.

No capítulo 5, hipotetizámos que a deficiência em αBc iria acelerar a severidade e progressão da doença de HD, como tinha sido previamente observado num modelo de Alzheimer. Nós testámos esta hipótese, cruzando animais nulos para αBc (e para HspB2) com os ratinhos BACHD, e monitorizando sintomas comportamentais e neuropatológicos de HD durante a progressão da doença. O nosso estudo mostrou que a eliminação genética de αBc não agravou a progressão da doença de HD. Em suma, os resultados apresentados nesta tese fornecem uma nova perspectiva no papel da αBc e da sua função em mecanismos celulares essenciais no contexto de HD. Este trabalho também apoia o crescente papel e significado de células neuronais em doenças neurológicas como a HD, sugerindo respostas adaptativas e diferenciadas que podem contribuír e/ou providenciar um caminho terapêutico de aspectos distintos de neurodegeneração. Por último, este conhecimento tem como objectivos, promover e realçar o impacto das sHsps, especialmente a αBc em HD e outras doenças relacionadas para ajudar a desenvolver terapêuticas promissoras para estas doenças devastadoras.

List of abbreviations

αBc – alpha B-crystallin

AD – Alzheimer's disease

ALS - Amyotrophic Lateral Sclerosis

BDNF - brain-derived neurotrophic factor

CNS – Central Nervous System

Cryab Tg – Cryab Transgene

DARPP-32 - dopamine and cyclic AMP-regulated protein

DR1 – dopamine receptor 1

DR2 – dopamine receptor 2

DTg – double transgenic

EAE - Experimental autoimmune encephalomyelitis

GFAP - glial fibrillary acidic protein

Glut1 – Glutamate receptor 1

GOF – gain of function

HD - Huntington's disease

Hsps - heat shock proteins

HSR – Heat Shock Response

Htt – huntingtin

HTT – huntingtin gene

Htt – huntingtin protein

IB – inclusion bodies

iNOS – inducible nitric oxide synthase

LOF – loss of function

mHtt – mutant huntingtin

NeuN – Neuronal marker Anti-NeuN antibody

PD – Parkinson's disease

polyQ – polyglutamine

PTMs - Post-translational modifications

ROS – reactive oxygen species

RPE - retinal pigment epithelial

sHsps - small heat shock proteins

TNF-α- Tumor Necrosis factor alpha

WT – wild type

Chapter 1.

General Introduction

Chapter 1. General Introduction

1. Huntington's Disease

1.1. Historical Background

Huntington's disease (HD), originally called simply 'chorea' or 'hereditary chorea', has been recognized as a disorder since the Middle Age. Nevertheless, it was just in 1872 that George Huntington, a young physician from Connecticut, published the first accurate description of the disease (1).

This neurological disease was described as dominantly inherited, affecting several family generations, and characterized by an excessive dance–like motor movements (the major motor abnormality occurring in HD), neuropsychological deficits, including cognitive and psychiatric impairment, and gradual deterioration that would ultimately lead to death (2).

In 1983, a study conducted by a consortium of researchers – The US-Venezuela Huntington's Disease Collaborative Research Project – took place in the Lake Maracaibo region of Venezuela. This region was known for its high density of HD cases and significant consanguinity, linked a polymorphic DNA marker genetically to HD (3). More than a century passed since the first description of HD until the underlying genetic mutation was identified (4). Shortly, the polymorphic DNA marker consists of an abnormal expansion of a CAG trinucleotide repeat sequence in the coding region of the HD IT15 (Interesting Transcript 15) or HTT gene, on the short arm of chromosome 4 (4p16.3). The CAG repeat encodes a polymorphic stretch of glutamines (Q) within the N-terminal region of a high molecular weight protein, with approximately 3144 amino acids (~348 kDa), known as Huntingtin (Htt) (5). Since identification of the disease-causing gene, several approaches and a number of genetically modified cellular and animal models were developed to enable the study of the molecular underpinnings of HD, to possibly bring us closer to identify possible therapeutic strategies for this devastating disease. The first HD mouse model, called R6/2, was created in 1996 (6) and a year later, accumulation of mutant Htt (mHtt) in intranuclear inclusions was discovered in the brain of this HD mouse model and related to the pathogenic mechanism in

HD (7). Similar neuropathological features were also found in the brains of HD patients (8). Despite the intense effort on HD research since its first discovery, no clinical interventions tested in cellular and animal models to date have delayed the disease progression in humans. However, these models provide an invaluable tool for both investigating the underlying pathogenic processes and developing new effective therapies.

The details of the genetic aspects of HD and Htt - inclusion bodies formation will be described throughout this Chapter as well as some of the most promising therapeutic approaches for HD.

1.2. Epidemiology

The prevalence of HD, incorporating both genetic and clinical diagnostic studies, is approximately 10-13 in 100,000 people worldwide (9, 10), but it can vary to a great extent and can affect 700 per 100,000 individuals in some secluded regions of Venezuela (11). The age of onset is typically between 35 and 50 years old, however 15% of the cases can occur before 20 years old, called juvenile HD cases. The life expectancy of this devastating and progressive disease is typically 15-20 years from onset of symptoms till death (12).

1.3. The disease: Clinical presentation

HD is typically characterized by movement impairment (Chorea), cognitive dysfunction and decline and psychiatric disorder (13, 14). Chorea is the most common and aggressive manifestation of HD. It consists of involuntary, abnormal and irregular movements (hyperkinetic movements) that can affect most of the body, in particular the limbs, trunk and face (15). As the disease progresses, chorea often stabilizes and bradykinesia and rigidity start taking place, which is a very common feature in other neurodegenerative disorders such as Parkinson's disease (PD) (16). Individuals in the last stages of HD suffer from gait disturbances which compromises their mobility, leading to falls (17). In the very last stage of the disease patients are not able to swallow and ultimately they are incapable of eating and also breathing (15, 18). Regarding cognitive dysfunction in HD, dementia is a common feature in the majority of the cases, varying from the designated subcortical dementia in

which individuals are not able to learn new motor skills and their visuospatial memory is also affected to a very broad of cognitive decline (13, 19). Lastly, the psychiatric disturbances in HD are extremely diverse, but the most typical in patients are irritability, apathy, anxiety, depression and impulsivity (13). HD patients also commonly suffer from progressive weight loss, alterations in sexual behavior, and disturbances in the wake-sleep cycle that occur very early in the course of the disease and may partly be explained by hypothalamic dysfunction (20). Suicide is also prevalent among HD patients (21, 22).

1.4. Genetic Factors and neuropathology of HD

As previously mentioned, HD is a devastating autosomal-dominant neurodegenerative disease caused by an abnormal expansion of the CAG triplet in the exon1 of the IT15 gene, which encodes a polyglutamine (polyQ) segment in the Htt protein (5, 14).

Unaffected alleles have CAG repeat size ranging from 10 to 35. With a median size of 18, the most common alleles in all populations contain repeats of 15-20 CAGs (15). HD-causing alleles are classified as: 1) Reduced- penetrance HD-causing alleles with 36-39 CAG repeats. An individual with an allele in this range is at risk for HD but may not develop symptoms. 2) Full-penetrance HD-causing alleles with 40 or more CAG repeats. Alleles of this size are associated with development of HD with great certainty (3). Individuals with adult-onset HD usually have a CAG expansion from 40 to 55. In that range, ~50-70% of age of symptom onset appears to be explained by the length of the polyQ stretch, whereas the remaining variance is plausible to occur by other modifying genes and environmental factors (23–25). In longer polyQ stretches, the length of the polyQ stretch explains a greater proportion of age of symptom onset. Like other polyQ disorders, there is an inverse correlation between the length of CAG repeats and the age of onset. Thus, the longer the CAG stretch, the earlier symptoms typically appear (Figure 1). HD juvenile onset cases have CAG expansions greater than 60 that are often inherited from the father (paternal transmission) (3, 26).

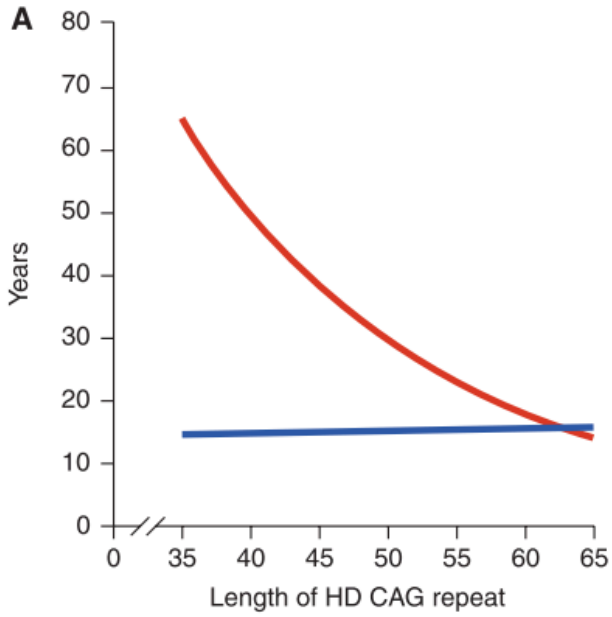

Figure 1. The role of the CAG expansion in IT15 on HD pathogenesis. (A) Correlation of HD CAG-repeat length with age at onset. Best-fit curves for age at neurological onset (red) and duration of disease from onset to death (blue), plotted against CAG- repeat length for the expanded mutant allele from HD patients. Age at onset is strongly correlated with the CAG-repeat length ($r^2 = 0.54$; $p < 0.001$), and duration of disease shows no correlation with the CAG-repeat length, suggesting that, after onset of HD, factors independent of the original trigger of pathogenesis determine the rate of progression. Adapted with permission from (5).

Although HD pathology has been observed in peripheral tissues (27) like other polyQ disorders, HD is predominantly a central nervous system (CNS) disorder, characterized by cell loss and atrophy (28), classified in five grades (0–4) designated in ascending order of severity (7, 29).

Within the brain, atrophy of the striatum (the largest component of the basal ganglia system) is the most prominent (17) (Figure 2), which primarily include a selective degeneration of medium spiny neurons (MSNs) (which represent about 96% of striatal neurons, and receive synaptic input primarily from the cortex) in the caudate nucleus and putamen, while aspiny interneurons (which represent around 2% of the striatal neurons) of the striatum are generally spared (30). Counts of neurons in the caudate nucleus revealed that 50% are lost in grade 1 and that 95% are lost in grade 4 (29).

Nevertheless, gradual MSN's degeneration in the caudate nucleus and putamen appears to be distinctive. At early stages of HD, striato-globus pallidus (GP) internal segments (GPi) medium spiny projection neurons (which express substance P/gamma-aminobutyric acid (GABA) and projects to and inhibit GPi resulting in thalamus disinhibition and subsequent excitation of upper motor neurons in the motor areas of the cortex, which increase movement - direct pathway) are relatively spared. In contrast, striato-GP external segments (GPe) (which express enkephalins and projects to and inhibit GPe resulting in

subthalamic nucleus inhibition and consequent less inhibition of substantia nigra (SN) pars reticulata (SNr) and GPi which inhibits thalamus resulting in the inhibition of upper motor neurons; thus decreasing movement - indirect pathway) and striato-SNr (which express substance P/GABA and projects to and inhibit SNr - direct pathway) medium spiny projection neurons degenerate (31); loss of striato-GPe neurons was also demonstrated in presymptomatic HD (32). The early and relatively selective loss of striato-GPe and striato-SNr neurons was suggested to be a plausible explanation for the chorea and oculomotor abnormalities that are prominent clinical features of early HD (33). However, in later stages of adult HD, both populations of striatal projection neurons are affected, with concomitant loss of markers of the direct pathway (substance P/GABA-containing neurons), including dopamine D1 receptors and substance P (31, 34). In addition, in juvenile cases of HD, degeneration of both direct and indirect pathway striatal neurons was observed (34). Thus, the degeneration of both the direct and indirect pathways was suggested to be functionally correlated with bradykinetic rigid phenotype observed in late stage and juvenile HD patients (34). Also, within the spared aspiny interneurons in HD there appears to be a differential level of vulnerability (35). In addition, non-striatal brain regions can also be affected, particularly in latter stages of the disease, and can include the SN, hippocampus, and mostly various regions of the cortex (36). Pyramidal neurons of deeper cortical layers appear to be more affected in HD, which seem to be correlated with dementia and personality changes in HD patients (17).

As previously discussed, brain atrophy and degeneration with marked neuronal cell loss in the regions mentioned above, putamen and caudate nucleus as well as cortex can occur before specific or severe motor symptoms appear in HD - asymptomatic patients – this period is defined by prodromal stage (Figure 2). At this point, affected patients can still perform usual functions although distress and discomfort may be felt (17).

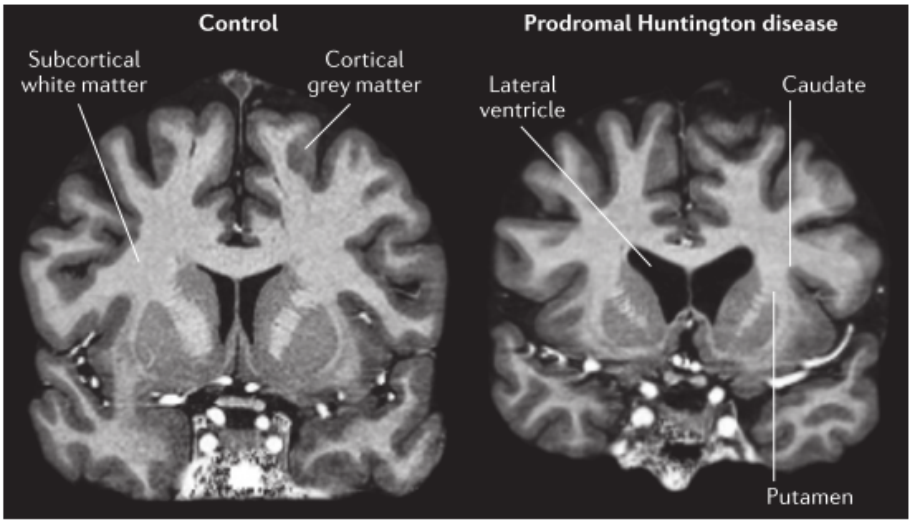

Figure 2. Atrophy in prodromal HD shown using 7T MRI. Bilateral atrophy of the caudate and putamen, and a concomitant increase in size of the fluid-filled lateral ventricle, is observed in the gene carrier compared with the control. This prodromal participant has only subtle signs and symptoms that are insufficient for diagnosing manifest HD. There are also subtle changes in the cortical grey matter and overall atrophy of subcortical white matter (26).

The reason why there is selective brain degeneration in HD remains unclear. However, it may be due to the role and importance of the Htt protein might have in the brain. The Htt polyQ tract begins at the 18 amino acid and is followed by a proline rich sequence (polyP) composed by 38 amino acids, which is considered to be important in Htt solubility (37). The first 17 amino acids of Htt are important for nuclear shuttling since they interact with TPR (translocated promoter region), a protein of the nuclear pore that actively exports proteins from the nucleus. Htt nuclear accumulation was observed when the first 17 amino acids were eliminated (38). Htt also contains multiple regions of so-called HEAT (Huntingtin, Elongation factor 3, a subunit of protein phosphatase 2ª nd the lipid kinase TOR) repeats, a sequence of ~40 amino acids named after the first four proteins in which it was discovered (39, 40) (Figure 3). Although the exact function of HEAT repeats is still unclear, studies have suggested that these domains play a role in a variety of interactions between proteins, including transportation in the cytoplasm and nucleus, microtubule dynamics and chromosome segregation (39).

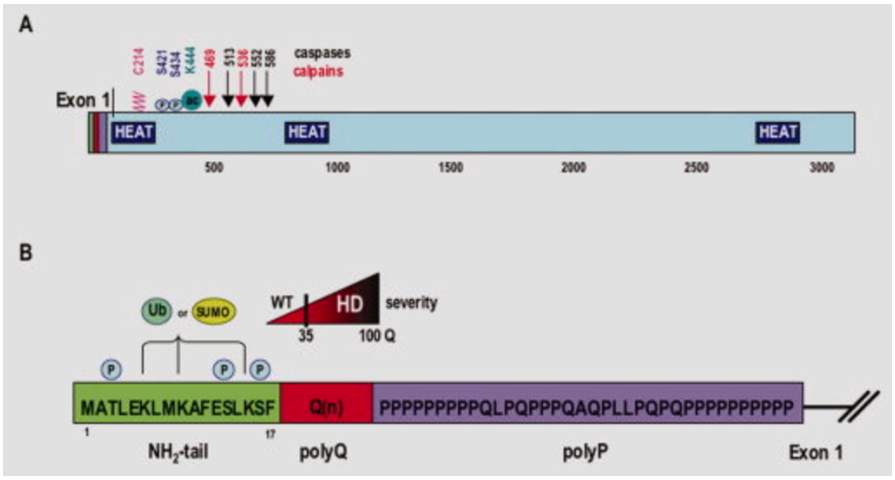

Figure 3. Structure of the Htt full-length protein (A) and of the N-terminal exon 1 of the gene (B). Panel (A) indicates the position of the three clusters of HEAT repeats, the caspase (black) and calpain (red) cleavage sites and some of the post-translational modification sites along Htt protein (C214 palmitoylation, S421, S434 phosphorylation, K444 acetylation). Panel (B) shows the N-terminal product of the exon 1 of the Htt gene, with the 17aa N-terminal tail (green) and the post-translational modifications reported to occur on the indicated residues (T3, S13, S16 phosphorylation; K6, K9, K15 ubiquitination and/or SUMOylation); Q(n) indicates the polyglutamine tract (red) and the upper insert shows the correlation between polyQ size and HD severity; the polyproline region downstream polyQ stretch is indicated in purple (41).

Htt mRNA and protein are ubiquitously expressed throughout development and in adulthood, in a variety of cells and peripheral tissues, and homogenously in the brain where it is higher expressed (8, 42), with a predominance of neuronal over glial expression (43–45). In the brain, Htt mRNA was detected in both grey and white matters (lowest expression levels), and the highest expression levels of Htt were found in the cortex (with differential expression between cortical layers), hippocampus, SN and cerebellum, followed by the striatum (43, 45). There are no differences in the distribution and levels of Htt mRNA between symptomatic HD patients and control individuals, except in the striatum where the intensity of labeling seems significantly reduced (42). However, presymptomatic HD brains revealed a striatal expression similar to controls and surviving striatal neurons in more advanced HD had an expression of Htt mRNA within normal limits. Therefore, HD brain selective degeneration does not seem to result from altered Htt mRNA expression (43). Wild-type (WT) Htt protein within neurons can be found mainly in the cytoplasm, but also in neurites and synapses. WT Htt can be associated with various organelles and structures, such as microtubules, plasma membrane, endosomal and endoplasmic compartments, clathrin-coated vesicles and mitochondria (46–48). Although mostly located in the cytoplasm, Htt is also detected in the nucleus (47). Due to its subcellular localization Htt interacts with numerous proteins involved

in gene expression, intracellular transport, signaling and metabolism, axonal trafficking of vesicles, transcriptional regulation and it also plays important functions in apoptosis and embryonic development (14, 49, 50). WT Htt is involved in embryonic development, since homozygous HTT locus knockout mice are lethally affected at early embryonic development stages (51–53). In contrast, the presence of one fully functional allele (at least 50% Htt expression) is compatible with life in humans and HD is not caused by a simple loss of function of the HTT gene (54). In fact, patients with Wolf-Hirschhorn syndrome, that have a partial deletion of chromosome 4 that comprises the CAG triplet repeats region and therefore contain only one copy of the HTT gene, are born and do not develop HD (3). WT Htt has an anti-apoptotic function in a gene and protein-dependent manner (55). In addition, WT Htt acts downstream mitochondrial cytochrome c release (a protein at the mitochondrial inter-membrane space that when released from mitochondria can bind to caspases to activate the cell death process), preventing the activation of both caspase-3 (56) and caspase-9 (57). Also, WT Htt physically interacts with active caspase-3 and inhibits its activity (58). Furthermore, Htt has been suggested to have a role in transcriptional regulation. For example, Htt was shown to regulate the genetic transcription of brain-derived neurotrophic factor protein (BDNF), a signaling neurotrophin essential for striatal neuronal survival and for the activity of cortico-striatal synapses, by binding and trapping in the cytoplasm (inhibit) the BDNF transcriptional repressor REST/NRSF (RE-1 silencing transcription factor/neuron- restrictive silencer factor) (14, 59–61). Apparently, WT Htt facilitates a de-repression of BDNF transcription but polyQ-expanded Htt does not (60). Thus, several studies have implicated that a reduction of BDNF at the transcriptional level is an important contributor to HD pathogenesis (60, 62).

In the disease context, the Htt protein with an expanded and abnormal polyQ, now denominated mutant Htt (mHtt) becomes aberrant and toxic that leads to neurodegeneration (6, 26). At the cellular level, HD neuropathology is characterized by the presence of neuritic, cytoplasmic and nuclear inclusions of mHtt (7, 8). mHtt accumulation and toxicity are associated with neuropathological damage characterized by brain atrophy and neuronal cell death, even at prodromal stages (Figure 2). How this polyQ-expanded mHtt causes selective and progressive dysfunction and neurodegeneration remains unclear. HD is one of at least nine genetic diseases caused by an abnormal expansion of a polyQ stretch, highlighting the

toxicity of polyQ-mediated protein misfolding in disease pathogenesis (54). However, increasing evidence points to the fundamental role that host protein context plays in pathogenesis. Expansion of its polyQ stretch beyond 36 repeats causes the protein to misfold and confers a toxic gain of function (GOF) (63). However, there is also evidence to support a contribution to disease pathogenesis from a loss of function of the WT allele (54). While a GOF is consistent with the autosomal dominant inheritance, there is also evidence to support a contribution to pathogenesis from loss of function (LOF) of the WT allele (14, 54). mHtt appears to have at least certain properties of WT Htt. In fact, mHtt can rescue the embryonic lethal phenotype seen in Htt-null knockout mice (64, 65). However, it is still not clear if neuronal cytotoxicity in HD is due to a LOF or GOF of Htt or actually both. Additionally, WT Htt has been implicated in a multitude of other cellular processes, including intracellular signaling, metabolism, gene expression, and intracellular transport, but its precise native function is still unknown (20, 21). Post-translational modifications (PTMs), in particular, greatly influence the toxicity of several different disease-associated polyQ proteins, including Htt (66). For instance, 4 several PTMs localized to the N-terminal 17 amino acids of Htt can modulate its toxicity (37, 67, 68). These residues, immediately preceding the polyQ stretch, are well positioned to alter the expansion's propensity to cause protein misfolding via both direct and indirect means. However, other Htt PTMs farther away from the polyQ repeat region by primary sequence also have been reported to modify mHtt toxicity (49, 69).

The proteolytic cleavage of mHtt into N-terminal fragments containing the polyQ stretch and their subsequent translocation to the nucleus and formation of intranuclear aggregates (8, 70) is an hallmark of the disease detected in post-mortem HD human brains. The aggregates can be found before the onset of the first symptoms (7), and the rate of aggregate formation was shown to correlate with the length of the polyQ repeat (71, 72). However, the toxicity of mHtt nuclear inclusions remains controversial, since their formation is correlated with disease progression, but it is not directly linked with neuronal degeneration as initially thought. In fact, several cellular studies, including many from our laboratory, have demonstrated that large mHtt inclusions can be protective against mHtt-induced toxicity and increase cell survival (8, 73, 74). Interestingly, exposure of mHtt-transfected striatal neurons to conditions in which nuclear localization of mHtt was blocked and consequently, suppressing its ability to form intranuclear inclusions, resulted in increased cell death,

suggesting that the formation of intranuclear inclusions might reflect a cellular mechanism to protect against mHtt-induced cell death (74). On the other hand, the decrease of proteolytic cleavage of mHtt reduced its toxicity and slowed disease progression (75, 76). In addition, expression of smaller N-terminal mHtt fragments resulted in increased toxicity in cultured cells (77) and transgenic animals (8, 78, 79), when compared to the full-length mHtt expression with the same polyQ expansion. These findings suggested that the susceptibility to neuronal death is greater with decreased protein length and increased polyQ size. Therefore, several HD models have been generated to mimic the neuropathological features that occur in humans. These models express only a fragment or a full-length (fl) mHtt to study the cellular and molecular mechanisms of mHtt-induce neurodegeneration.

1.5. HD models

A wide variety of species, including the invertebrate worm *(Caenorhabditis elegans)* and fly *(Drosophila melanogaster)* models, non-mammalian species as zebrafish *(Danio rerio)* and mammals, such as mouse *(Mus musculus)* and rat *(Rattus norvegicus)*, have also been genetically engineered to express the HD mutation (80–83). A large number of mouse models of HD that show different degrees of similarity to the human condition have been generated. Models that express either truncated, full-length human or mouse mHtt display significant phenotypic differences that may be caused by the influence of the protein context, mouse strain, or regulatory sequences between the mouse and human HTT genes (80). To overcome these problems, a group of researchers also considered the generation of large HD genetic models such as sheep (84), mini-pig (85), and the non-human primate (86, 87). With their size, organ capacity, and physiology resembling in several aspects that of humans, these models may be well suited for preclinical trials and long-term safety studies. However, in some cases, ethical concerns have been raised. In this section, we describe especially the most common HD mouse models that have particularly enlightened in the search for targets and for compounds capable of interfering with mHtt toxicity.

1.5.1. Transgenic models

In transgenic mouse models, full-length or a fragment of the mutant HTT gene is inserted randomly into the mouse genome, leading to the expression of a mutant protein in addition to the endogenous Htt. Thus, transgenic mouse models of HD express N- terminal mHtt fragments or full-length human HTT gene with an expanded polyQ tract (28).

1.5.1.1. N-terminal huntingtin transgenic models

The first transgenic mice model of HD, named R6/2 mice, include the insertion of a fragment of the human HTT gene. R6/2 mice contain a mutant N-terminal segment of the exon 1 of the human HTT gene with ~144-150 CAG repeats (6). These mice display choreiform-like movements and mHtt inclusion formation as early as at 4-5 weeks. At 6-8 weeks their physical appearance deteriorates and motor symptoms become very severe, followed by an early death around 12-14 weeks. Despite their severe motor impairment and brain atrophy, these mice display fewer neuronal death when compared to human HD patients (6, 79, 81). Due to their high number of CAG repeats, R6/2 mice seem to recapitulate the disease features of juvenile cases of HD (88). In parallel, another transgenic model was developed - the R6/1 model of HD. This mouse model expresses a truncated HTT gene with around 115 CAG repeats, and exhibits a progressive pathology and lower expression of the mutant transgene. A marked decline in rotarod performance and other locomotor activities is observed at 13-20 weeks, correlating with the numbers of striatal neurons exhibiting intranuclear inclusions of mHtt, and with death occurring within 4-5 months of age (8, 28). The R6/1 model is not used as often as the R6/2 model and is therefore less well understood.

The N171-82Q mouse model of HD contains a longer N-terminal fragment of mHtt (exon 1 and exon 2) with 82 CAG repeats. Its lifespan is ~17-20 weeks with HD-like symptoms beginning at 10-12 weeks of age. In these mice, neuropathological features are more similar to human HD, therefore brain atrophy and neuronal loss is more prominent and seems more selective for the striatum (78, 81). HTT is driven from a prion promoter, restricting expression solely to neurons and not glia. But in human HD, Htt is expressed in both neurons and glia (80).

1.5.1.2 Full-lenght huntingtin transgenic models

Transgenic mice expressing full-length htt have in some cases been more successful than N-terminal fragment models regarding neuronal deterioration and loss and the capability to recapitulate more closely the sequence of events leading to HD. Two genomic transgenic models expressing full-length mHtt from the human genomic locus on a yeast artificial chromosome (YAC) (64, 89, 90) or on a bacterial artificial chromosome (BAC) (91) were generated. A series of YAC transgenic models of HD expressing full-length human mHtt with 18, 46, 72, and 128 CAG repeats (i.e., YAC18, YAC46, YAC72, and YAC128) were created after microinjection of YAC DNA construct into the friend virus B strain (FVB/N) pronuclei and maintained on the inbred mouse FVB/N background strain; in contrast to the C57BL/6 background strain common to most HD mouse models, the FVB/N strain shows higher neuronal loss when exposed to excitotoxic stress after injection of kainic- or quinolinic acid (QA) (64, 89, 90). YAC128 mice are the latest of the series and exhibit by far the most robust phenotypes among all the YAC models; therefore, YAC128 is used as a preclinical model in HD (89). At the protein level, the YAC128 line expresses human mHtt at about 75% of the level of the endogenous murine Hdh (80). YAC128 mice exhibit hyperactivity at 2 months of age and hypoactivity at 8–12 months of age. They also exhibit rotarod deficits at 4 months of age, which become more prominent at 6 months of age (92–94). mHtt nuclear localization is detected in the striatum at 1-2 months and in the cortex and hippocampus at 3 months of age. Nuclear inclusions are detected only at 18 months in the striatum. As in humans, selective atrophy in the striatum and cortex, but not in cerebellum is detected (93).

BACHD, the model we have used in this study, is a more recent generated transgenic mouse model of HD and also maintained in the FVB/N background strain. Under the control of endogenous HTT regulatory machinery on the BAC, the 97 polyQ repeat within full length mHtt in BACHD mice is encoded by a mixed CAA-CAG repeat, which is stable in both the germline and somatic tissues including the cortex and striatum at the onset of neuropathology (91). The BACHD mice exhibit progressive motor deficits and selective late-onset neuropathology without somatic repeat instability in the aged brain. BACHD mice exhibit mild rotarod deficits at 2 months, with progressive deficits and hypoactivity at 6 months of age. At 12 months of age, cortical and striatal atrophy is detected. However, unlike previous

full-length mHtt mouse models, BACHD mice do not show early and diffuse mHtt inclusions (91, 95). By 12 months of age, BACHD brains have only a few small aggregates predominantly in the neuropil in the cortex and small aggregates in the striatum (82), suggesting that diffuse nuclear accumulation of aggregated mHtt in striatum and cortex is not necessarily associated with the slowly progressive and selective pathological process in the BACHD mice. Importantly, a relatively steady-state level of predominantly full-length mHtt and a small amount of mHtt N-terminal fragments, present in both the nucleus and cytoplasm, may be responsible for the onset of neuropathology (91, 96). Thus, BACHD mice represent a robust *in vivo* paradigm to study HD pathogenesis and treatment.

1.5.2. Knock-in models

Knock-in HD models were generated by targeting an expanded polyQ repeat and/or adjacent human mHtt exon 1 sequences (including the polyP region) to replace the corresponding sequences in the endogenous murine HD homologue gene (Hdh) (97). Therefore, differently from the transgenic model, the mHtt in the Knock-in models is expressed from the endogenous Hdh locus in a similar manner to the expression in HD patients, making this model considered one of the most precise genetic HD mouse models (98). When compared to N- terminal mHtt fragments expressing models, Hdh knock-in mice display slow progression and moderately mild phenotypes, and their lifespan is usually normal. This mouse model is important to evaluate early pathological processes induced by mHtt in humans (95). The first knock-in models generated were disappointing to the community because their extended stretch of 50 or 80 CAG repeats into the endogenous mouse Hdh gene (HdhQ50; HdhQ80) showed no behavioural phenotypes or abnormalities, or even mHtt aggregates (99, 100). For these reasons, other knock-in models were generated to better represent the human pathology.

1.5.2.1. HdhQ111

The HdhQ111 model is a knock-in mouse model of HD with an insertion of a chimeric murine Hdh/human mHtt exon 1 into the endogenous Hdh locus; the human mHtt portion

includes 111 CAG repeats and a polyP region (88). The behavioral phenotypes of HdhQ111 are very mild and slowly progressive. Rotarod, clasping or open field abnormalities were not detected in heterozygous or homozygous HdhQ111 mice until 17 months of age, and gait abnormalities were detected only at 24 months of age (101). HdhQ111 homozygous mice show selective and progressive accumulation of nuclear mHtt at 2.5 months of age, nuclear inclusion formation at 10 months of age, and reactive gliosis in the striatum at 24 months of age (101).

1.5.2.2. CAG140

The CAG140 HD knock-in mice model was generated by replacing the endogenous murine Hdh exon 1 with a chimeric mouse and human exon 1 with 140 CAG repeats (102). CAG140 HD mice display early hyperactivity at 1 month of age, followed by hypoactivity at 4 months of age, gait abnormality at 12 months of age, with nuclear mHtt micro-aggregates in the striatum and cortex, and nuclear inclusions in the striatum at 4 months of age and in the cortex at 6 months (103). However, nuclear micro-aggregates were also observed at 6 months of age in the cerebellum, a relatively spared region in human HD brain, but presented no cell loss or brain atrophy (95, 103).

1.5.2.3. Hdh(CAG)150

Hdh(CAG)150 HD knock-in mice was developed by a replacement of the short CAG repeat in the murine Hdh exon 1 with a stretch of 150 CAG repeats (104). Homozygous Hdh(CAG) 150 mice revealed several slowly progressive motor abnormalities (105, 106). Homozygous HdhCAG(150) mice display progressive rotarod deficits at 18 months of age and mHtt aggregates in the striatum and hippocampus at 6 months and widespread in the brain at 10 months of age (107). Striatal neuronal loss is observed at 100 week-old (105).

1.6. Diagnosis, Screening and Prevention of HD

HD is easily diagnosed based on the appearance of physical symptoms specific to the disease. As previously described, the motor symptoms are the first clinical features to be diagnosed, specifically abrupt, excessive and random timing of involuntary movement (26). Characterized by its dominant inheritance, the available genetic test for HD consists of a simple blood examination to confirm the number of CAG repeats in the HTT gene. However, a positive result is not considered a differential diagnosis since it can be obtained before the onset of symptoms. This test is very important to rule out the disease and also because its result may dramatically influence personal and family planning decisions. Longitudinal analyses show a consistent increase in the prevalence of HD over the past two decades, coinciding with wider availability of the genetic test. Since HD is an autosomal dominantly transmitted disorder, there is a 50 % chance of children from an affected individual inheriting the disease (15, 26). Prenatal testing can also be performed using non-invasive techniques to determine the carrier status of the fetus. The progression of the disease can be measured based on the unified HD rating scale (UHDRS) that characterizes the relevant clinical features of HD (108). Medical functional imaging, such as fMRI and PET, are very important in the early detection of HD since they can show changes in the brain activity before symptoms onset in addition to monitoring the disease progression (15, 26).

HD is devastating to patients and their families and unfortunately, at the present, there is no effective treatment to stop or slow the disease progression.

The current available therapies act mainly on motor symptoms in order to improve patients' quality of life. These therapies are mainly focused to treat movement disorders such as chorea and dystonia, as well as gait, speech, swallowing and fine motor tasks (16). The only drug currently approved and specifically licensed by the US Food and Drug Administration (FDA) in 2008 to treat chorea in HD patients is tetrabenazine (109). As a synaptic vesicular amine transporter inhibitor, tetrabenazine acts by reducing the quantity of dopamine released from vesicles in the brain by reversibly inhibiting the monoamine transporter type 2 (VMAT2) and therefore depleting central monoamines (110). Tetrabenazine is also responsible for reducing dopamine by blocking dopamine receptors. Unfortunately, this drug is also associated with some adverse side effects, namely, sedation

and somnolence, agitation, depression, akathisia, anxiety and hyperkinesia (108, 110). Several studies are underway to investigate other potential treatments for chorea in patients with HD, including pallidal deep-brain stimulation (111, 112) and a deuterated tetrabenazine molecule (111, 113, 114). In fact, many reviews have emphasized the weak evidence supporting any other pharmacological intervention in the treatment of HD (115, 116).

In an effort to diminish therapeutic nihilism in the absence of established and accurately proven treatments, a series of algorithms for the treatment of chorea, irritability and obsessive–compulsive behaviors were reported in 2011 by an international group based on surveys of HD experts (117). Until better treatments arise, the clinicians must adopt an attitude that therapeutics providing benefit to patients without HD, who have neuropsychiatric symptoms, may be also expected to help HD patients that share the same symptoms. As an example, some pharmacological approaches to treat or ameliorate the neuropsychiatric symptoms in HD include: olanzapine for weight loss, selective serotonin reuptake inhibitors and mirtazapine for depression, antipsychotic drugs for psychiatric and behavioral aspects of this pathology. Although these pharmacological compounds are not specific for HD (116), clinicians should proceed thoughtfully to optimize the patients' quality of life with available medications and supportive therapies.

1.7. Novel Strategies for Therapeutic Intervention in HD

In this section I briefly describe new possible and promising therapeutic targets as well as potential disease-modifying therapies underlying the pathobiology of mHtt, that are currently being studied. Figure 4 highlights some of the current and potential disease-modifying strategies for HD. Special emphasis will be given to chaperone-mediated folding and aggregation, and also pathways involving protein homeostasis, since it is the central topic for this thesis work.

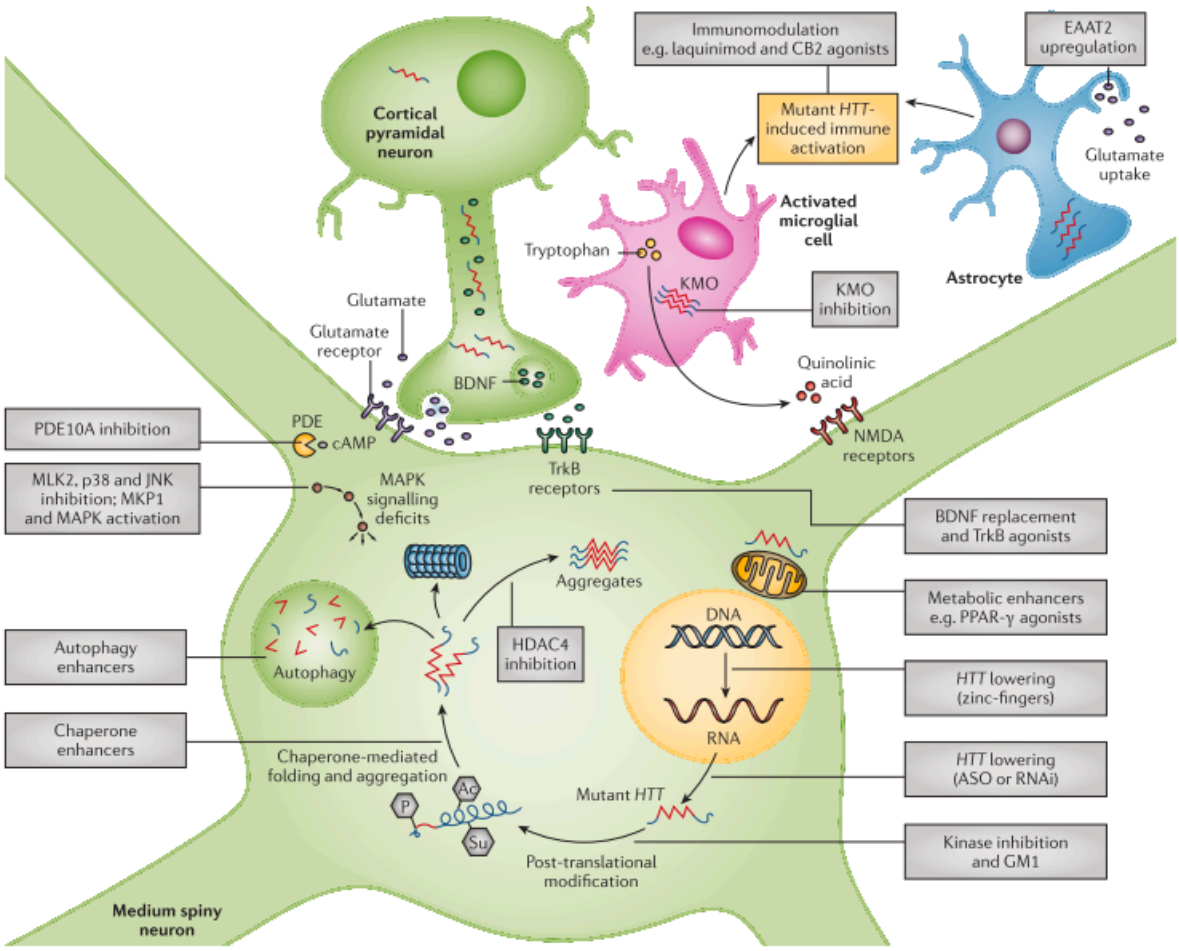

Figure 4. Current priority preclinical therapeutic targets under investigation for Huntington disease. Several targets have been identified for potential exploitation in therapy, with strategies that include Htt lowering and immunomodulation (118) . Ac, acetyl group; ASO, antisense oligonucleotide; BDNF, brain-derived neurotrophic factor; CB2, cannabinoid receptor 2; EAAT2, excitatory amino acid transporter 2; GM1, monosialotetrahexosylganglioside; HDAC4, histone deacetylase 4; JNK, c-Jun N-terminal kinase (MAPK8, MAPK9 and MAPK10); KMO, kynurenine 3-monooxygenase; MAPK, mitogen-activated protein kinase; NMDA, N-methyl-d-aspartate; P, phosphate group; p38, mitogen-activated protein kinase (MAPK11, MAPK12, MAPK13 and MAPK14); PDE, phosphodiesterase; PPAR-γ, peroxisome proliferator- activated receptor-γ; RNAi, RNA interference; Su, sumoyl group; TrkB, tyrosine receptor kinase B. Figure adapted from (26).

1.7.1. Protein Homeostasis

Protein homeostasis is essential for cell function and survival, because proteins are involved in all aspects of cellular function varying from cell metabolism and cell division to the cellular response to environmental stressors. Protein homeostasis is tightly regulated by

the synthesis, folding, trafficking and clearance of proteins, all of which act in an orchestrated manner to ensure proteome stability (119). The protein quality control system is composed of stress response pathways, which take action whenever the proteome is challenged by environmental or physiological stress. Aging, however, damages the proteome, and such damage is thought to be associated with age-related diseases. In the next sections I will discuss the different cellular processes that define the protein quality control system and focus on their role in protein conformational diseases.

1.7.2. Protein Quality Control Systems

Dysregulation of protein quality control is a key event in HD pathogenesis. The accumulation of misfolded proteins is a hallmark of many human diseases, including several incurable neurological disorders, such as HD. In HD, expansion of the polyQ stretch within the first exon of the Htt protein leads to Htt misfolding, aberrant protein aggregation, and disease onset (50). The accumulation of aberrant mHtt and other polyQ disease proteins form insoluble aggregates and, as mentioned above, the role that aggregation has in the pathogenesis of polyQ diseases remains contentious (50, 73, 122). Neurons, as post-mitotic cells with a high metabolic activity, are extremely sensitive to protein accumulation and the presence of aberrant proteins lead to neuronal cell death. Thus, the *post-mortem* confirmation of the presence of protein aggregates in the brain of patients with neurodegenerative diseases such as HD emphasizes the importance of protein turnover in neuronal homeostasis. To prevent the deleterious process of misfolded proteins accumulation, cells have specific quality control mechanisms that include the molecular chaperones, including the heat shock proteins (Hsps), the ubiquitin-proteasome system (UPS) activation, autophagy-mediated protein degradation. While chaperones help other proteins in the folding process, refolding misfolded proteins to their native conformation, the UPS and autophagy are responsible for the targeting and degradation of unfolded or mutant proteins (123). This degradation mechanism is critical to clear the cytosolic space from these toxic proteins that might disturb the essential cellular processes, and also to recycle amino acids (119, 123). Impairment of the cell quality control mechanisms is commonly associated with neurodegenerative diseases such as HD, and therefore the focus of intensive research in the field (119).

1.7.2.1 Heat Shock Proteins (Hsps)

Hsps, are able to bind specifically and non-covalently to interactive proteins surfaces that are transiently exposed during cellular processes (124). The controlled binding and release of substrate proteins facilitates the correct fate of the protein in the cell, whether this be correct folding assembly into oligomers, transport to a specific subcellular compartment, membrane translocation, or even degradation (125). Hsps protect the cells against a variety of stresses by preventing abnormal protein aggregation and by keeping proteins in a state competent for either refolding or degradation (121). Some chaperones interact with a variety of polypetide chains, whereas other act on specific targets via substrate specific binding domains. For example the 70 kDa Hsps recognize hydrophobic protein surfaces or amino acid residues that are generally exposed by non-native proteins and newly synthesized polypeptide chains (126). The ClpX/Hsp100 family can illustrate an example of specificity of some molecular chaperones. Proteins of this family form ring-like subunit architectures and are able to disassemble multimeric or aggregated forms of certain proteins in an ATP dependent fashion (127). Two members of this family (Clp X and ClpaA) recognize specific C-terminal sequences on target proteins. This property has been extensively characterized for the interaction between *E.coli* Clp X and the transposase of phage Mu (MuA protein) (128). Molecular chaperones were originally termed Hsps due to their initial discovery in *Drosophila melanogaster* cells exposed to elevated temperatures. Despite the name, the Hsps are also known to be induced by a wide variety of environmental or metabolic stresses including anoxia, ischemia and viral agents (121, 129). Hsps can be divided into ATP dependent and ATP independent families as well as being subdivided into families according to their molecular weight. The ATP-dependent Hsps require ATP hydrolysis to facilitate the folding process (129).

1.7.2.1 Hsp families

The name of the members of the Hsp family is derived from the molecular weight of the main representative protein (Table 1) (121, 130). Additionally, the nomenclature is based on systematic gene symbols that have been assigned by the HUGO Gene Nomenclature Committee (HGNC) (131).

Table 1. Major families of Hsps

Chaperone	Binding topology	Action
HSP100		Disaggregates
HSP90		Supports nearly mature conformations; signal transducers
HSP70		Binds linear polypeptide for folding; translocation assembly of multiprotein complexes
HSP60 (GroEL,TriC)		Folds 'molten globule' proteins or domains
Small HSPs		Prevents aggregation, particularly during heat shock

Different Hsps families recognize structural features that are specific to immature and unstable proteins at different of folding and unfolding. The Hsp70 chaperones, rin-shaped chaperonins and Hsp90 are involved successively more advanced stages of protein folding and function, whereas the small Hsps and Hsp100 act predominantly during stress (132).

1.7.2.3. Small heat shock proteins (sHsps) family

Small heat shock proteins (sHsps) have molecular weights between 12 and 43 kDa, distinguishing them in size from larger Hsps (133, 134). There are ten human sHsps: HSPB1–HSPB10 (134, 135). They share common structural characteristics, including a highly conserved 90 amino acid long Hsp20 domain, usually referred to as the alpha-crystallin (α-crystallin) domain, and the capacity to form large dynamic oligomers (136). Thus, sHsps can be found as homo- or heteromeric complexes, consisting of 2-40 subunits (137). The α-crystallin domain consists of two layers of three and five anti-parallel strands, respectively, connected by a short inter-domain loop, forming a β-sheet (138). The α-crystallin domains of two monomers interact tightly to form dimeric building block of the sHsp oligomers. The N-terminal region contains α-helical components and is variable in structure (139). The N-terminal of many of the sHps contains a small prolinephenylalanine-rich region with one or two WD/EDF motifs. This region seems to be important in oligomeric complex formation and also for chaperone activity (140). The C-terminal tail is highly motile and flexible, and is also involved in stabilizing the oligomeric structure through contacts between a conserved motif in the C-terminal region and a hydrophobic patch in the α-crystallin domain of a neighboring subunit (139).

As chaperone proteins, sHsps bind misfolded proteins and prevent them from aggregating. However, they are unable to actively refold the protein themselves because in contrast to other Hsps families, the sHsps do not require ATPase activity for their chaperone function (141). Instead, sHsps sequester the misfolded proteins within the cell, forming large dynamic oligomeric structures that are able to bind several non-native proteins per oligomeric complex, to prevent aggregation until a large Hsp, as Hsp70 or Hsp40, can assist in refolding (134, 137, 142) (Figure 5).

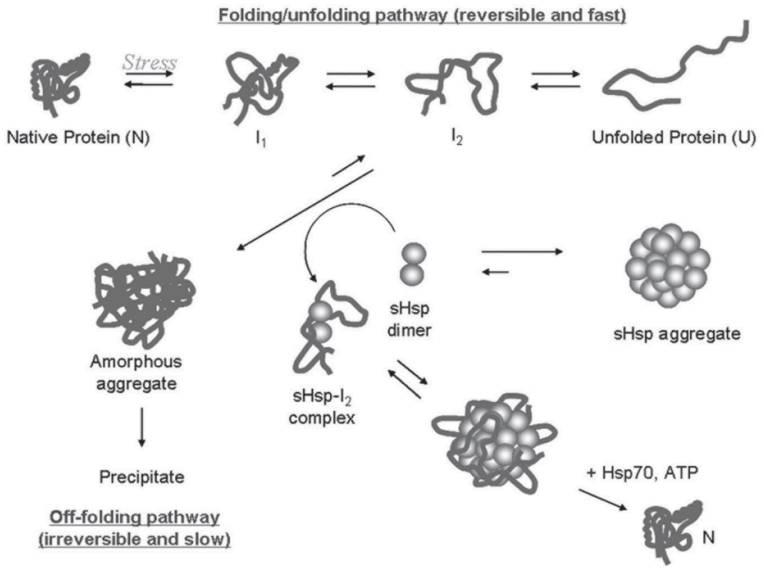

Figure 5. Mechanism of sHsp chaperone interaction with amorphously aggregating target proteins sHsps selectively interact with and stabilize slowly aggregating, intermediately folded target proteins on their amorphous off-folding pathway. The intermediates (I2) are relatively disordered in structurewith only some elements of secondary structure in place.The dynamic nature of the equilibrium between the monomeric and aggregated I2 species facilitates interaction with the similarly dynamic sHsp. There is some evidence that the dissociated, dimeric form of the sHsp is the chaperone-active species which interacts with I2 and is subsequently sequestered into a high-mass complex containing both proteins. It is possible to recover natively folded target protein (N) via the action of another chaperone, for example by Hsp70 action coupled to ATP hydrolysis (124, 137).

Historically, sHsps have been extensively studied in the context of being intracellular molecular chaperones. However, recent studies looking at the role of sHsps in neurological diseases have demonstrated that despite being found in areas of damage, sHsps show therapeutic effects by transgenic overexpression and exogenous administration in various experimental disease paradigms (143). In addition to acting as molecular chaperones and preventing protein aggregation, sHsps have been suggested to be strongly involved in

apoptosis inhibition, anti-inflammation, organization of the cytoskeleton (134, 137). The most intensively studied sHsps are the Hsp27 or HSPB1 and αB-crystallin (αBc) or HSPB5 (144).

1.7.2.4. αB-crystallin/HSPB5

αB-crystallin (αBc) or HSPB5 is a ubiquitously expressed protein and is a major constituent of the eye lens (145), and in the brain is mainly expressed in astrocytes and oligodendrocytes (146).

αBc acts as a molecular chaperone by preventing the aggregation of unfolded proteins and is know to be a multi-tasking chaperone by playing a role in several cellular functions: protein turnover, redox homeostasis, apoptosis and inflammation inhibition, cytoskeletal assembly and architecture (147). It is associated with cytoskeleton proteins, for example, αBc modulates the assembly of the intermediate filament protein vimentin, of the glial fibrillary acidic protein (GFAP) and stabilizes actin filaments in a phosphorylation-dependent manner (148). In addition, αBc also associates with tubulin, and microtubule-associated protein (MAP) and this is mediated through the α-crystallin domain (149, 150). αBc might play a role on proteosome degradation, UPS pathway, since it has been found to interact with FBX4, and F-box-containing protein that is a component of the ubiquitin-protein isopeptide ligase SCF (SKP1/CUL1/F-box). This interaction is dependent on phosphorylation of αBc (151). The chaperone activity or cytoprotective activity of αBc can be regulated by phosphorylation. Interestingly, in the brain, some of the αBc isolated from the proteinaceous aggregates of patients with amyloid plaques and Lewy bodies is phosphorylated (152). However, it remains unclear whether there is a preference for the phosphorylated forms of αBc to interact with the proteins associated with these deposits (153).

αBc has three phosphorylation sites, serines 59, 45, and 19 (153). The triple phosphomimic of αBc (i.e. S19D, S45D, S59D αBc or 3D αBc) is a more effective chaperone in preventing fibril formation by the natively unstructured target proteins k-casein and α-synuclein compared to the WT protein, but is less effective against the ccb-Trp peptide which adopts a well-structured coiled-coil configuration in its native state prior to fibril formation (154).

At the least two pathways are implicated in αBc phosphorylation: the MAPKAPK2 kinases phosphorylate serine 59 whereas serine 45 may be regulated by p42/p44 MAPK. The kinase involved is the phosphorylation of serine 19 is still unknown (140) (Figure 6).

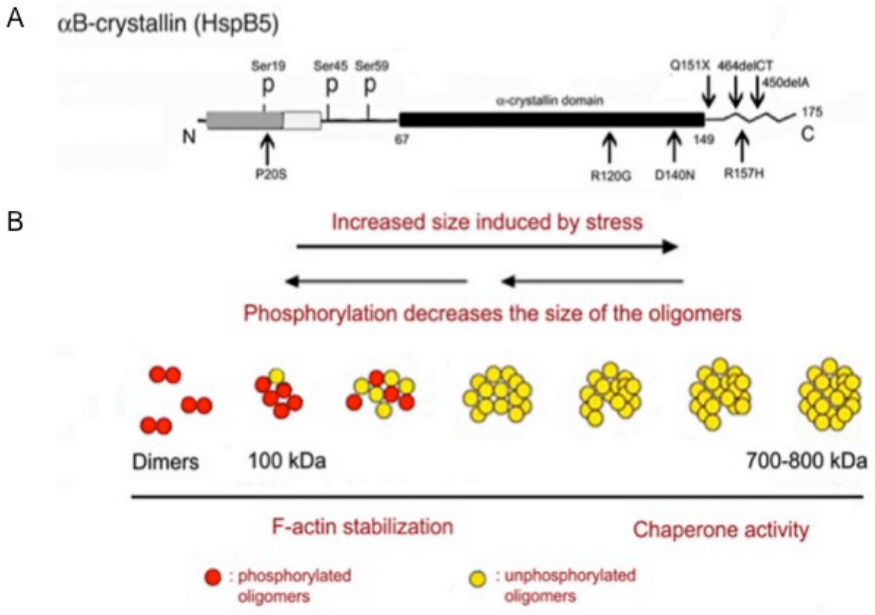

Figure 6. Domain structure and biochemical properties of αB-crystallin (αBc).
A) Light box - conserved region in N-terminus; black box - α-cystallin domain; grey box – WDPF domain; ^^^ - flexible domain; P – phosphorylated serine residues. Arrows indicate positions of point mutations that are responsible for pathologies. B) Biochemical properties of sHsps. Large oligomeric structures are favored under conditions of stress and associate with unfolded proteins. Phosphorylation decreases the size of the oligomers. Large non-phosphorylated oligomers of αBc (and Hsp27) (>300 KDa) can protect cells through their chaperone activity, and small oligomers may act at the level of F-actin polymerization/depolymerization (133).

Mutations in the sHsps, namely in αBc, have been reported in a number of human diseases. Some of these mutations have been found as genes responsible for human degenerative myopathy, cardiomyopathy and congenital cataracts (Table 2). Regarding the myopathies, recent studies have revealed the importance of αBc towards desmin network (148, 155). The majority of mutations found in αBc (and other sHsps) are contained in the conserved α-crystallin domain, suggesting that oligomerization and chaperone function of αBc is impaired (156).

Table 2. Mutations in αBc and the corresponding pathologies. Adapted from (144).

Mutations	Associated Pathologies	Ref
R120G	Myofibrillar myopathy, cardiomyopathy, cataract	(155)
Q151X	Myofibrillar myopathy	(157)
464delCT	Myofibrillar myopathy	(157)
R157H	Cardiomyopathy	(158)
PS20S	Cataract	(159)
D140N	Cataract	(160)
450delA	Cataract	(161)

The crystal structures of αBc and other sHsps may provide insights into understanding how some of these mutations have pathological consequences (162).

In the absence of αBc, knockout mice show normal lens development and age-related degeneration of skeletal muscle, but otherwise have no overt phenotype (163). A recent study however show αBc -/- mice to be more susceptible to experimental autoimmune encephalomyelitis (EAE) - mouse model of Multiple Sclerosis (MS), with an increase in inflammation and glial apoptosis (153). This study enlightens the anti-inflammatory properties of αBc and suggested its therapeutic effect in autoimmune diseases. In addition, αBc has anti-apoptotic functions through its potential interactions with the p53 and caspase-3 pathway (164, 165). Its expression is also correlated with TRAIL resistance in a number of human cancer cell lines (166). Several studies have highlighted αBc antioxidant properties and its role in preventing oxidative stress, αBc was able to reduce the levels of hydrogen peroxide (H_2O_2) on a study in C6 astroglioma cell lines (167). In addition, an oligomer of αBc was reported to bind Cu^{2+} with close to picomolar affinity and to sequester a large number (~150) of Cu^{2+} ions. Therefore acting like a "Cu^{2+} sponge", αBc has been shown to inhibit Cu^{2+}- induced oxidation of ascorbate and hence preventing the production of oxygen species (168). Due to the diverse protective properties of αBc, intensive research has shown the role of endogenous αBc in various pathologies (147). However, recent studies have used recombinant αBc and its peptides as therapeutic agents for diseases including neurodegenerative diseases, myopathies, inflammation, stroke, retinal pathology, platelet

aggregation, and H_2O_2-injury by transgenic overexpression or exogenous administration using *in vivo* and in *vitro* models (132, 133, 147).

Whether or not the endogenous release of αBc from cells occurs is still unclear. The primary sequence of αBc does not have a peptide signal sequence and therefore whether αBc can be secreted remains in debate. Nevertheless, several studies have reported the extracellular presence of several sHsp (169–171). Interestingly, extracellular lipoprotein drusen deposits and the inter-photoreceptor matrix contain αBc as a component, suggesting an extracellular function for αBc (172). Supporting this data, the apical secretion of αBc was reported in a non-conventional pathway via exosomes in polarized retinal pigment epithelial (RPE) cells (173), and it was also demonstrated that αBc efficiently neutralized extracellular misfolded oligomers and suppressed oligomer-induced toxicity (174). This insight has highlighted the possibility of αBc as novel therapeutic target for HD and other neurodegenerative diseases.

1.7.2.5. αB-cystallin in Neurodegenerative Diseases and other CNS injuries

Mounting evidence over the past two decades suggests that αBc may not only play a role in maintaining a healthy body, but that they also have protective functions in disease or injury to the central nervous system (CNS) (132, 133, 175).

Important findings and support to my thesis work resulted from a study conducted in a mouse model of Alexander disease (AxD), a primary disorder of astrocytes caused by dominant mutations in the GFAP gene. In this study, loss of αBc led to increased mortality, while overexpression of αBc rescued animals from terminal seizures (176). Remarkably, in this model, restoration of αBc expression through the GFAP promoter reversed this lethal outcome, showing the rescue effect is astrocyte-specific. Overexpression of αBc results in a markedly reduced CNS stress response, restores expression of the glutamate transporter Glt1 (EAAT2), and protects these animals from death (176, 177). Several other studies reporting the therapeutic and protective role of αBc in devastating neurological disorders and other CNS injuries has been widely studied (Table 3).

Table 3. Therapeutic role of αBc in neurological disorders and other CNS injuries.

Disease	Model	Delivery/ Administration Route	Therapeutic Efficiency	Ref
Huntington's Parkinson's diseases	WT and gmr Q92, UAS- α syn Transgenic (Tg) Drosophila model	P element-mediated germ line transformation with pUAS-αBc-HA	Suppressed compound eye: degeneration induced by polyQ & α- synuclein-induced rough eye phenotype	(178)
Alexander's disease	GFAPTg and GFAP+/R236H mouse model of Multiple sclerosis	αBc over expression under GFAP promoter	Reduced CNS stress response, restored expression of the Glt1 Protected mice from terminal seizures – death	(179)
Parkinson disease, CNS inflammation	Drd2-null mice, Drd2hGFAP cKO, cultured astrocytes, and Parkinson disease mouse	αBC over expression under GFAP promoter in Drd2-null mice, and αBc over expression in cultured astrocytes null for Drd2.	Suppressed the proinflammatory mediators like IL-1β, IL-2, IL-6, IFN-γ, and IL-12β Suppressed	(180)
Alzheimer's disease	Tg2576 Mouse model of AD	CRYAB-/-;HSPB2-/- (αBc/HspB2 null mice) in AD	Severed impaired locomotion Exacerbation of protein aggregation in CRYAB-/-;HSPB2-/-; Tg2576 mice	(181)
Multiple sclerosis (MS)	EAE Mouse model of MS	Intraperitoneum	Decreased clinical score when administered at peak of disease, Reduced apoptosis in CNS	(182–184)
Brain Stroke	WT and CRYAB−/− mouse	Intraperitoneum	Reduced both stroke volume and inflammatory cytokines associated with stroke	(185)
Ischemic injury Myocardial	Adult and neonatal Rat	Viral vector	Protected against ischemic injury	
Spinal cord contusion injury	Mouse	Intravenous	Improvement in locomotor skills, amelioration of secondary tissue damage. Modulation of inflammatory response	(186)
H_2O_2 induced injury (Oxidative stress)	Human lens epithelial (HLE) cells	Pretreatment of HLE cells with gC-CPP tagged αBC (gC-αBC) and TAT fused αBC (TAT-αBC) separately.	Protected the HLE cells from oxidative stress induced cell death.	(187)
Endothelial injury & platelet aggregation	Human platelet rich plasma (PRP) and hamster	Incubation of PRP with αBC Intracellular	Reduced thrombin-induced calcium influx and phosphoinositide hydrolysis by phospholipase C in human platelets	(188)
Optic nerve crush Endothelial	Rat	Intravenous	Increased the number of retinal ganglion cells (RGCs), decreased the number of retinal microglial cells (RMCs), and decreased the protein expression of TNF-α, iNOS. Reduced	(189)

CNS: central nervous system; Drd2: dopamine D2 receptor; EAE: experimental autoimmune encephalomyelitis; GFAP: glial fibrillary acidic protein; RGC: retinal ganglion cells.

Because of the beneficial effects of αBc in many neurodegenerative diseases and other pathologies as well, αBc is a molecule of great interest in the field. In the context of HD, the main focus for this study, αBc has show neuroprotective effects on different polyQ proteins: it has prevented the *in vitro* aggregation of ataxin-3 (190), and it has supressed the mHtt-induced toxicity in mice lens (191). In more detail, expression of the mHtt fragments 46Q and 72Q in mice lacking this major lens chaperone, αBc, markedly accelerated the onset and severity of aggregation, leading to cataracts. This demonstrated that the endogenous chaperone activity of αBc suppresses aggregation *in vivo* (191).

In addition, studies conducted in a transgenic Drosophila model have shown that αBc overexpression suppressed both polyQ-induced compound-eye degeneration and α-synuclein-induced rough-eye phenotype, suggesting a protective role for αBc in HD and Parkinson's diseases (178).

Although many studies have examined the expression and modulation of αBc in neurological diseases, to date the potential neuroprotective role of αBc has not been tested *in vivo* in a mouse model of HD. Hence, this thesis will focus on deciphering the role of αBc in the progression of the disease of the BACHD mouse model of HD.

1.8. References

1. Huntington,G. (1872) On Chorea. *Med Surg Rep*, **26**, 317–321.
2. Huntington,G. (2003) On chorea. *J. Neuropsychiatry Clin. Neurosci.*, **15**, 109–112.
3. Gusella J.F., Wexler, N.S., Conneally, P.M., et al (1983) A polymorphic DNA marker genetically linked to Huntington's disease. *Nature*, **306**, 234–238.
4. Lione,L.A., Carter,R.J., Hunt,M.J., Bates,G.P., Morton,A.J. and Dunnett,S.B. (1999) Selective Discrimination Learning Impairments in Mice Expressing the Human Huntington ' s Disease Mutation. **19**, 10428–10437.
5. Finkbeiner,S. (2011) Huntington's disease. *Cold Spring Harb. Perspect. Biol.*, **3**, 1–24.
6. Mangiarini L., Sathasivam K., Seller M., Cozens, B., Harper, A., Hetherington, C., Lawton, M., Trottier, Y., Lehrach, H., Davies, S.W., Bates, G.P. (1996) Exon 1 of the HD gene with an expanded CAG repeat is sufficient to cause a progressive neurological phenotype in transgenic mice. *Cell*, **87(3)**, 493–506.
7. DiFiglia,M., Sapp,E., Chase,K.O., Davies,S.W., Bates,G.P., Vonsattel,J.P. and Aronin,N. (1997) Aggregation of huntingtin in neuronal intranuclear inclusions and dystrophic neurites in brain. *Science*, **277**, 1990–1993.
8. Davies, S.W., Turmaine, M., Cozens, B.A., DiFiglia, M., Sharp, A.H., Ross, C.A., Scherzinger, E., Wanker, E.E., Mangiarini, L., Bates,G.P. (1997) Formation of neuronal intranuclear inclusions underlies the neurological dysfunction in mice transgenic for the HD mutation. *Cell*, **90**, 537–548.
9. Fisher, E. R. & Hayden,M.R. (2014) Multisource ascertainment of Huntington disease in Canada:

prevalence and population at risk. *Mov. Disord.*, **29**, 105–114.
10. Evans, S. J. W., et al. (2013) Prevalence of adult Huntington's disease in the UK based on diagnoses recorded in general practice records. *J. Neurol. Neurosurg. Psychiatry*, **84**, 1156–1160.
11. Paradisi, I., Hernández, A., Arias,S. (2008) Huntington disease mutation in Venezuela: age of onset, haplotype analyses and geographic aggregation. *J Hum Genet*, **53**, 127–35.
12. Lawrence,A.D., Sahakian,B.J., Hodges,J.R., Rosser,A.E., Lange,K.W. and Robbins,T.W. (1996) Executive and mnemonic functions in early Huntington's disease. *Brain*, **119**, 1633–1645.
13. Paulsen,J.S., Ready,R.E., Hamilton,J.M., Mega,M.S. and Cummings,J.L. (2001) Neuropsychiatric aspects of Huntington's disease. *J. Neurol. Neurosurg. Psychiatry*, **71**, 310–4.
14. Zuccato,C., Valenza,M. and Cattaneo,E. (2010) Molecular Mechanisms and Potential Therapeutical Targets in Huntington ' s Disease. *Physiol. Rev*, 10.1152/physrev.00041.2009.
15. Walker,F.O. (2007) Huntington ' s disease. *Lancet*, **369**, 218–228.
16. Thompson,J.C., Ph,D., Harris,J., Sc,B., Sollom,A.C., Stopford,C.L., Howard,E., Snowden,J.S., Craufurd,D. and Sc,M. (2012) Longitudinal Evaluation of Neuropsychiatric Symptoms in Huntington ' s Disease. *J Neuropsychiatry Clin Neurosci*.
17. Vonsattel, Jean Paul,D.M. (1998) Hungtington's disease. *J. Neuropathol. Exp. Neurol.*
18. Sturrock, A., Leavitt,B.R. (2010) The clinical and genetic features of Huntington disease 23(4):243–59 22. *J Geriatr Psychiatry Neurol*, **23**, 243–59 22.
19. Hamilton,J.M., Salmon,D.P., Corey-Bloom,J., Gamst, a, Paulsen,J.S., Jerkins,S., Jacobson,M.W. and Peavy,G. (2003) Behavioural abnormalities contribute to functional decline in Huntington's disease. *J. Neurol. Neurosurg. Psychiatry*, **74**, 120–122.
20. Politis, M., Pavese, N., Tai, Y.F., Tabrizi, S.J, Barker, R.A., Piccini,P. (2008) Hypothalamic involvement in Huntington's disease: an in vivo PET study. *Brain*, **131**, 2860–2869.
21. Farrer,L. (1986) Suicide and attempted suicide in Huntington disease: implications for preclinical testing of persons at risk. *Am J Med Genet*, **24**, 305–311.
22. Paulsen, J.S., Hoth, K.F., Nehl , C., Stierman,L. (2012) Critical Periods of Suicide Risk in Huntington ' s Disease. *Am J Psychiatry*, **162**, 725–731.
23. Project,T.U.S. –Venezuel. C.R. and Wexler,N.S. (2004) Venezuelan kindreds reveal that genetic and environmental factors modulate Huntington's disease age of onset. *Proc. Natl. Acad. Sci. United States Am.* , **101**, 3498–3503.
24. Rubinsztein, D.C., Leggo, J., Coles, R., et al (1996) Phenotypic characterization of individuals with 30-40 CAG repeats in the Huntington disease (HD) gene reveals HD cases with 36 repeats and apparently normal elderly individuals with 36-39 repeats. *Am J Hum Genet*, **59**, 16–35.
25. Gayán,J., Brocklebank,D., Andresen,J.M., Alkorta-Aranburu,G., Cader,M.Z., Roberts,S. a., Cherny,S.S., Wexler,N.S., Cardon,L.R. and Housman,D.E. (2008) Genomewide linkage scan reveals novel loci modifying age of onset of Huntington's disease in the Venezuelan HD kindreds. *Genet. Epidemiol.*, **32**, 445–453.
26. Bates,G.P., Dorsey,R., Gusella,J.F., Hayden,M.R., Kay,C., Leavitt,B.R., Nance,M., Ross,C. a., Scahill,R.I., Wetzel,R., *et al.* (2015) Huntington disease. *Nat. Rev. Dis. Prim.*, **1**, 1–21.
27. Björkqvist,M., Wild,E.J., Thiele,J., Silvestroni,A., Andre,R., Lahiri,N., Raibon,E., Lee,R. V, Benn,C.L., Soulet,D., *et al.* (2008) A novel pathogenic pathway of immune activation detectable before clinical onset in Huntington's disease. *J. Exp. Med.*, **205**, 1869–77.
28. Sathasivam,K., Hobbs,C., Mangiarini,L., Mahal, a, Turmaine,M., Doherty,P., Davies,S.W. and Bates,G.P. (1999) Transgenic models of Huntington's disease. *Philos. Trans. R. Soc. Lond. B. Biol. Sci.*, **354**, 963–969.
29. Vonsattel,J.P., Myers,R.H., Stevens,T.J., Ferrante,R.J., Bird,E.D. and Richardson Jr.,E.P. (1985) Neuropathological classification of Huntington's disease. *J Neuropathol Exp Neurol*, **44**, 559–577.
30. Cowan,C.M. and Raymond,L.A. (2006) Selective Neuronal Degeneration in Huntington's Disease. *Curr. Top. Dev. Biol.*, **75**, 25–71.
31. Reiner,A., Albin,R.L., Anderson,K.D., D'Amato,C.J., Penney,J.B. and Young,A.B. (1988)

Differential loss of striatal projection neurons in Huntington disease. *Proc. Natl. Acad. Sci. U. S. A.*, **85**, 5733–7.
32. Albin,R., Reiner,A., Anderson,K.D., Dure,L.S., Handelin,B., Balfour,R., Whetsell,W.O., Penney,J.B. and Young, a B. (1992) Preferential loss of striato-external pallidal projection neurons in presymptomatic Huntington's disease. *Ann. Neurol.*, **31**, 425–430.
33. Albin,R.L. and Tagle,D.A. (1995) Genetics and molecular biology of Huntington's disease. *Trends Neurosci.*, **18**, 11–14.
34. Albin,R.L., Reiner,A., Anderson,K.D., Penney,J.B. and Young,A.B. (1990) Striatal and nigral neuron subpopulations in rigid Huntington's disease: Implications for the functional anatomy of chorea and rigidity-akinesia. *Ann. Neurol.*, **27**, 357–365.
35. Ehrlich,M.E. (2012) Huntington's disease and the striatal medium spiny neuron: cell-autonomous and non-cell-autonomous mechanisms of disease. *Neurotherapeutics*, **9**, 270–84.
36. Van Raamsdonk,J.M., Pearson,J., Slow,E.J., Hossain,S.M., Leavitt,B.R. and Hayden,M.R. (2005) Cognitive dysfunction precedes neuropathology and motor abnormalities in the YAC128 mouse model of Huntington's disease. *J. Neurosci.*, **25**, 4169–80.
37. Steffan,J.S., Agrawal,N., Pallos,J., Rockabrand,E., Trotman,L.C., Slepko,N., Illes,K., Lukacsovich,T., Zhu,Y.-Z., Cattaneo,E., *et al.* (2004) SUMO modification of Huntingtin and Huntington's disease pathology. *Science*, **304**, 100–104.
38. Cornett,J., Cao,F., Wang,C.-E., Ross,C. a, Bates,G.P., Li,S.-H. and Li,X.-J. (2005) Polyglutamine expansion of huntingtin impairs its nuclear export. *Nat. Genet.*, **37**, 198–204.
39. Neuwald,A.F. and Hirano,T. (2000) HEAT repeats associated with condensins, cohesins, and other complexes involved in chromosome-related functions. *Genome Res.*, **10**, 1445–1452.
40. Andrade,M.A., Petosa,C., O'Donoghue,S.I., Müller,C.W. and Bork,P. (2001) Comparison of ARM and HEAT protein repeats. *J. Mol. Biol.*, **309**, 1–18.
41. Giacomello,M., Hudec,R. and Lopreiato,R. (2011) Huntington's disease, calcium, and mitochondria. *BioFactors*, **37**, 206–218.
42. Li,S.H. and Li,X.J. (2004) Huntingtin-protein interactions and the pathogenesis of Huntington's disease. *Trends Genet.*, **20**, 146–154.
43. Landwehrmeyer,G.B., McNeil,S.M., Dure IV,L.S., Ge,P., Aizawa,H., Huang,Q., Ambrose,C.M., Duyao,M.P., Bird,E.D., Bonilla,E., *et al.* (1995) Huntington's disease gene: Regional and cellular expression in brain of normal and affected individuals. *Ann. Neurol.*, **37**, 218–230.
44. Sapp,E., Schwarz,C., Chase,K., Bhide,P.G., Young,A.B., Penney,J., Vonsattel,J.P., Aronin,N. and DiFiglia,M. (1997) Huntingtin localization in brains of normal and Huntington's disease patients. *Ann. Neurol.*, **42**, 604–612.
45. Strong,T. V, Tagle,D. a, Valdes,J.M., Elmer,L.W., Boehm,K., Swaroop,M., Kaatz,K.W., Collins,F.S. and Albin,R.L. (1993) Widespread expression of the human and rat Huntington's disease gene in brain and nonneural tissues. *Nat. Genet.*, **5**, 259–265.
46. DiFiglia,M., Sapp,E., Chase,K., Schwarz,C., Meloni, a, Young,C., Martin,E., Vonsattel,J.P., Carraway,R. and Reeves,S. a (1995) Huntingtin is a cytoplasmic protein associated with vesicles in human and rat brain neurons. *Neuron*, **14**, 1075–81.
47. Gutekunst,C. a, Levey, a I., Heilman,C.J., Whaley,W.L., Yi,H., Nash,N.R., Rees,H.D., Madden,J.J. and Hersch,S.M. (1995) Identification and localization of huntingtin in brain and human lymphoblastoid cell lines with anti-fusion protein antibodies. *Proc. Natl. Acad. Sci. U. S. A.*, **92**, 8710–8714.
48. Kegel,K.B., Meloni,A.R., Yi,Y., Kim,Y.J., Doyle,E., Cuiffo,B.G., Sapp,E., Wang,Y., Qin,Z.H., Don Chen,J., *et al.* (2002) Huntingtin is present in the nucleus, interacts with the transcriptional corepressor C-terminal binding protein, and represses transcription. *J. Biol. Chem.*, **277**, 7466–7476.
49. Borrell-Pagès, M., Zala, D., Humbert, S., Saudou,F. (2006) Huntington's disease: from huntingtin function and dysfunction to therapeutic strategies. *Cell Mol Life Sci*, **63**, 2642–60.
50. Landles,C. and Bates,G.P. (2004) Huntingtin and the molecular pathogenesis of Huntington's

disease. Fourth in molecular medicine review series. *EMBO Rep.*, **5**, 958–63.
51. Macdonald,M.E., Duyao,M., Calzonetti,T., Auerbach,A., Ryan,A., Barnes,G., White,J.K., Auerbach,W., Vonsattel,J.P., Gusella,J.F., *et al.* (1996) Targeted inactivation of the mouse Huntington's disease gene homolog Hdh. In *Cold Spring Harbor Symposia on Quantitative Biology*.Vol. 61, pp. 627–638.
52. Barnes,G.T., Duyao,M.P., Ambrose,C.M., McNeil,S., Persichetti,F., Srinidhi,J., Gusella,J.F. and MacDonald,M.E. (1994) Mouse Huntington's disease gene homolog (Hdh). *Somat. Cell Mol. Genet.*, **20**, 87–97.
53. Woda,J.M., Calzonetti,T., Hilditch-Maguire,P., Duyao,M.P., Conlon,R. a and MacDonald,M.E. (2005) Inactivation of the Huntington's disease gene (Hdh) impairs anterior streak formation and early patterning of the mouse embryo. *BMC Dev. Biol.*, **5**, 17.
54. Cattaneo, E., Zuccato, C., and Tartari, M. (2005) Normal huntingtin function: an alternative approach to Huntington's disease. *Nat Rev Neurosci*, **6**, 919–930.
55. Leavitt,B.R., Van Raamsdonk,J.M., Shehadeh,J., Fernandes,H., Murphy,Z., Graham,R.K., Wellington,C.L., Raymond,L.A. and Hayden,M.R. (2006) Wild-type huntingtin protects neurons from excitotoxicity. *J. Neurochem.*, **96**, 1121–1129.
56. Rigamonti,D., Bauer,J.H., De-Fraja,C., Conti,L., Sipione,S., Sciorati,C., Clementi,E., Hackam,A., Hayden,M.R., Li,Y., *et al.* (2000) Wild-type huntingtin protects from apoptosis upstream of caspase-3. *J. Neurosci.*, **20**, 3705–13.
57. Rigamonti,D., Sipione,S., Goffredo,D., Zuccato,C., Fossale,E. and Cattaneo,E. (2001) Huntingtin's Neuroprotective Activity Occurs via Inhibition of Procaspase-9 Processing. *J. Biol. Chem.*, **276**, 14545–14548.
58. Zhang,Y., Leavitt,B.R., van Raamsdonk,J.M., Dragatsis,I., Goldowitz,D., MacDonald,M.E., Hayden,M.R. and Friedlander,R.M. (2006) Huntingtin inhibits caspase-3 activation. *EMBO J.*, **25**, 5896–5906.
59. Gauthier,L.R., Charrin,B.C., Borrell-Pagès,M., Dompierre,J.P., Rangone,H., Cordelières,F.P., De Mey,J., MacDonald,M.E., Leßmann,V., Humbert,S., *et al.* (2004) Huntingtin controls neurotrophic support and survival of neurons by enhancing BDNF vesicular transport along microtubules. *Cell*, **118**, 127–138.
60. Zuccato, C., Ciammola, A., Rigamonti, D., Leavitt, B.R., Goffredo, D., Conti, L., MacDonald, M.E., Friedlander, R.M., Silani, V., Hayden, M.R., Timmusk, T., Sipione, S., Cattaneo,E. (2001) Loss of huntingtin-mediated BDNF gene transcription in Huntington's disease. *Science (80-.).*, **293**, 493–498.
61. Zuccato,C., Tartari,M., Crotti,A., Goffredo,D., Valenza,M., Conti,L., Cataudella,T., Leavitt,B.R., Hayden,M.R., Timmusk,T., *et al.* (2003) Huntingtin interacts with REST/NRSF to modulate the transcription of NRSE-controlled neuronal genes. *Nat. Genet.*, **35**, 76–83.
62. Ferrer,I., Goutan,E., Marín,C., Rey,M.. and Ribalta,T. (2000) Brain-derived neurotrophic factor in Huntington disease. *Brain Res.*, **866**, 257–261.
63. Gil,J.M. and Rego,A.C. (2008) Mechanisms of neurodegeneration in Huntington's disease. *Eur. J. Neurosci.*, **27**, 2803–20.
64. Hodgson,J.G., Smith,D.J., McCutcheon,K., Koide,H.B., Nishiyama,K., Dinulos,M.B., Stevens,M.E., Bissada,N., Nasir,J., Kanazawa,I., *et al.* (1996) Human huntingtin derived from YAC transgenes compensates for loss of murine huntingtin by rescue of the embryonic lethal phenotype. *Hum. Mol. Genet.*, **5**, 1875–85.
65. Dragatsis,I., Efstratiadis,A. and Zeitlin,S. (1998) Mouse mutant embryos lacking huntingtin are rescued from lethality by wild-type extraembryonic tissues. *Development*, **125**, 1529–1539.
66. Pennuto,M., Palazzolo,I. and Poletti,A. (2009) Post-translational modifications of expanded polyglutamine proteins: Impact on neurotoxicity. *Hum. Mol. Genet.*, **18**.
67. Gu,X., Greiner,E.R., Mishra,R., Kodali,R., Osmand,A., Finkbeiner,S., Steffan,J.S., Thompson,L.M., Wetzel,R. and Yang,X.W. (2009) Serines 13 and 16 Are Critical Determinants of Full-Length Human Mutant Huntingtin Induced Disease Pathogenesis in HD Mice. *Neuron*,

64, 828–840.
68. Rockabrand,E., Slepko,N., Pantalone,A., Nukala,V.N., Kazantsev,A., Marsh,J.L., Sullivan,P.G., Steffan,J.S., Sensi,S.L. and Thompson,L.M. (2007) The first 17 amino acids of Huntingtin modulate its sub-cellular localization, aggregation and effects on calcium homeostasis. *Hum. Mol. Genet.*, **16**, 61–77.
69. Ehrnhoefer,D.E., Sutton,L. and Hayden,M.R. (2011) Small changes, big impact: posttranslational modifications and function of huntingtin in Huntington disease. *Neuroscientist*, **17**, 475–92.
70. Belloni E, Muenke M, Roessler E, Traverso G, Siegel-Bartelt J, Frumkin A, Mitchell HF, Donis-Keller H, Helms C, Hing AV, Heng HH, Koop B, Martindale D, Rommens JM, Tsui LC,S.S. (1996) Cleavage of huntingtin by apopain, a proaoptotic cysteine protease, is modulated by the polyglutamine tract. *Nat Genet.*, **14**, 353–6.
71. Legleiter,J., Mitchell,E., Lotz,G.P., Sapp,E., Ng,C., DiFiglia,M., Thompson,L.M. and Muchowski,P.J. (2010) Mutant huntingtin fragments form oligomers in a polyglutamine length-dependent manner in Vitro and in Vivo. *J. Biol. Chem.*, **285**, 14777–14790.
72. Miller,J., Arrasate,M., Brooks,E., Libeu,C.P., Legleiter,J., Hatters,D., Curtis,J., Cheung,K., Krishnan,P., Mitra,S., *et al.* (2012) Identifying polyglutamine protein species in situ that best predict neurodegeneration. *Nat. Chem. Biol.*, **8**, 318–318.
73. Arrasate,M., Mitra,S., Schweitzer,E.S., Segal,M.R. and Finkbeiner,S. (2004) Inclusion body formation reduces levels of mutant huntingtin and the risk of neuronal death. *Nature*, **431**, 805–10.
74. Saudou, F., Finkbeiner, S., Devys, D., Greenberg,M.E. (1998) Huntingtin acts in the nucleus to induce apoptosis but death does not correlate with the formation of intranuclear inclusions. *Cell*, **95**, 55–66.
75. Gafni,J., Hermel,E., Young,J.E., Wellington,C.L., Hayden,M.R. and Ellerby,L.M. (2004) Inhibition of calpain cleavage of Huntingtin reduces toxicity: Accumulation of calpain/caspase fragments in the nucleus. *J. Biol. Chem.*, **279**, 20211–20220.
76. Wellington,C.L., Singaraja,R., Ellerby,L., Savill,J., Roy,S., Leavitt,B., Cattaneo,E., Hackam,A., Sharp,A., Thornberry,N., *et al.* (2000) Inhibiting caspase cleavage of huntingtin reduces toxicity and aggregate formation in neuronal and nonneuronal cells. *J. Biol. Chem.*, **275**, 19831–19838.
77. Hackam,A.S., Singaraja,R., Wellington,C.L., Metzler,M., McCutcheon,K., Zhang,T., Kalchman,M. and Hayden,M.R. (1998) The influence of huntingtin protein size on nuclear localization and cellular toxicity. *J. Cell Biol.*, **141**, 1097–1105.
78. Schilling,G., Becher,M.W., Sharp,A.H., Jinnah,H.A., Duan,K., Kotzuk,J.A., Slunt,H.H., Ratovitski,T., Cooper,J.K., Jenkins,N.A., *et al.* (1999) Intranuclear inclusions and neuritic aggregates in transgenic mice expressing a mutant N-terminal fragment of huntingtin. *Hum. Mol. Genet.*, **8**, 397–407.
79. Yu,Z.-X., Li,S.-H., Evans,J., Pillarisetti,A., Li,H. and Li,X.-J. (2003) Mutant huntingtin causes context-dependent neurodegeneration in mice with Huntington's disease. *J. Neurosci.*, **23**, 2193–2202.
80. Ramaswamy,S., Mcbride,J.L. and Kordower,J.H. Animal Models of Huntington's Disease.
81. Hersch,S.M. and Ferrante,R.J. (2004) Translating therapies for Huntington's disease from genetic animal models to clinical trials. *NeuroRx*, **1**, 298–306.
82. Menalled,L. and Brunner,D. (2014) Animal Models of Huntington ' s Disease for Translation to the Clinic : Best Practices ABSTRACT : One Mouse Model Does Not Fit All Needs : Know Your Model. **29**.
83. Heng,M.Y., Detloff,P.J. and Albin,R.L. (2008) Rodent genetic models of Huntington disease. *Neurobiol. Dis.*, **32**, 1–9.
84. Jennifer Morton,A., Rudiger,S.R., Wood,N.I., Sawiak,S.J., Brown,G.C., Mclaughlan,C.J., Kuchel,T.R., Snell,R.G., Faull,R.L.M. and Simon Bawden,C. (2014) Early and progressive circadian abnormalities in Huntington's disease sheep are unmasked by social environment. *Hum. Mol. Genet.*, **23**, 3375–3383.

85. Morton,A.J. and Howland,D.S. (2013) Large genetic animal models of Huntington's Disease. *J. Huntingtons. Dis.*, **2**, 3–19.
86. Yang,S.-H., Cheng,P.-H., Banta,H., Piotrowska-Nitsche,K., Yang,J.-J., Cheng,E.C.H., Snyder,B., Larkin,K., Liu,J., Orkin,J., *et al.* (2008) Towards a transgenic model of Huntington's disease in a non-human primate. *Nature*, **453**, 921–4.
87. Chan,A.W., Xu,Y., Jiang,J., Rahim,T., Zhao,D., Kocerha,J., Chi,T., Moran,S., Engelhardt,H., Larkin,K., *et al.* (2014) A Two Years Longitudinal Study of a Transgenic Huntington Disease Monkey. *BMC Neurosci.*, **15**, 15–36.
88. Wheeler,V.C., Auerbach,W., White,J.K., Srinidhi,J., Auerbach,A., Ryan,A., Duyao,M.P., Vrbanac,V., Weaver,M., Gusella,J.F., *et al.* (1999) Length-dependent gametic CAG repeat instability in the Huntington's disease knock-in mouse. *Hum. Mol. Genet.*, **8**, 115–122.
89. Slow,E.J., van Raamsdonk,J., Rogers,D., Coleman,S.H., Graham,R.K., Deng,Y., Oh,R., Bissada,N., Hossain,S.M., Yang,Y.Z., *et al.* (2003) Selective striatal neuronal loss in a YAC128 mouse model of Huntington disease. *Hum. Mol. Genet.*, **12**, 1555–1567.
90. Van Raamsdonk,J.M., Metzler,M., Slow,E., Pearson,J., Schwab,C., Carroll,J., Graham,R.K., Leavitt,B.R. and Hayden,M.R. (2007) Phenotypic abnormalities in the YAC128 mouse model of Huntington disease are penetrant on multiple genetic backgrounds and modulated by strain. *Neurobiol. Dis.*, **26**, 189–200.
91. Gray,M., Shirasaki,D.I., Cepeda,C., André,V.M., Wilburn,B., Lu,X.-H., Tao,J., Yamazaki,I., Li,S.-H., Sun,Y.E., *et al.* (2008) Full-length human mutant huntingtin with a stable polyglutamine repeat can elicit progressive and selective neuropathogenesis in BACHD mice. *J. Neurosci.*, **28**, 6182–95.
92. Graham,R.K., Slow,E.J., Deng,Y., Bissada,N., Lu,G., Pearson,J., Shehadeh,J., Leavitt,B.R., Raymond,L.A. and Hayden,M.R. (2006) Levels of mutant huntingtin influence the phenotypic severity of Huntington disease in YAC128 mouse models. *Neurobiol. Dis.*, **21**, 444–455.
93. Van Raamsdonk,J.M., Murphy,Z., Slow,E.J., Leavitt,B.R. and Hayden,M.R. (2005) Selective degeneration and nuclear localization of mutant huntingtin in the YAC128 mouse model of Huntington disease. *Hum. Mol. Genet.*, **14**, 3823–3835.
94. Van Raamsdonk,J.M., Metzler,M., Slow,E., Pearson,J., Schwab,C., Carroll,J., Graham,R.K., Leavitt,B.R. and Hayden,M.R. (2007) Phenotypic abnormalities in the YAC128 mouse model of Huntington disease are penetrant on multiple genetic backgrounds and modulated by strain. *Neurobiol. Dis.*, **26**, 189–200.
95. Menalled,L., El-Khodor,B.F., Patry,M., Suárez-Fariñas,M., Orenstein,S.J., Zahasky,B., Leahy,C., Wheeler,V., Yang,X.W., MacDonald,M., *et al.* (2009) Systematic behavioral evaluation of Huntington's disease transgenic and knock-in mouse models. *Neurobiol. Dis.*, **35**, 319–36.
96. Pouladi,M. a, Stanek,L.M., Xie,Y., Franciosi,S., Southwell,A.L., Deng,Y., Butland,S., Zhang,W., Cheng,S.H., Shihabuddin,L.S., *et al.* (2012) Marked differences in neurochemistry and aggregates despite similar behavioural and neuropathological features of Huntington disease in the full-length BACHD and YAC128 mice. *Hum. Mol. Genet.*, **21**, 2219–32.
97. Lee,J.M., Pinto,R.M., Gillis,T., St. Claire,J.C. and Wheeler,V.C. (2011) Quantification of age-dependent somatic CAG repeat instability in Hdh CAG knock-in mice reveals different expansion dynamics in striatum and liver. *PLoS One*, **6**.
98. Gusella,J.F. and MacDonald,M.E. (2006) Huntington's disease: seeing the pathogenic process through a genetic lens. *Trends Biochem. Sci.*, **31**, 533–540.
99. Shelbourne,P.F., Killeen,N., Hevner,R.F., Johnston,H.M., Tecott,L., Lewandoski,M., Ennis,M., Ramirez,L., Li,Z., Iannicola,C., *et al.* (1999) A Huntington's disease CAG expansion at the murine Hdh locus is unstable and associated with behavioural abnormalities in mice. *Hum. Mol. Genet.*, **8**, 763–774.
100. White,J.K., Auerbach,W., Duyao,M.P., Vonsattel,J.P., Gusella,J.F., Joyner,A.L. and MacDonald,M.E. (1997) Huntingtin is required for neurogenesis and is not impaired by the Huntington's disease CAG expansion. *Nat. Genet.*, **17**, 404–10.

101. Wheeler,V.C., Persichetti,F., McNeil,S.M., Mysore,J.S., Mysore,S.S., MacDonald,M.E., Myers,R.H., Gusella,J.F. and Wexler,N.S. (2007) Factors associated with HD CAG repeat instability in Huntington disease. *J. Med. Genet.*, **44**, 695–701.
102. Xia,J., Lee,D.H., Taylor,J., Vandelft,M. and Truant,R. (2003) Huntingtin contains a highly conserved nuclear export signal. *Hum. Mol. Genet.*, **12**, 1393–1403.
103. Hickey,M.A., Zhu,C., Medvedeva,V., Lerner,R.P., Patassini,S., Franich,N.R., Maiti,P., Frautschy,S.A., Zeitlin,S., Levine,M.S., *et al.* (2012) Improvement of neuropathology and transcriptional deficits in CAG 140 knock-in mice supports a beneficial effect of dietary curcumin in Huntington's disease. *Mol. Neurodegener.*, **7**, 12.
104. Lin,C.H., Tallaksen-Greene,S., Chien,W.M., Cearley,J.A., Jackson,W.S., Crouse,A.B., Ren,S., Li,X.J., Albin,R.L. and Detloff,P.J. (2001) Neurological abnormalities in a knock-in mouse model of Huntington's disease. *Hum. Mol. Genet.*, **10**, 137–44.
105. Heng,M.Y., Tallaksen-Greene,S.J., Detloff,P.J. and Albin,R.L. (2007) Longitudinal evaluation of the Hdh(CAG)150 knock-in murine model of Huntington's disease. *J. Neurosci.*, **27**, 8989–98.
106. Luthi-Carter, R., Hanson, S.A., Strand, A.D., Bergstrom, D.A., Chun, W., Peters, N.L., Woods, A.M., Chan, E.Y., Kooperberg, C., Krainc, D., Young, A.B., Tapscott, S.J., Olson,J.M. (2002) Dysregulation of gene expression in the R6/2 model of polyglutamine disease: parallel changes in muscle and brain. *Hum. Mol. Genet.*, **11**, 1911–1926.
107. Tallaksen-Greene,S.J., Crouse,A.B., Hunter,J.M., Detloff,P.J. and Albin,R.L. (2005) Neuronal intranuclear inclusions and neuropil aggregates in Hdh CAG(150) knockin mice. *Neuroscience*, **131**, 843–852.
108. Group,H.S. (1996) Unified Huntington's Disease Rating Scale: reliability and consistency. *Huntingt. Study Group. Mov. Disord.*, **11**, 136–142.
109. Group,H.S. (2006) Tetrabenazine as antichorea therapy in Huntington disease: a randomized controlled trial. *Neurology*, **66**, 366–372.
110. Frank,S. (2010) Tetrabenazine: the first approved drug for the treatment of chorea in US patients with Huntington disease. *Neuropsychiatr Dis Treat*, **6**, 657–665.
111. Jankovic, J. & Roos,R.A.C. (2014) Chorea associated with Huntington's disease: to treat or not to treat? *Mov. Disord.*, **29**, 1414–1418.
112. Gonzalez,V. et al. (2014) Deep brain stimulation for Huntington's disease: long-term results of a prospective open-label study. *J. Neurosurg.*, **121**, 114–122.
113. Pfizer (2014) Study evaluating the safety, tolerability and brain function of 2 doses of PF-02545920 in subjects with early Huntington's disease. *[online], https//www. Clin.*
114. First time use of SD-809 in Huntington disease (first-HD) (2014) *[online], https://clinicaltrials.gov/ct2/show/ NCT01795859*.
115. Mestre, T. A. & Ferreira,J.J. (2012) An evidence-based approach in the treatment of Huntington's disease. *Park. Relat. Disord.*, **18**, 316–320.
116. Bonelli, R. M. & Hofmann,P. (2007) A systematic review of the treatment studies in Huntington's disease since 1990. *Expert Opin. Pharmacother.*, **8**, 141–153.
117. Groves,M., Van Duijn,E., Anderson,K., Craufurd,D., Guttman, M., Edmondson,M., Van Kammen,D., Giuliano, J., Perlman, S., Burgunder,J.-M., Goodman,N. and Goodman,L. (2012) International survey-based algorithms for the pharmacological treatment of irritability and perseverative behaviors in huntington's disease. *Neurotherapeutics*, **9**, 227.
118. Wild, E. J. & Tabrizi,S.J. (2014) Targets for future clinical trials in Huntington's disease: what's in the pipeline? *Mov. Disord.*, **29**, 1434–1445.
119. Labbadia,J. and Morimoto,R.I. (2014) The Biology of Proteostasis in Aging and Disease. *Annu. Rev. Biochem.*, **84**, 150317182619002.
120. Valastyan,J.S. and Lindquist,S. (2014) Mechanisms of protein-folding diseases at a glance. *Dis. Model. Mech.*, **7**, 9–14.
121. Lindquist,S. (1986) THE HEAT-SHOCK RESPONSE. *Ann. Rev. Biochem.*, **55**, 1151–91.
122. Arrasate,M., Finkbeiner, S. Protein aggregates in Huntington's disease. *Exp Neurol*, **238**, 1–11.

123. Jansen,A.H.P., Reits,E. a J. and Hol,E.M. (2014) The ubiquitin proteasome system in glia and its role in neurodegenerative diseases. *Front. Mol. Neurosci.*, **7**, 73.
124. Carver,J.A., Rekas,A., Thorn,D.C. and Wilson,M.R. (2003) Review Article Small Heat-shock Proteins and Clusterin : Intra- and Extracellular Molecular Chaperones with a Common Mechanism of Action and Function ? *IUBMB Life*, **55**, 661–668.
125. Quraishe,S., Asuni,A., Boelens,W.C., O'Connor,V. and Wyttenbach,A. (2008) Expression of the small heat shock protein family in the mouse CNS: Differential anatomical and biochemical compartmentalization. *Neuroscience*, **153**, 483–491.
126. Muchowski,P.J., Schaffar,G., Sittler, a, Wanker,E.E., Hayer-Hartl,M.K. and Hartl,F.U. (2000) Hsp70 and hsp40 chaperones can inhibit self-assembly of polyglutamine proteins into amyloid-like fibrils. *Proc. Natl. Acad. Sci. U. S. A.*, **97**, 7841–6.
127. Vacher,C., Garcia-Oroz,L. and Rubinsztein,D.C. (2005) Overexpression of yeast hsp104 reduces polyglutamine aggregation and prolongs survival of a transgenic mouse model of Huntington's disease. *Hum. Mol. Genet.*, **14**, 3425–3433.
128. Lindberg,I., Shorter,J., Wiseman,R.L., Chiti,F., Dickey,C. a and McLean,P.J. (2015) Chaperones in Neurodegeneration. *J. Neurosci.*, **35**, 13853–9.
129. Saibil,H. (2000) Molecular chaperones: Containers and surfaces for folding, stabilising or unfolding proteins. *Curr. Opin. Struct. Biol.*, **10**, 251–258.
130. Saibil,H. (2013) Chaperone machines for protein folding, unfolding and disaggregation. *Nat. Rev. Mol. Cell Biol.*, **14**, 630–642.
131. Bruford,E., Lush,M.J., Wright,M.W., Sneddon,T.P., Povey,S. and Birney,E. (2008) The HGNC database in 2008: A resource for the human genome. *Nucleic Acids Res.*, **36**.
132. Brownell,S.E., Becker,R.A. and Steinman,L. (2012) The protective and therapeutic function of small heat shock proteins in neurological diseases. *Front. Immunol.*, **3**, 1–10.
133. Arrigo,A.-P., Simon,S., Gibert,B., Kretz-Remy,C., Nivon,M., Czekalla,A., Guillet,D., Moulin,M., Diaz-Latoud,C. and Vicart,P. (2007) Hsp27 (HspB1) and alphaB-crystallin (HspB5) as therapeutic targets. *FEBS Lett.*, **581**, 3665–74.
134. Clark,J.I. and Muchowski,P.J. (2000) Small heat-shock proteins and their potential role in human disease. *Curr. Opin. Struct. Biol.*, **10**, 52–9.
135. Kappé, G., Franck, E., Verschuure, P., Boelens, W. C., Leunissen, J. A., and de Jong,W.W. (2003) The human genome encodes 10 alpha-crystallin-related small heat shock proteins: HspB1-10. *Cell Stress Chaperones*, **8**, 53–61.
136. Horwitz,J. (2003) Alpha-crystallin. *Exp. Eye Res.*, **76**, 145–153.
137. Ecroyd,H. and Carver,J. a (2009) Crystallin proteins and amyloid fibrils. *Cell. Mol. Life Sci.*, **66**, 62–81.
138. Horwitz,J., Bova,M.P., Ding,L.L., Haley,D. a and Stewart,P.L. (1999) Lens alpha-crystallin: function and structure. *Eye (Lond).*, **13 (Pt 3b**, 403–408.
139. Horwitz,J. (1992) Alpha-crystallin can function as a molecular chaperone. *Proc. Natl. Acad. Sci. U. S. A.*, **89**, 10449–53.
140. Ecroyd,H. and Carver,J.A. (2009) Review Crystallin proteins and amyloid fibrils. **66**, 62–81.
141. Morrow,G., Hightower,L.E. and Tanguay,R.M. (2015) Small heat shock proteins: big folding machines. *Cell Stress Chaperones*, **20**, 207–212.
142. Narberhaus,F. (2002) Alpha-crystallin-type heat shock proteins: socializing minichaperones in the context of a multichaperone network. *Microbiol. Mol. Biol. Rev.*, **66**, 64–93; table of contents.
143. Garrido,C., Paul,C., Seigneuric,R. and Kampinga,H.H. (2012) The small heat shock proteins family: the long forgotten chaperones. *Int. J. Biochem. Cell Biol.*, **44**, 1588–92.
144. Arrigo,A.P., Simon,S., Gibert,B., Kretz-Remy,C., Nivon,M., Czekalla,A., Guillet,D., Moulin,M., Diaz-Latoud,C. and Vicart,P. (2007) Hsp27 (HspB1) and αB-crystallin (HspB5) as therapeutic targets. *FEBS Lett.*, **581**, 3665–3674.
145. Klemenz,R., Fröhli,E., Steiger,R.H., Schäfer,R. and Aoyama,A. (1991) Alpha B-crystallin is a

small heat shock protein. *Proc. Natl. Acad. Sci. U. S. A.*, **88**, 3652–6.
146. Iwaki,T., Wisniewski,T., Iwaki, a, Corbin,E., Tomokane,N., Tateishi,J. and Goldman,J.E. (1992) Accumulation of alpha B-crystallin in central nervous system glia and neurons in pathologic conditions. *Am. J. Pathol.*, **140**, 345–56.
147. Reddy,V.S. and Reddy,G.B. (2015) Emerging Role for α B-Crystallin as a Therapeutic Agent : Pros and Cons.
148. Elliott,J.L., Der Perng,M., Prescott,A.R., Jansen,K. a, Koenderink,G.H. and Quinlan,R. a (2013) The specificity of the interaction between αB-crystallin and desmin filaments and its impact on filament aggregation and cell viability. *Philos. Trans. R. Soc. Lond. B. Biol. Sci.*, **368**, 20120375.
149. Almeida-Souza,L., Asselbergh,B., d'Ydewalle,C., Moonens,K., Goethals,S., de Winter,V., Azmi,A., Irobi,J., Timmermans,J.-P., Gevaert,K., *et al.* (2011) Small heat-shock protein HSPB1 mutants stabilize microtubules in Charcot-Marie-Tooth neuropathy. *J. Neurosci.*, **31**, 15320–8.
150. Ghosh,J.G., Houck,S.A. and Clark,J.I. (2008) Interactive sequences in the molecular chaperone, human alphaB crystallin modulate the fibrillation of amyloidogenic proteins. *Int. J. Biochem. Cell Biol.*, **40**, 954–67.
151. den Engelsman,J., Keijsers,V., de Jong,W.W. and Boelens,W.C. (2003) The small heat-shock protein alpha B-crystallin promotes FBX4-dependent ubiquitination. *J. Biol. Chem.*, **278**, 4699–704.
152. Pountney,D.L., Treweek,T.M., Chataway,T., Huang,Y., Chegini,F., Blumbergs,P.C., Raftery,M.J. and Gai,W.P. (2005) ??B-Crystallin is a major component of glial cytoplasmic inclusions in multiple system atrophy. *Neurotox. Res.*, **7**, 77–85.
153. Ito, H., Okamoto, K., Nakayama, H., et al. (1997) Phosphorylation of alphaB-crystallin in response to various types of stress. *J Biol Chem*, **272**, 29934–41.
154. Ecroyd,H. and Carver,J. a (2008) The effect of small molecules in modulating the chaperone activity of alphaB-crystallin against ordered and disordered protein aggregation. *FEBS J.*, **275**, 935–47.
155. Bova,M.P., Yaron,O., Huang,Q., Ding,L., Haley,D. a, Stewart,P.L. and Horwitz,J. (1999) Mutation R120G in alphaB-crystallin, which is linked to a desmin-related myopathy, results in an irregular structure and defective chaperone-like function. *Proc. Natl. Acad. Sci. U. S. A.*, **96**, 6137–6142.
156. Rajasekaran,N.S., Connell,P., Christians,E.S., Yan,L.J., Taylor,R.P., Orosz,A., Zhang,X.Q., Stevenson,T.J., Peshock,R.M., Leopold,J. a., *et al.* (2007) Human αB-Crystallin Mutation Causes Oxido-Reductive Stress and Protein Aggregation Cardiomyopathy in Mice. *Cell*, **130**, 427–439.
157. Selcen,D. and Engel, a G. (2003) Myofibrillar myopathy caused by novel dominant negative alpha B- crystallin mutations. *Ann Neurol*, **54**, 804–810.
158. Inagaki,N., Hayashi,T., Arimura,T., Koga,Y., Takahashi,M., Shibata,H., Teraoka,K., Chikamori,T., Yamashina,A. and Kimura,A. (2006) αB-crystallin mutation in dilated cardiomyopathy. *Biochem. Biophys. Res. Commun.*, **342**, 379–386.
159. Liu,M., Ke,T., Wang,Z., Yang,Q., Chang,W., Jiang,F., Tang,Z., Li,H., Ren,X., Wang,X., *et al.* (2006) Identification of a CRYAB mutation associated with autosomal dominant posterior polar cataract in a Chinese family. *Investig. Ophthalmol. Vis. Sci.*, **47**, 3461–3466.
160. Berry,V., Francis,P., Reddy,M.A., Collyer,D., Vithana,E., MacKay,I., Dawson,G., Carey,A.H., Moore,A., Bhattacharya,S.S., *et al.* (2001) Alpha-B crystallin gene (CRYAB) mutation causes dominant congenital posterior polar cataract in humans. *Am. J. Hum. Genet.*, **69**, 1141–5.
161. Liu,Y., Zhang,X., Luo,L., Wu,M., Zeng,R., Cheng,G., Hu,B., Liu,B., Liang,J.J. and Shang,F. (2006) A novel αB-crystallin mutation associated with autosomal dominant congenital lamellar cataract. *Investig. Ophthalmol. Vis. Sci.*, **47**, 1069–1075.
162. Raju,I. and Abraham,E.C. (2013) Biochemical and Biophysical Research Communications Mutants of human a B-crystallin cause enhanced protein aggregation and apoptosis in mammalian cells : Influence of co-expression of HspB1. **430**, 107–112.
163. Brady,J.P., Garland,D.L., Green,D.E., Tamm,E.R., Giblin,F.J. and Wawrousek,E.F. (2001)

AlphaB-crystallin in lens development and muscle integrity: a gene knockout approach. *Invest. Ophthalmol. Vis. Sci.*, **42**, 2924–34.
164. Kamradt,M.C., Chen,F., Sam,S. and Cryns,V.L. (2002) The small heat shock protein aB-crystallin negatively regulates apoptosis during myogenic differentiation by inhibiting caspase-3 activation. *J. Biol. Chem.*, **277**, 38731–38736.
165. Kamradt,M.C., Chen,F. and Cryns,V.L. (2001) The Small Heat Shock Protein aB-Crystallin Negatively Regulates Cytochrome c- and Caspase-8-dependent Activation of Caspase-3 by Inhibiting Its Autoproteolytic Maturation. *J. Biol. Chem.*, **276**, 16059–16063.
166. Kamradt,M.C., Lu,M., Werner,M.E., Kwan,T., Chen,F., Strohecker,A., Oshita,S., Wilkinson,J.C., Yu,C., Oliver,P.G., *et al.* (2005) The small heat shock protein aB-crystallin is a novel inhibitor of TRAIL-induced apoptosis that suppresses the activation of caspase-3. *J. Biol. Chem.*, **280**, 11059–66.
167. Shin,J.-H., Kim,S.-W., Lim,C.-M., Jeong,J.-Y., Piao,C.-S. and Lee,J.-K. (2009) aB-crystallin suppresses oxidative stress-induced astrocyte apoptosis by inhibiting caspase-3 activation. *Neurosci. Res.*, **64**, 355–61.
168. Prabhu,S., Srinivas,V., Ramakrishna,T., Raman,B. and Rao,C.M. (2011) Inhibition of Cu2+-mediated generation of reactive oxygen species by the small heat shock protein αB-crystallin: the relative contributions of the N- and C-terminal domains. *Free Radic. Biol. Med.*, **51**, 755–62.
169. Oh, J.Y., Choi, H., Lee, R.H., et al. (2012) Identification of the HSPB4/TLR2/NF-kappaB axis in macrophage as a therapeutic target for sterile inflammation of the cornea. *EMBO Mol Med*, **4**, 435–48.
170. Campisi, J., Leem, T.H., Fleshner,M. (2003) Stress-induced extracellular Hsp72 is a functionally significant danger signal to the immune system. *Cell Stress Chaperones*, **8**.
171. Lai, Y., Stange, C., Wisniewski, S.R., et al. (2006) Mitochondrial heat shock protein 60 is increased in cerebrospinal fluid following pediatric traumatic brain injury. *Dev Neurosci*, **28**, 336–41.
172. Gangalum, R.K., Atanasov, I.C., Zhou, Z.H., Bhat,S.P. (2011) AlphaB- crystallin is found in detergent-resistant membrane microdomains and is secreted via exosomes from human retinal pigment epithelial cells. *J Biol Chem*, **286**, 3261–3269.
173. Sreekumar,P.G., Kannan,R., Kitamura,M., Spee,C., Barron,E., Ryan,S.J. and Hinton,D.R. (2010) αB crystallin is apically secreted within exosomes by polarized human retinal pigment epithelium and provides neuroprotection to adjacent cells. *PLoS One*, **5**.
174. Mannini,B., Cascella,R., Zampagni,M., van Waarde-Verhagen,M., Meehan,S., Roodveldt,C., Campioni,S., Boninsegna,M., Penco, a., Relini, a., *et al.* (2012) Molecular mechanisms used by chaperones to reduce the toxicity of aberrant protein oligomers. *Proc. Natl. Acad. Sci.*, **109**, 12479–12484.
175. Rothbard,J.B., Zhao,X., Sharpe,O., Strohman,M.J., Kurnellas,M., Mellins,E.D., Robinson,W.H. and Steinman,L. (2011) Chaperone activity of α B-crystallin is responsible for its incorrect assignment as an autoantigen in multiple sclerosis. *J. Immunol.*, **186**, 4263–8.
176. Hagemann,T.L., Boelens,W.C., Wawrousek,E.F. and Messing,A. (2009) Suppression of GFAP toxicity by alphaB-crystallin in mouse models of Alexander disease. *Hum. Mol. Genet.*, **18**, 1190–9.
177. Quraishe,S. (2010) The sHsp expression signature in the brain and modulation in models of chronic neurodegeneration.
178. Tue,N.T., Shimaji,K., Tanaka,N. and Yamaguchi,M. (2012) Effect of alphaB-crystallin on protein aggregation in drosophila. *J. Biomed. Biotechnol.*, **2012**.
179. Hagemann,T.L., Boelens,W.C., Wawrousek,E.F. and Messing,A. (2009) Suppression of GFAP toxicity by alphaB-crystallin in mouse models of Alexander disease. *Hum. Mol. Genet.*, **18**, 1190–9.
180. Shao,W., Zhang,S., Tang,M., Zhang,X., Zhou,Z., Yin,Y., Zhou,Q., Huang,Y., Liu,Y., Wawrousek,E., *et al.* (2013) Suppression of neuroinflammation by astrocytic dopamine D2

receptors via αB-crystallin. *Nature*, **494**, 90–4.
181. Ojha,J., Karmegam,R. V, Masilamoni,J.G., Terry,A. V and Cashikar,A.G. (2011) Behavioral defects in chaperone-deficient Alzheimer's disease model mice. *PLoS One*, **6**, e16550.
182. Ousman, S.S., Tomooka, B.H., van Noort, J.M., et al. Protective and therapeutic role for alphaB-crystallin in autoimmune demyelination. 2007; : *Nature*, **448**, 474–9.
183. Quach,Q.L., Metz,L.M., Thomas,J.C., Rothbard,J.B., Steinman,L. and Ousman,S.S. (2013) CRYAB modulates the activation of CD4+ T cells from relapsing-remitting multiple sclerosis patients. *Mult. Scler.*, **19**, 1867–77.
184. Rothbard, J.B., Kurnellas, M.P., Brownell, S., et al. (2012) Therapeutic effects of systemic administration of chaperone alphaB- crystallin associated with binding proinflammatory plasma proteins. *J Biol Chem*, **287**, 9708–21.
185. Arac, A., Brownell, S.E., Rothbard, J.B., et al. (2011) Systemic augmentation of alphaB-crystallin provides therapeutic benefit twelve hours post-stroke onset via immune modulation. *Proc Natl Acad Sci*, **108**, 13287–92.
186. Klopstein,A., Santos-Nogueira,E., Francos-Quijorna,I., Redensek,A., David,S., Navarro,X. and López-Vales,R. (2012) Beneficial effects of αB-crystallin in spinal cord contusion injury. *J. Neurosci.*, **32**, 14478–88.
187. Christopher, K.L., Pedler, M.G., Shieh, B., et al. (2014) Alpha-crystallin- mediated protection of lens cells against heat and oxidative stress-induced cell death. *Biochim Biophys Acta*, **1843**, 309–15.
188. Kozawa, O., Matsuno, H., Niwa, M., et al. (2001) AlphaB-crystallin, a low-molecular-weight heat shock protein, acts as a regulator of platelet function. *Cell Stress Chaperones*, **6**, 21–8.
189. Wu, N., Yu, J., Chen, S., et al. (2014) alpha-Crystallin protects RGC survival and inhibits microglial activation after optic nerve crush. *Life Sci*, **94**, 17–23.
190. Robertson,A.L., Headey,S.J., Saunders,H.M., Ecroyd,H., Scanlon,M.J., Carver,J. a and Bottomley,S.P. (2010) Small heat-shock proteins interact with a flanking domain to suppress polyglutamine aggregation. *Proc. Natl. Acad. Sci. U. S. A.*, **107**, 10424–9.
191. Muchowski,P.J., Ramsden,R., Nguyen,Q., Arnett,E.E., Greiling,T.M., Anderson,S.K. and Clark,J.I. (2008) Noninvasive measurement of protein aggregation by mutant huntingtin fragments or alpha-synuclein in the lens. *J. Biol. Chem.*, **283**, 6330–6.

Chapter 2.

Aims of the project

Aims of the project

As introduced earlier, HD is a devastating neurodegenerative disorder. How the polyQ-expanded mHtt causes selective and progressive dysfunction and neurodegeneration remains unclear. Therefore, at the present there is no cure for HD.

Protein misfolding and aggregation of mHtt play a central role in HD, and growing evidence has been shown that transgenic overexpression and exogenous administration of the sHsp αBc may represent a strong candidate for HD therapeutic targets.

The main aims of this project were to investigate whether modulating the levels of αBc affected mHtt toxicity and influenced pathogenesis in a mouse model of HD. Thus, the aims of this thesis were:

1. Determine whether αBc overexpression in astrocytes affects the onset and severity of HD phenotype and neurotoxicity induced by mHtt *in vivo* (Chapter 3)

We tested whether astrocytic αBc overexpression was able to modulate behavioral and neuropathological deficits in a mouse model of HD. Thus, we crossed the well characterized BACHD mouse model of HD with αBc transgenic mice in which αBc is regulated by the GFAP promotor, driving its expression in astrocytes.

2. Explore the relation of αBc overexpression with fundamental cellular pathways that are impaired in HD
(Chapter 4)

We clarified important cellular mechanisms where αBc could potentially be involved in alleviating mHtt-induced toxicity. We investigated potential αBc interactors in the progression of HD.

3. Determine whether αBc deficiency affects the onset and severity of HD phenotype and neurotoxicity induced by mHtt *in vivo*

(Chapter 5)

We tested whether endogenous αBc was able to modulate behavioral and neuropathological deficits found in the BACHD mouse model of HD. Thus, we crossed BACHD mice with αBc deficient mice ($\alpha Bc^{-/-}$). This KO model also targets HspB2, due to the proximity of the promoter sequences of both sHsps genes.

Chapter 3.

αB-crystallin overexpression in astrocytes modulates the phenotype of the BACHD mouse model of Huntington's disease

αB-crystallin over-expression in astrocytes modulates the phenotype of the BACHD mouse model of Huntington's disease

Ana Osório Oliveira[1,2,3], Alexander Osmand[4], Tiago Fleming Outeiro[2,5,6], Paul Joseph Muchowski[7] , Steven Finkbeiner [3,8,9,10]

1 Lisbon Academic Medical Center PhD Program

2 Cell and Molecular Neuroscience Unit, Instituto de Medicina Molecular, Faculdade de Medicina de Lisboa, Portugal

3 Gladstone Institute for Neurological Disease, J. David Gladstone Institutes San Francisco, CA, USA

4 Department of Biochemistry and Cellular and Molecular Biology, University of Tennessee, Knoxville, TN, USA

5 CEDOC – Chronic Diseases Research Center, Faculdade de Ciências Médicas, Universidade Nova de Lisboa, Lisboa, Portugal

6 Department of Neurodegeneration and Restorative Research, University Medical Center Goettingen, Goettingen, Germany

7 Soteria Therapeutics, San Francisco, CA, USA

8 Department of Neurology, University of California at San Francisco, San Francisco, CA, USA

9 Department of Physiology, University of California at San Francisco, San Francisco, CA, USA

10 Taube/Koret Center for Neurodegenerative Disease Research San Francisco, CA, USA

3.1. Introduction

Huntington's disease (HD) is a fatal autosomal, dominantly inherited, progressive neurodegenerative disorder (1). The mutation responsible for HD leads to abnormally long CAG/polyglutamine (polyQ) repeats in the IT15 gene, which encodes the ubiquitously expressed protein huntingtin (Htt) (2). The polyQ expansion makes Htt prone to misfold and accumulate, which is thought to confer a toxic gain of function (3). The deposition of inclusion bodies of misfolded Htt fragments containing the expanded polyQ region is a neuropathological hallmark of HD (4).

This accumulation of misfolded proteins in cells triggers a protective stress response that includes the up-regulation of heat shock proteins (Hsps) that function as molecular chaperones either to prevent protein misfolding or to rescue misfolded proteins to help restore cellular homeostasis (5, 6). Overexpression of molecular chaperones reduces Htt aggregation and increases lifespan in HD *Drosophila* and mice (7–10). Manipulating the expression of chaperones that mitigate protein misfolding or facilitate its clearance may represent an approachable therapeutic target to decrease toxicity and slow disease progression in HD models.

The small Hsp (sHsp) family of molecular chaperones includes proteins of small molecular mass (15–30 kDa) that accumulate in the cells after many different environmental, physiological or pathological stresses (11). sHsps are protective in many pathways that are implicated in HD, including native and non-native protein folding, cytoprotection from numerous stresses, such as oxidative damage and modulation of cell death and survival pathways (6). Structurally, all sHsps share a central C-terminal domain, referred to as the alpha-crystallin domain, consisting of 80–90 residues in eight beta strands that form an intermolecular beta- sheet interaction site (12, 13). The most studied sHsps (i.e., Hsp27/HSPB1, αA-crystallin/HSPB4, αB-crystallin/HSPB5, Hsp22/HSPB8 and Hsp16.2/HSPB11) have strong anti-aggregation chaperone activity through their ability to recognize and interact with partially folded protein intermediates (14, 15). Chaperones include eligible candidates for neuroprotection in HD (6, 16), and their potential has been evaluated *in vitro* (17), in *Caenorhabditis elegans* (18), mammalian cells (8, 19), and *in vivo* models of HD (20). Our study focused on the αB-crystallin (αBc) or HspB5 protein. This sHsp has a

chaperone-like function and binds to the unfolded proteins to inhibit its aggregation (21), suggesting that αBc has an impact on several protein conformation disorders. αBc prevents the aggregation and elongation of α-synuclein fibrils (22, 23), implicated in Parkinson's disease (PD). Furthermore, αBc is a potent inhibitor of amyloid fibril formation and, by slowing the rate of its aggregation, effectively reduces the toxicity of amyloid-β peptide in cells (24), suggesting a protective role for αBc in a Alzheimer's disease (AD) *in vitro* model. Amyotrophic lateral sclerosis (ALS) is a progressively paralytic neurodegenerative disease that can be caused by mutations in Cu,Zn-superoxide dismutase 1 (SOD1). Completely eliminating αBc in mice expressing two different SOD1 mutants (G37R and L126Z) reduced the interval to disease end stage by 20–30 days in mice expressing either mutant (25). These results suggest that the activity of αBc modulates the cellular specificity of mutant SOD1 accumulation. In addition, over-expression of αBc in a mouse model of Alexander disease (AxD), a rare and fatal neurodegenerative disorder of childhood, rescued the AxD mice from terminal seizures. Consistently, loss of αBc resulted in increased mortality of these mice (26).

We previously showed that expressing a mutant Htt (mHtt) fragment in the lens of mice lacking αBc markedly accelerated the onset and severity of mHtt aggregation (27). In addition, overexpression of αBc in a transgenic drosophila model of HD suppressed mHtt toxicity, suggesting a protective role for αBc in HD (28). Downregulation of a number of molecular chaperones, including αBc, was reported in the brains of the exon-1 fragment mouse model R6/2 (20, 29), suggesting αBc may be associated with HD pathogenesis *in vivo*, and that restoration of chaperone levels could be neuroprotective against disease. Interestingly, current evidence suggests expression of the sHsps, such as αBc, is predominantly in non-neuronal cells (7). In the brain, αBc is mainly found in astrocytes and oligodendrocytes. The role of astrocytes and oligodendrocytes in HD is not entirely clear. However, evidence suggests that non cell-autonomous functions of glial cells are an important mechanism of supporting neuronal health (30). We focused on astrocytes because recent studies in different HD mice models have shown that astrocytes contribute to neuronal dysfunction *in vivo,* by a marked decreased expression of both glutamate transporters, GLAST and GLT-1, and of glutamate uptake (31), by a decrease on potassium (K+) ion channel expression in astrocytes and disturbances of astrocyte-mediated K(+) homeostasis (32) or by being a source of oxidative stress to neurons *in vivo* (33).

Here we investigated the effects of αBc overexpression in astrocytes on behavioral and neuropathological phenotypes in a full-length HD mouse model, BACHD. These mice exhibit early (2–3 months of age) robust and progressive motor deficits, and late-onset selective neuropathology, including significant cortical and striatal atrophy (34). αBc astrocytic overexpression in BACHD mice improved motor and cognitive symptoms. The improvements in behavioral deficits correlated with prevention of the cortical and striatal neuron loss that is observed in HD. We observed a decreased level of soluble mHtt, and decreased size of mHtt inclusions in BACHD brain. Our results suggest that αBc is protective in HD through an astrocyte-mediated chaperone function related to regulating mHtt protein levels and aggregation in BACHD brains.

3.2. Materials and Methods

Animals and breeding strategy

Experiments involving mice were approved by the Institutional Animal Care and Use Committee of the University of California, San Francisco. Mice were housed, bred and maintained in compliance with National Institutes of Health guidelines. BACHD (BACHD ^{tg}) mice (34) were obtained from William Yang (University of California, Los Angeles). Cryab Tg (Cryab ^{tg}) mice with wild-type hamster Cryab gene under the control of the human GFAP promoter (35) were obtained from Albee Messing (University of Wisconsin, Madison). Both lines were maintained by breeding to WT FVB/NJ animals from the Jackson Laboratory (Bar Harbor, ME). To test if over-expression of αB-crystallin improved HD progression, we crossed the Cryab Tg mice to BACHD mice. Progeny from this breeding included Cryab ^{Tg}, BACHD, Cryab ^{tg};BACHD (double transgenic, DTg) and littermate controls, wild-type (WT) mice and were used for behavioral studies and HD-associated neuropathological studies.

Genotyping

Mouse-tail DNA was analyzed by PCR to determine the genotypes. The BACHD transgene was identified as described (34). The Cryab transgene was identified as described (35).

Behavioral assays

For all behavior experiments, experimenters were blinded to genotype. Experimental readouts were analyzed at 3, 7, 10 and 13 months for elevated plus maze, open field, rotarod and balance beam to evaluate HD phenotype progression. All cages contained at least one mouse from each genotype, and mice were given environmental enrichment. Mice were subject to a 12-h light/dark cycle. Behavioral analysis of WT, Cryab Tg, BACHD and DTg mice was done blind to genotype.

Before starting the behavioral analyses at the first time point (3 months), two mice from our cohort presented tumors in their legs (one was WT and the other BACHD). In our water-T-maze study (at 13 months), one mouse (from the double transgenic - DTg group) was removed from testing because he was an aggressive male that bit the tester during the pre-training phase. This mouse's aggressive behavior resulted in the need to house this mouse singly and to be excluded from the last behavioral assay. In both cases, these mice were excluded but the exclusion was not based on behavioral performance and so did not introduce an obvious bias into the measurements.

Elevated Plus Maze

The elevated plus maze has been described as a simple method for assessing anxiety responses in mice (36). Anxiety levels were measured in a cross-shaped maze, with two open arms and two closed arms linked to automated computer software. Entries and time spent on both open and closed arms were detected by photobeam arrays underlying the four arms platform. Each mouse had 3 sessions (15 min each) and returned to its initial cage after testing. Testing arms were cleaned with 70% alcohol after each session to remove any dirt or smell accumulated on the apparatus.

To note: In our study, the BACHD mice did not display an anxious phenotype in the elevated plus maze test during the disease progression.

Open field

Spontaneous locomotor activity was measured using an automated Photobeam Activity System (San Diego Instruments, San Diego, CA). Before testing, mice were

acclimated in the testing room for 1 h. During testing, mice were placed into a clear plastic testing chamber (41 × 41 × 30 cm) for 15 min. Horizontal and vertical movements were detected by photobeam arrays traversing the testing chamber. Testing chambers were cleaned with 70% alcohol after each session.

To note: In our study, the BACHD mice did not display a locomotor phenotype in the open field test during the disease progression.

Rotarod

An accelerating rotarod (Med Associates ENV-577M) was used to analyze motor coordination and balance. Baseline behavior was performed at 3 months, and mice were placed into balanced cohorts based on sex, and genotype. Mice were trained three times at a constant speed of 16 rpm for maximum of 300 s. During testing, mice were subjected to beam acceleration of 4–40 rpm for a maximum of 300 s, three times per session (1 day) for a total of three sessions/days (37). Performance was quantified by measuring the latency to fall off of the rotarod apparatus.

Balance beam

The balance beam was also used to assess motor coordination and balance. This test consisted of three sessions with three trials in each session: one session of training, one session of testing on large diameter beam, one session of testing on medium diameter beam. Motor performance was assessed by measuring the time it takes for the mouse to traverse the beam, the number of hind paw slips, and the number of falls during this process (38).

Water T-maze

Normal phase swimming T-maze test

The full-length mHtt model—YAC128 mice—show multiple cognitive deficits in swimming T-maze test (39). We decided to test cognitive deficits in BACHD mice at 13 months.

Mice were tested to assess spatial learning and memory. They were placed in the base of a water-filled T-maze and trained to swim to an escape platform located in the right or left arm of the maze (mice were divided in two groups and trained to reach the platform to the

right or to the left side to be unbiased in the test). Mice must learn to turn to the correct arm to reach the platform directly.

During this test, mice received three trials per day for 7 days. To successfully complete this task, mice must remember either the location of or the path to the escape platform. Because FVB/N mice have severe retinal degeneration at the age tested (40), learning to swim to the correct arm of the maze likely relies on internal rather than external cues.

Reversal phase swimming T-maze test

After 1 day of rest, we included a reversal phase to the swimming T-maze test to assess the ability of the mice to replace a previously learned strategy. For this test, the platform was switched to the opposite arm (used in the first phase) of the T-maze. Mice received three trials per day for 5 days.

For the two phases of the T-maze test, the time to reach the platform, the swim velocity and the distance taken to reach the platform were recorded. Swimming through the incorrect arm was arbitrarily given a score of 0, whereas swimming into the correct arm where the platform was located was given a score of 1.

Protein extraction

Mice were anesthetized with Avertin (tribromoethanol, 250 mg per kg) and perfused transcardially with 0.9% saline. Brains were removed, microdissected in ice-cold PBS, and homogenized in ice-cold standard RIPA buffer (150 mM NaCl, 1% NP-40, 0.1% sodium dodecyl sulfate, 0.5% sodium deoxycholate, 50 mM Tris, pH 7.4) supplemented with complete protease inhibitors (Roche Applied Science) and spun at 14,000 × g for 20 min at 4 °C.

Western blotting

Proteins (10–20 μg/well) were separated on a 4–12% NuPAGE Bis-Tris gel (Life Technologies) and transferred onto nitrocellulose membranes, which were incubated for 1 h in 5% bovine serum albumin (Sigma-Aldrich) diluted in Tris-buffered saline containing 0.05% Tween (BSA-TBST). Immunoblots were probed and incubated overnight at 4 °C in rabbit anti-αB-crystallin (1:1,000, Stressgen), or anti-B-tubulin (Abcam, ab6046, 1:20000), 4H7H7

(1:2000, made in the Lab), 1C2 (1:1000, made in the Lab) antibodies diluted in BSA-TBST. Appropriate IRDye secondary antibodies (LI-COR Biosci) were used at a 1:20,000 dilution. Images were captured with the Odyssey CLx (LI-COR Biosci).

Neuropathology

Mice were anesthetized with avertin (tribromoethanol, 250 mg/kg) and perfused with saline. Hemi-brains were then drop fixed in 4% paraformaldehyde for 48 h. For mHtt inclusions, multiple perfusion-fixed brains were embedded in gelatin blocks, post-fixed, and freeze-cut into coronal 35 μm sections in 24 sequential series (NeuroScience Associates Inc., Knoxville, TN). These were stored at -20° C in cryoprotectant as individual series of sections and stained for mhtt-derived aggregates with an affinity purified preparation of the sheep anti-htt antibody S830 (30 ng/mL), GFAP (10 ng/mL) and Iba1 (10 ng/mL) under uniform free-floating conditions modified from previous descriptions (41). Binding was visualized using ultra-sensitive HRP-based Ni++/DAB immunohistochemistry. Images (590 μ x 470 μ) were collected with a Nikon DS-RI1 Digital Sight camera on a Nikon Eclipse Ni microscope under control of NIS-Elements V4.30. Extended depth-of-field images were converted to gray scale and numbers and size of immunoreactive inclusion bodies determined using Fiji-ImageJ.

<u>For striatal and cortical counts:</u>

Fixed brains were sectioned into 40 μm sections with a Leica Vibratome in 24 sequential series. Free-floating sections were incubated in either 10% goat or donkey serum in 0.1% Triton X-100 for 1 h before incubation with primary antibodies at 4°C for 24 h. Sections were then immunostained with anti-DARPP32 (1:1000, Cell Signaling) and NeuN (1:1000, Chemicon). The specific areas analyzed were striatum/medial caudate/putamen and M1/M2 cortex. For all neuropathological analysis, at least three sections were analyzed per mouse and for each section and each area (cortex or striatum), we obtained 6 to 7 fields of view/micrographs and cell counts were averaged per area/per mice. For comparison across genotypes, we selected sections from the same sequential series. Confocal micrographs for DARPP-32- and NeuN-positive cells were analyzed with original proprietary programs that were written in MATLAB.

The following steps used on a Matlab Script were used for all images from the different groups of mice, and analyzed simultaneously.

(1) The script first reads the input image and filters it using an adaptive thresholding method based on the paper "Adaptive Thresholding for the DigitalDesk" by Pierre Wellner (42). We used median filtering and relative thresholds instead of absolute as they gave more accurate results.

(2) After thresholding, we end up with a binary image where the objects of interest are labeled with 1's. This image also has some noise in the form of small white objects that need to be removed. Hence, we use morphology to remove all objects that are smaller than 200 pixels in area. This helps clean up the thresholded image and we are left with the cells of interest (that will be examined/reviewed to counteract possible shrunken and smaller cells to avoid therefore a different cell count in one of the genotypes compared with the other; this revision is done blindly for each genotype). The images below illustrate the application of this algorithm to image data, and demonstrate that the program is capable of accurately identifying and counting cells as objects, despite a fairly wide variation in cell size and morphology.

(3) After morphological cleanup, we still need to process these images further because there may be touching cells that need to be separated. This is done using a recursive watershed method to split merged objects, as described in (43) for the iterative watershed method.

(4) At this point we now have separate objects in each image that we count for each image. (see example in the supplementary Fig S2).

The program applies a constant threshold for pixel intensity to quantify cell diameter among four genotypes in an unbiased manner. Results from the analysis program were reviewed and minimally hand curated to avoid artifacts (false negative cells) and to make sure that if neurons did shrink in size, they did not fall below a certain area to be counted. For all studies, the experimenter was blind to the genotype of the mice.

Statistical Analyses

All data are expressed as the mean ± SEM. Variances between two groups were compared by F test and differences between two groups by unpaired Student's *t* test (two-tailed, unless indicated otherwise in the figure legends). Differences among multiple groups were assessed by one-way or two-way ANOVA, followed by Tukey multiple comparisons

post-hoc tests, as specified in the figure legends. Correlations were assessed by linear regression and Spearman's correlation. Null hypotheses were rejected at $p < 0.05$. All statistical analysis was performed using Prism (Graphpad, GraphPad Prism v6.0; GraphPad Software La Jolla, CA).

To address concerns related with winner's curse on our data, we presented a very common summary statistic, *Cohen's d*, whose single value can be plugged directly into standard statistical software (such as R, SAS, SPSS, STATA) or online sample size calculators (http://www.danielsoper.com/statcalc3/calc.aspx?id=47) to calculate the required sample size. If readers want to address issues of potential upward bias of the effect size, they could scale the estimate of the *Cohen's d* by say 30% and then use this smaller effect size to calculate the necessary sample size (Supplementary Tables S1-S5).

3.3. Results

3.3.1. αB-Crystallin levels decrease over time in BACHD mice

Sequestering chaperones into aggregates decreases the number of soluble chaperones that are available in the cell, and this presumably enhances abnormal protein folding (20). Levels of αBc and other chaperones decrease in the brains of an exon1 fragment HD model (29). Although mHtt exon1 is sufficient to cause disease, it lacks features of full-length Htt, such as post-translational modification sites, and protein interaction or signaling domains that may be important for regulating Htt proteostasis and toxicity. We wanted to determine if a decrease in endogenous αBc levels is altered during the progression of disease in the full-length mouse model of HD – BACHD mice. This model shows a robust phenotypic behavioral deficit and neuropathological features, and full-length mHtt expression with 97 polyQ is governed by the human Htt promoter, and so, it presumably recapitulates any cell- and time-dependent expression patterns seen in humans (44).

Whole-brain lysates from BACHD mice and wild type (WT) littermates from 3, 6, 9 and 12 months, corresponding to early- and late-onset stages of disease, were harvested. At 3 and 6 months of age, the protein levels of αBc were not different in BACHD and WT mice. However, at 9 and 12 months of age, BACHD mice had significantly lower brain levels of

αBc than WT littermates (Fig. 1). The decreased protein levels of αBc over time in BACHD mice, especially after 6 months, correspond to the period where the behavioral and motor deficits in BACHD mice begin to be clearly detected (21). These data raise the possibility that a decline in αBc protein levels is involved in mediating pathogenesis.

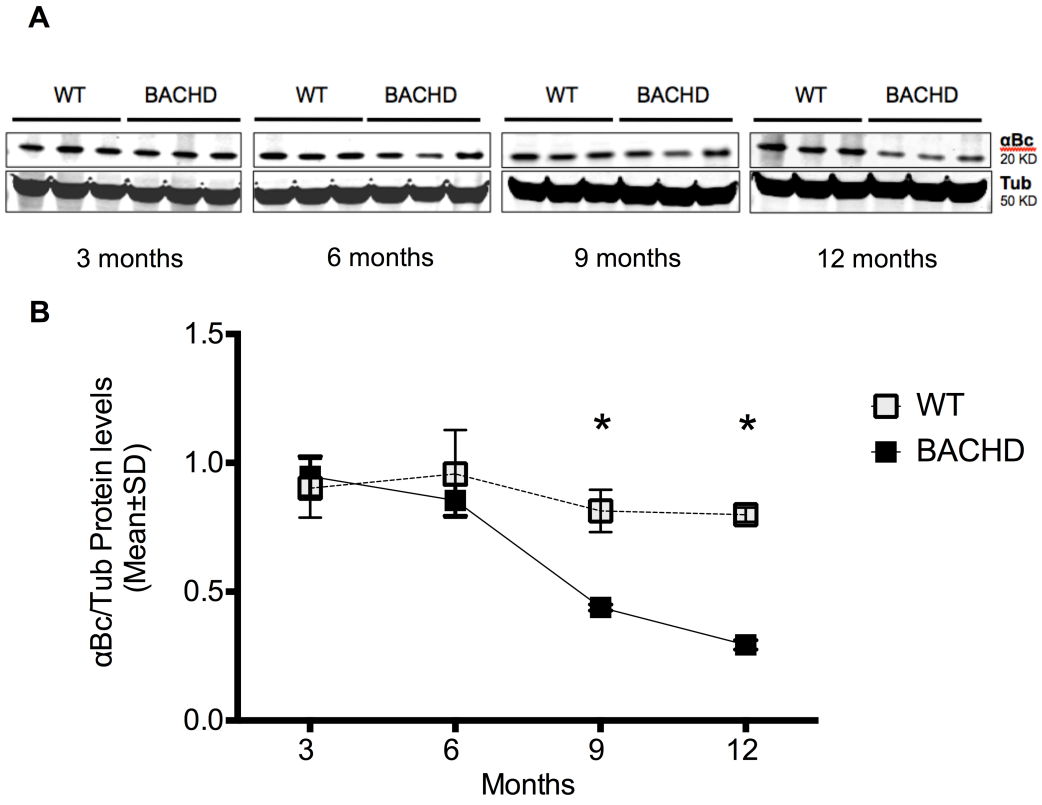

Figure 1. αB-crystallin levels decrease over time in BACHD mice. (A,B) BACHD (n=5) and WT (n=5) littermates were sacrificed at 3, 6, 9 and 12 months of age. Protein levels of αBc were determined by western blot analysis with whole-brain homogenates of BACHD and WT mice. **(A)** Immunoblots showing αBc protein level is decreased in BACHD, in an age-dependent manner, specifically after 6 months (when the motor symptoms are more robust in this mice model). **(B)** Respective quantifications of protein levels of αBc normalized to anti-β-tubulin (to show relative loading levels). Error bars represent standard errors of the mean (Means ± SEM). Data were tested for statistically significant differences using t-tests (*=$p<0.05$; **=$p<0.01$).

3.3.2. Over-expression of αBc in astrocytes improves motor performance in BACHD mice

To determine if the decline in αBc levels is an incidental finding or is playing a role in disease progression in BACHD mice, we sought to overexpress αBc and determine if it affected disease-associated phenotypes. To do so, we crossed BACHD mice with transgenic

mice expressing the WT αBc gene, Cryab. Since aBc is predominantly expressed in glia, we chose a model in which Cryab is under the control of the human GFAP promoter that targets expression to astrocytes (26). We evaluated motor behaviors at 3, 7, 10 and 13 months of age. These ages in mice correspond to early-, mid- and late-stage disease with regard to symptomatology and neuropathology (34). Deficits in rotarod latency to fall (34, 45) and balance beam latency to cross (38, 46) were previously reported in BACHD. In these assays, BACHD mice had performance deficits in an age-dependent manner (Fig. 2). In our study, BACHD behavioral deficits were detected as early as 3 months of age in rotarod and balance beam tests. BACHD mice fall off an accelerating rotarod sooner than WT littermates and Cryab Tg mice (significant at 3, 7, 10 and 13 months), and this effect is partially rescued by astrocytic over-expression of the Cryab transgene in BACHD mice (double transgenic, DTg) at all time points tested (Fig. 2A).

During the balance beam evaluation, the mice cohort was tested with a large-sized and a medium-sized balance beam (37). For our analyses, we used the data from the medium beam, which requires more motor coordination to cross than the large beam. BACHD mice took significantly more time to cross the medium beam than WT and Cryab Tg mice at 3, 7, 10 and 13 months (Fig. 2B). αBc over-expression rescues this phenotype in BACHD only at the 7 months; therefore, αBc does not improve the overall latency to cross the balance beam of the BACHD mice (Fig. 2B). We also tested the ability to stay on the beam by measuring the number of slips and falls. DTg mice were significantly better on the medium beam than BACHD with fewer slips (Fig. 2C) and falls (Fig. 2D) at later stages of disease progression. The number of slips and falls of Cryab Tg mice was similar to WT mice (Fig. 2C,D). These results indicate a specific genetic interaction of αBc and mhtt that mediates the onset and severity of motor deficits in BACHD mice as measured by balance beam and rotarod assays.

We found that BACHD and DTg mice gain significantly more weight (an average of 20–30%) than WT and Cryab Tg controls, between 3 and 7 months until 13 months of age (Fig. 3). Since weight could affect motor performance, we examined the relationship of weight and rotarod and balance beam performance in BACHD mice. We found that the rotarod and balance beam performance in this cohort of BACHD and DTg mice at 3, 7, 10 and 13 months was not significantly correlated with body weight (Fig. 4). Therefore, the improvement seen in the DTg is not explained by weight differences or the effect of weight

on motor performance. Thus, we conclude that astrocytic αBc positively affects BACHD motor performance.

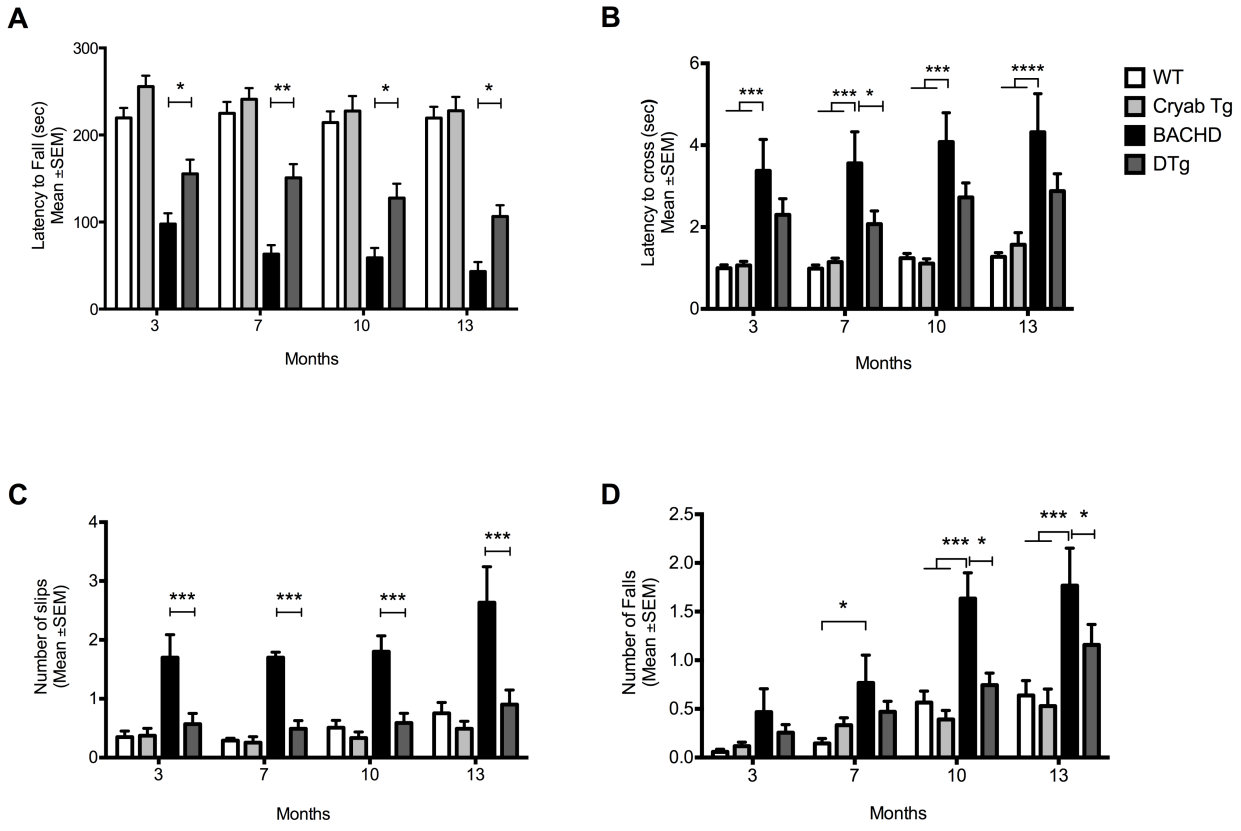

Figure 2. αBc overexpression improves behavioral readouts in BACHD mice.
Behavioral readouts of disease progression in BACHD were measured at 3, 7, 10 and 13 months of age using rotarod and balance beam. Data at each time point were tested for statistically significant differences using two-way ANOVA with multiple comparisons tests corrected by Tukey post-hoc tests. At 3 months of age, group sizes were as follows: WT (n=20), Cryab Tg (n=19), BACHD (n=14), DTg (n=17). Values are means ± SEM. * = $p < 0.05$, ** = $p < 0.01$ or ***= < 0.001 for main effect of the BACHD transgene by two-way ANOVA. **(A)** Rotarod. BACHD mice fall off an accelerating rotarod sooner than WT littermates and Cryab tg mice (significant main effect of the BACHD transgene). αBc over-expression partially rescues the BACHD motor impairment on DTg mice, and this is significant at all different time points at 3, 7, 10 and 13 months. **(B)** BACHD mice take significantly more time to cross the balance beam than WT littermates and Cryab tg mice. **(C-D)** The BACHD group also showed significant higher number of slips and falls during this task. αBc over-expression reduces the number of slips **(C)** and falls **(D)** in BACHD mice during the balance beam test. αBc overexpression does only change the overall latency to cross in DTg mice at 7 months, however, reduces significantly the number of slips (7, 10 and 13 months) and falls (10 and 13 months) of BACHD mice in the balance beam transversal assay.

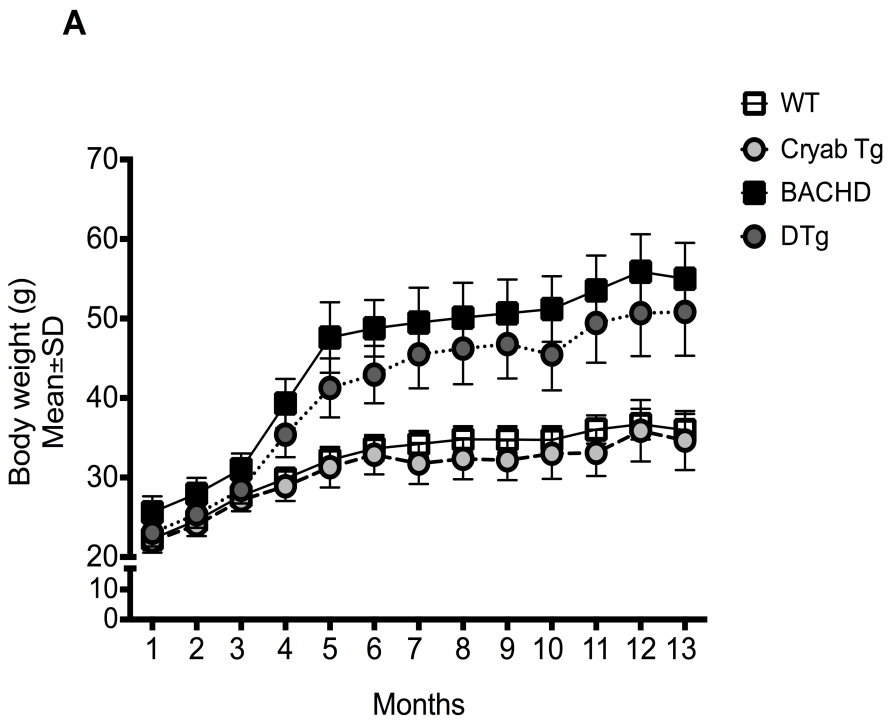

Figure 3. DTg mice display the obesity-with-age phenotype seen in BACHD mice. Monthly weight measurements of the cohort of WT (n=20), Cryab Tg (n=19), BACHD (n=14), and DTg (n=17) mice, prior to the initiation of behavioral testing at each time-point. The body weight of DTg mice is not different from BACHD mice. Data were analyzed by two-way repeated measures ANOVA followed by comparisons of the means with Tukey post-hoc tests.

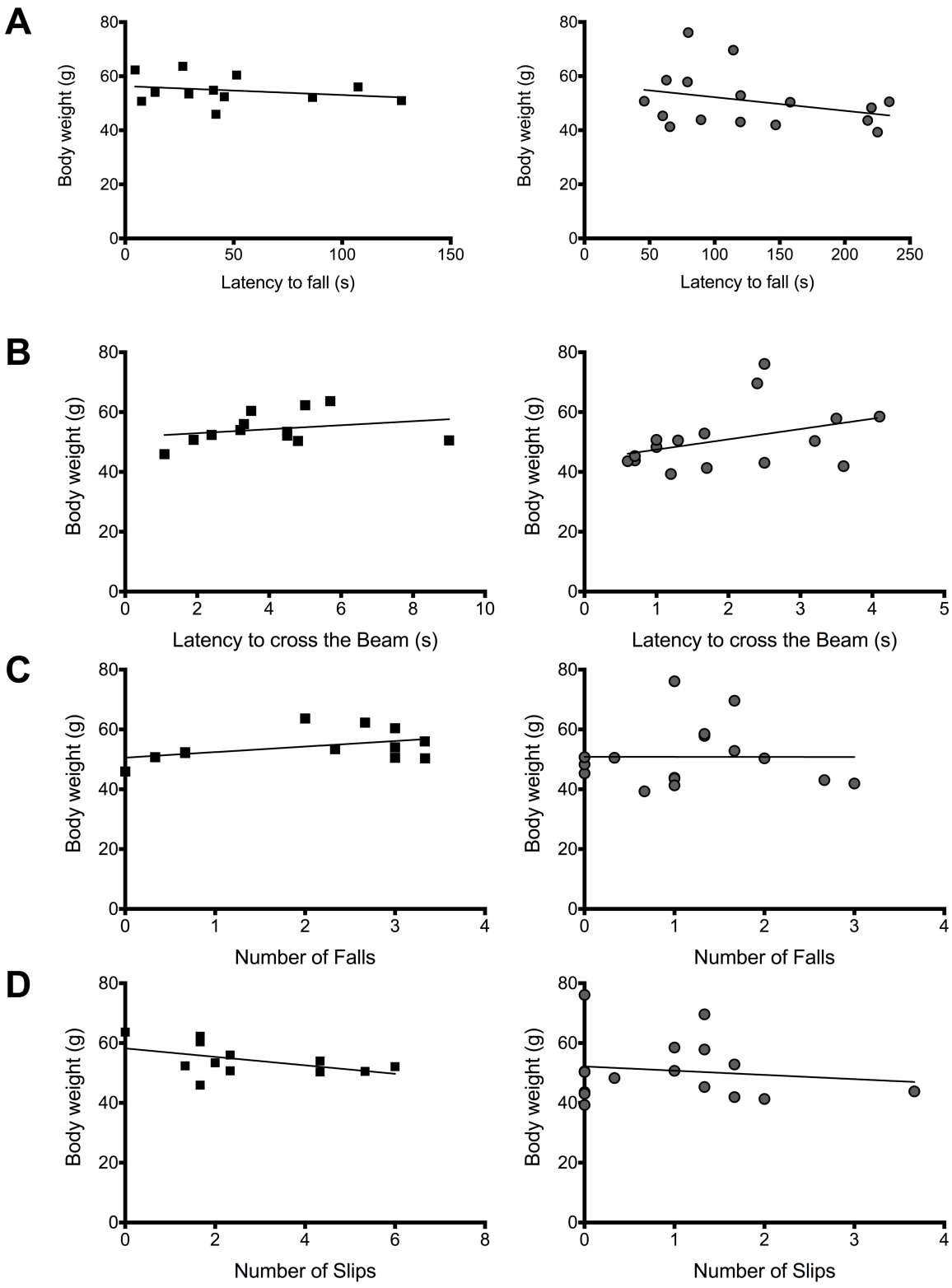

Figure 4. BACHD and DTg mice body weight phenotype does not correlate with their motor performance. The correlation between body weight and rotarod and balance beam performance in BACHD (n=12) and DTg mice (n=16) was examined. Correlations graphs for BACHD and DTg groups are in the left and right panel, respectively.

(A) Body weight correlation with latency to fall in rotarod at 13 months.
(B) Body weight correlation with latency to cross the balance beam at 7 months (only time point BACHD and DTg were significantly different).
(C) Body weight correlation with number of falls in balance beam at 13 months.
(D) Body weight correlation with number of slips in balance beam at 13 months
Our data indicate that the rotarod and balance beam BACHD and DTg mice motor performance is not correlated with their higher body weight at any time point (data not shown for 3, 7, 10 months). Therefore, the improvement seen in the DTg compared to the BACHD is not explained by weight differences or the effect of weight on motor performance. Data were analyzed by using the nonparametric Spearman correlation coefficient.

3.3.3. Expression of αBc in astrocytes improves strategy shifting in BACHD mice

In addition to motor performance, BACHD mice also exhibit cognitive decline at a later stage of the disease (47, 48), similar to what is observed in HD patients (49, 50). Therefore, we wanted to examine the effect of αBc over-expression on cognitive performance in a sensitive striatal learning-dependent assay, the swimming T-maze test. We used this test to measure procedural and spatial learning in symptomatic BACHD at the last time point of behavioral evaluation, when the mice were 13 months of age (a time known for more accentuated neurobehavioral dysfunction and cognitive decline in BACHD mice). The test was performed at only one time point in the course of disease progression to avoid any bias related to recall or long-term memory of the task. This task was previously tested in a different mouse model of full-length Htt, YAC128 mice, as a simple two-choice test of striatal dependent- learning and memory to facilitate rapid training and testing in visually cognitive-impaired mice (39). A schematic representation of the water T-maze task is presented in Fig. 5A. Briefly, on the first day, the mice were trained to swim and enter the correct arm on the T-maze, where a hidden platform was placed (right or left to avoid side biases). Upon reaching the platform, which completes the task, mice are rewarded by being allowed to return to their cages. Every day consisted of three trials. During normal phase swimming (i.e., days 2–7), the mice from all groups learned the task and made more correct choices over the course of the test (Fig. 5A). We observed no difference among genotypes performing the task during the 7-day trial. Thus, the BACHD and DTg groups learned to find the platform similar to their control littermates (Fig. 5B). The time to reach the platform (Fig. 5D), the swim velocity and the distance taken to reach the platform were not different among groups.

To assess the ability of BACHD mice to change strategy, we incorporated a reversal

phase into the swimming T-maze test by switching the platform to the opposite arm of the maze. Mice that were trained to swim directly to the right or left arm would now have to change their strategy to find the shortest path to the platform. WT, Cryab Tg and DTg mice swam down the arm they were trained initially, and after discovering that the platform was no longer present, immediately swam down the unvisited opposite arm of the maze and found the platform. Similar to the WT mice, all of the BACHD mice entered the arm of the T-maze they initially trained to. However, after discovering that the platform was not present in the opposite arm of the maze, the majority of the BACHD mice swam back to the start of the T-maze where they had already been. We measured this abnormality by quantifying the number of arms of the maze entered en route to the platform. This pattern of response resulted in the BACHD mice having more arm entries than WT, Cryab Tg and DTg mice, as it was apparently more difficult for the BACHD group to attain the 50% correct arm entries in the reversal arm over the course of the test (Fig. 5C). These results are consistent with findings observed in HD patients: during a re-learning process, HD patients tend to perseverate and have more difficulties in strategy-shifting, than healthy subjects (51–57). The difference between the number of correct entries of the BACHD group was significantly lower (below 50%) than in the DTg group from day 3 to day 5 in the reversal test. In addition, DTg mice took significantly less time to relocate the hidden platform (Fig. 5E) than BACHD mice. DTg mice were not different from the WT and Cryab Tg groups.

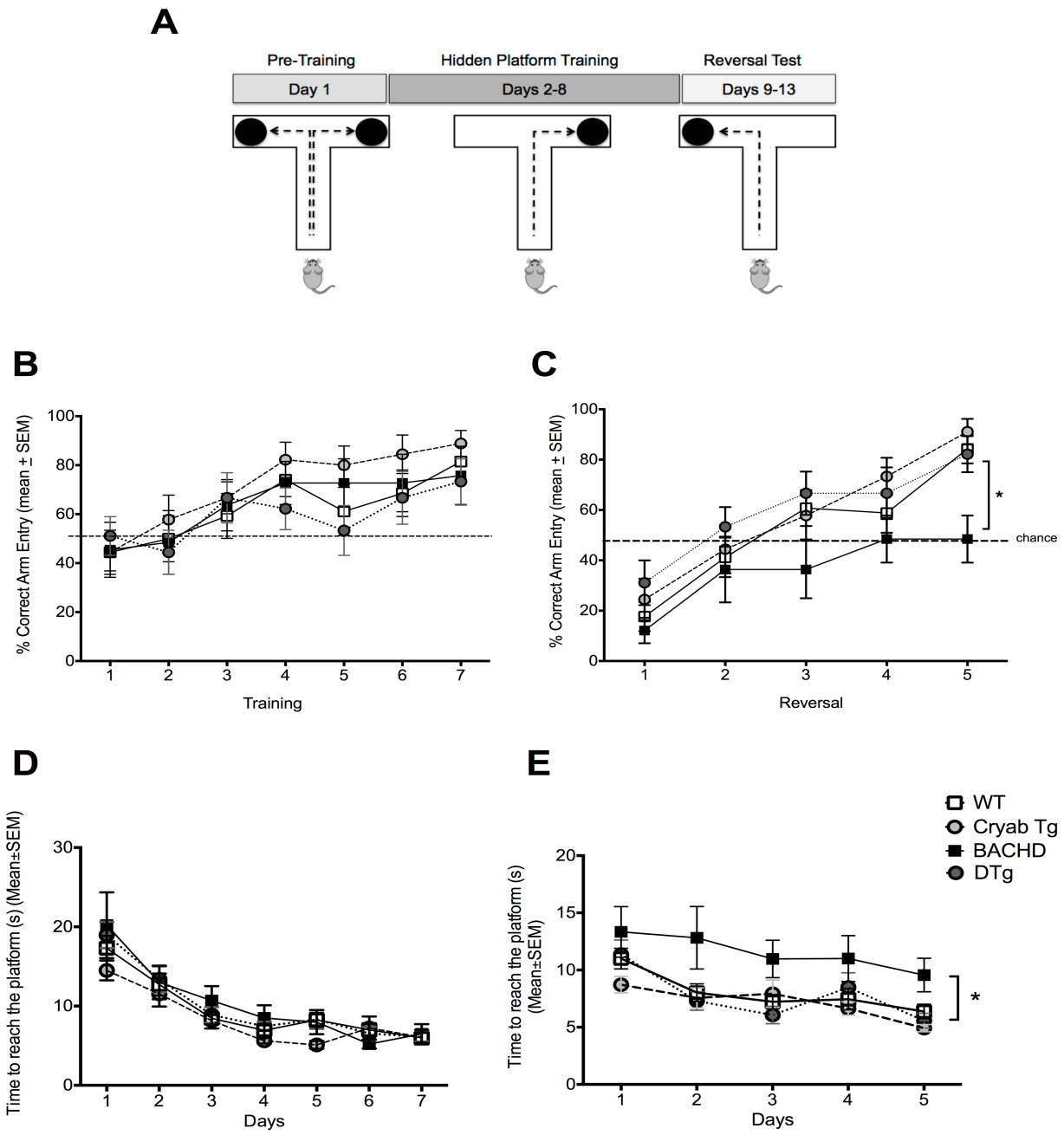

Figure 5. αBc over-expression improves BACHD strategy shifting in the water-T maze test.
(A) Water-T maze test diagram. BACHD mice were tested in the swimming T-maze with reversal. At 13 months of age, group sizes were as follows: WT (n=18), Cryab Tg (n=17), BACHD (n=10), DTg (n=15). Symptomatic BACHD show cognitive deficits in strategy shifting, and αBc overexpression rescues this impairment. **(B)** During the normal phase of the test, the four distinct groups learned to swim to the platform, and no differences were observed in the percentage of correct arm entries, having the four groups reaching ≥ 80% of correct entries, and **(D)** in the time to reach the platform. **(C)** During the reversal phase, when the location of the platform was switched, BACHD mice showed

a significant lower number of correct entries in the reversal arm and **(E)** required significantly more time to find the platform than the other groups from day 3 to day 5. Speed (cm/s) and distance (cm) to locate the platform in either training and reversal phases was not different among the four genotypes during this test performance. A two-way Anova was performed, with multiple comparisons tests, corrected by Tukey Test. *=$p< 0.05$.

3.3.4. αB-crystallin overexpression modulates levels of mhtt and inclusion body formation BACHD mice

To determine if the improved motor and cognitive behavioral phenotypes in DTg mice correlated with neuropathological changes, we examined disease features, such as inclusion body (IB) formation and neuronal cell loss. IB formation with mhtt is a hallmark of HD pathology. Aged BACHD mice develop IBs that are similar to those in the human disease and can be visualized histologically with specific htt antibodies. We examined serial sections from cortex and caudate-putamen/ striatum of 13-month-old mice of this cohort and observed differences in the density or size of inclusion bodies. Staining with the polyclonal antibody S830, which selectively recognizes expanded mhtt (34, 58), revealed prominent IBs in both the cortex and striatum of BACHD and DTG but not WT and Cryab Tg mice, as expected (Fig. 6C,D). Although there is a trend for a decrease of IB numbers in DTG when compared to BACHD, this difference did not reach statistical significance. However, there were significantly fewer larger inclusions (>1 μm) in DTg mice than in BACHD mice (Fig. 6D), indicating an overall reduction in size of inclusions.

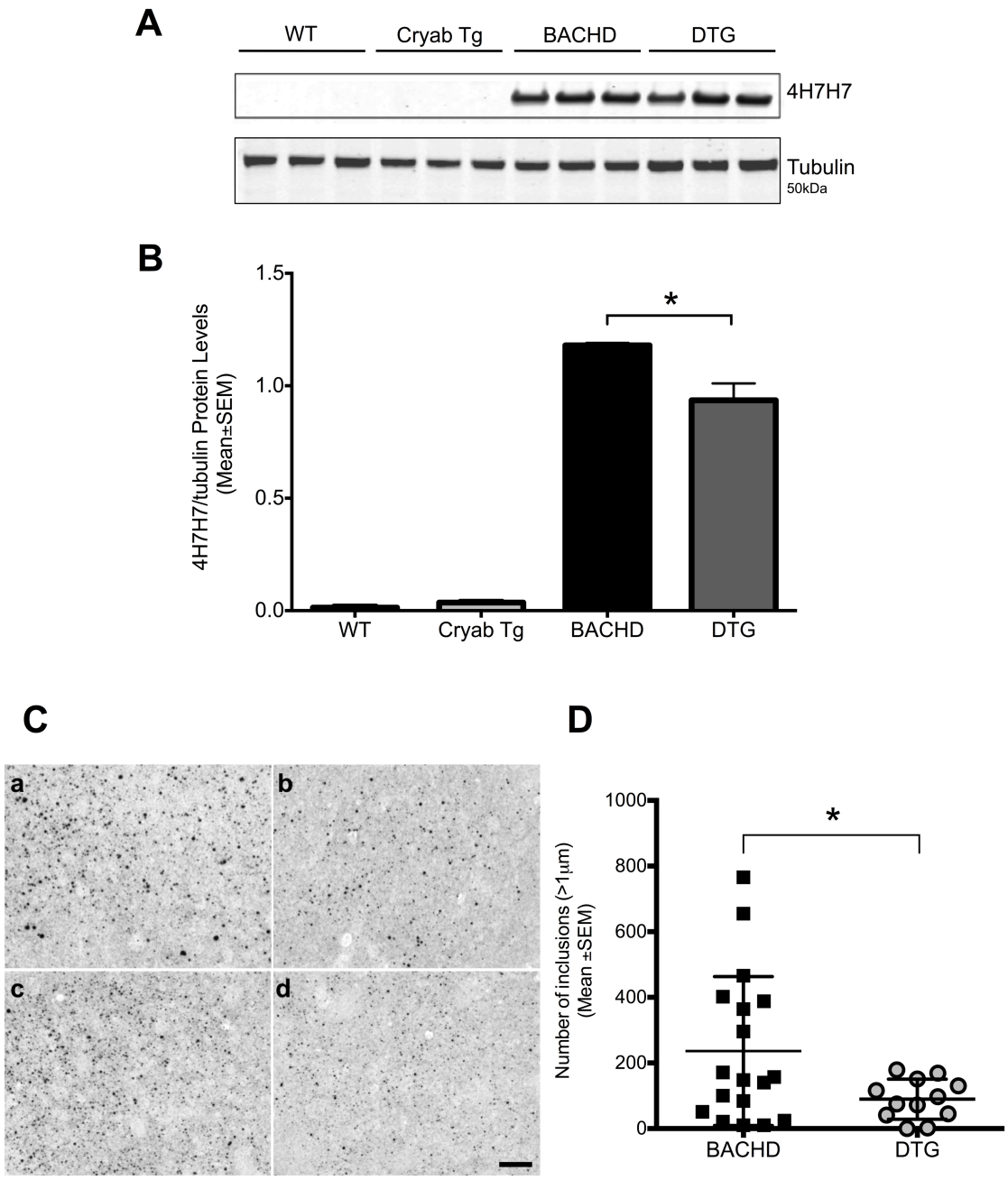

Figure 6. αBc over-expression decreases soluble levels of mutant huntingtin and reduces the size of S830 inclusion bodies in BACHD mice.

(A) Representative western blot of WT, Cryab Tg, DTg and BACHD (n=4) cortical lysates with 4H7H7 and anti-β-tubulin as a loading control and **(B)** subsequent quantification of signal intensity. Values are based on the mean of three independent 4H7H7 blots of four mice per group compared across different blots. All value were first normalized for input using the anti-β-tubulin controls. **(C)** Immunohistochemistry with polyoclonal S830 revealed prominent immunoreactive inclusion bodies in BACHD and DTg mice cortex and striatum but not in the WT and Cryab Tg littermate controls (data not shown). S830 immunohistochemistry in (**a, c**) BACHD and **(b, d)** DTg representative mouse

brains with average levels of aggregate counts and density for the two groups: **(a,b)** M1/M2 cortex layer III and **(c,d)** striatum/medial caudate/putamen, using Renyi/Entropy threshold and >1µm diameter. The scale bar represents 100 µm and the field size is 205 µm X 150µm. **(D)** The number of mHtt nuclear inclusions >1 µm were significantly reduced in the DTg when compared to BACHD mice. Values are means±SD; BACHD (n=9) and DTg (N=6), *=p< 0.05 by Student's unpaired t-test.

The difference in IBs mediated by αBc suggested that other features of mHtt proteostasis might also be altered. Since expression level of mHtt is a strong predictor of neurodegeneration in polyQ transfected rodent primary neurons (59, 60) and correlated with deficits in HD animal models (44), we compared the steady-state levels of soluble mHtt in cortical lysates.

Using the mouse monoclonal antibody 4H7H7, which preferentially recognizes pathogenic polyQ stretches (61), we found that DTg mice have a modest but reproducible and statistically significant reduction in soluble mHtt protein, compared to levels in BACHD mice (Fig. 6 A,B). Similar results were found with the mouse monoclonal antibody 1C2, selective for mHtt, in which a small but reproducible and significant decrease in soluble mHtt protein of the DTg mice when compared to BACHD mice (data not shown). In summary, these results suggest that αBc is involved in modulating mHtt protein levels and mHtt IB size, two prominent hallmarks of HD pathogenesis.

3.3.5. αB-crystallin overexpression prevents cortical and striatal neurodegeneration caused by the expression of mHtt in BACHD mice

Pathological examination of brains of HD patients reveals profound atrophy and cell death of medium spiny neurons (MSNs) of the striatum, with cortical loss also a feature as the disease progresses (4). BACHD mice present intranuclear inclusions and also show selective degeneration of the MSNs, in addition to significant atrophy of the forebrain without accompanying changes in the cerebellum (34), similar to the pattern of degeneration in human HD (62, 63).

Having found that αBc overexpression improves both motor and cognitive-like phenotypes in BACHD mice and may help reduce the levels of the mHtt–protein, we next sought to determine if the overexpression of αBc influences other neuropathological features of disease, looking at the striatum and cortex atrophy and/or cell loss. In BACHD brains at

late stage of disease (13 months of age), more than 95% of MSNs express dopamine and cyclic AMP-regulated protein (32 kDa, also known as DARPP-32) (64). We have used a sophisticated system for quantitative immunofluorescence and morphometry to measure the expression of striatal spiny neuron–specific protein, DARPP-32, in BACHD, DTg, Cryab Tg and WT mice (Fig. 7A, B). We found fewer DARPP-32+ cells in BACHD striatum than in the other genotypes. In the DTg mice, the number of DARPP-32+ cells was similar to those on WT and Cryab Tg mice (Fig. 7A, B).

Although HD is predominantly associated with degeneration of the striatum, it also involves cortical areas (30). To measure striatal and cortical neuronal cell loss, we stained brain sections with the NeuN antibody, which recognizes neuron-specific nuclear protein (Fig. 7C–F). We observed a significant decrease of both striatal (Fig. 7 C,D) and cortical (Fig. 7 E,F) NeuN+ counts when compared to WT mice, Cryab Tg and DTg mice. Taken together, our results indicate that astrocytic expression of αBc is associated with a significant reduction in striatal and cortical neuropathology in the BACHD model. Given that astrocytic overexpression of αBc significantly mitigates pathology in neurons, it further suggests that αBc overexpression may be acting in a non-cell autonomous manner.

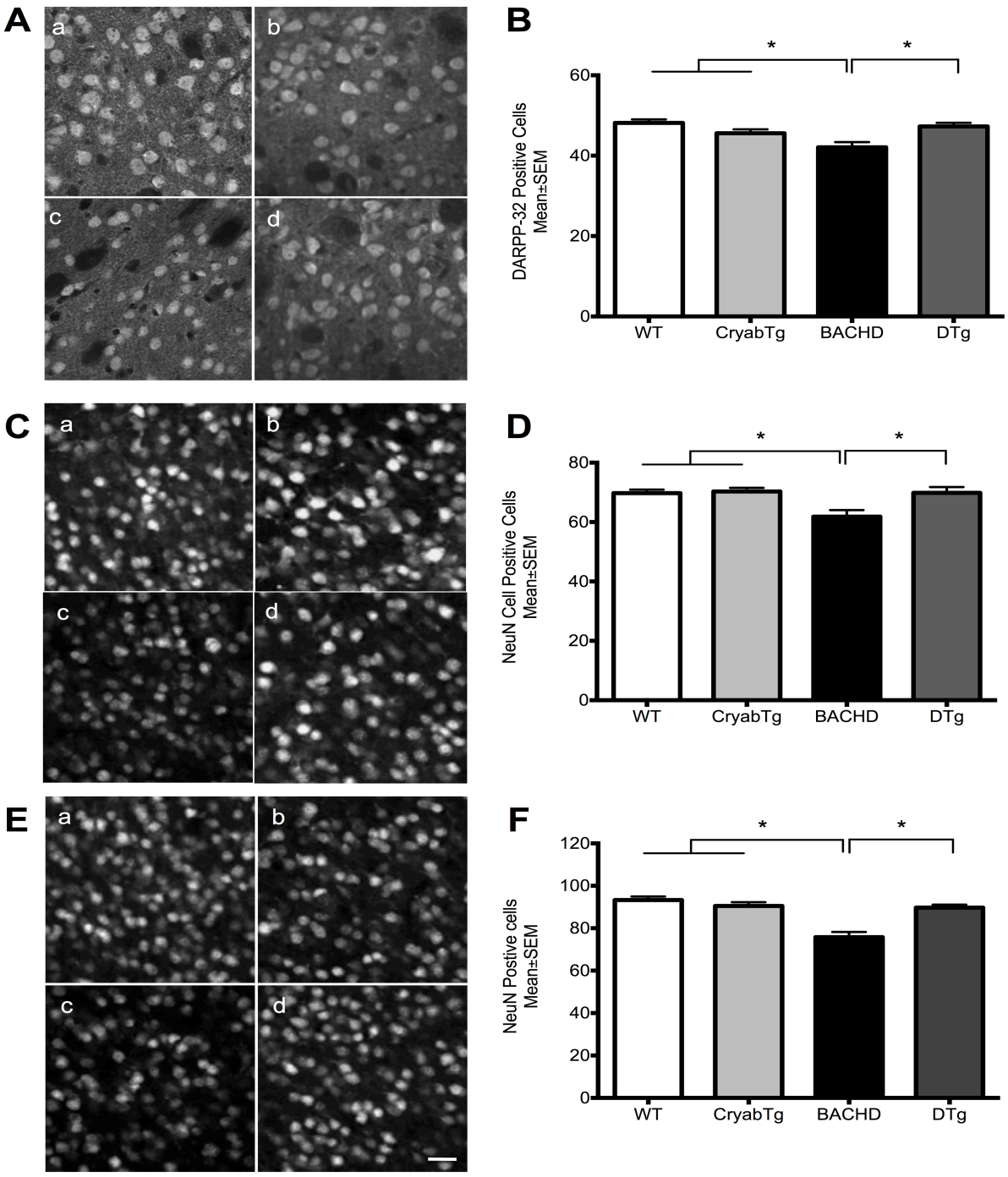

Figure 7. αBc over-expression rescues the neurodegeneration caused by expression of full-length mutant huntingtin at 13 months of age in BACHD.

Measurement of striatal DARPP-32-positive cells and striatal cortical NeuN-positive cells in **a**: WT (n=5), **b**: Cryab Tg (n=5), **c**: BACHD (n=8), **d**: DTg (n=7).

(A) Representative confocal micrographs of DARPP-32 immunostaining and **(B)** DARPP-32 positive cells quantification plots. (**C,E**) Representative confocal micrographs of NeuN immunostaining in the striatum/medial caudate/putamen (**C**) and M1/M2 cortex (**E**), followed by NeuN-positive cells

quantification plots **(D, F).** Each field is 600 x 600 μm, and the scale bar represents 20 μm. Values represent means ± SEM. *p < 0.05, one-way ANOVA with multiple Tukey multiple comparisons correction.

3.4. Discussion

No therapeutics directly and effectively target and remediate the protein-misfolding events and selective neuronal vulnerability associated with many devastating neurodegenerative disorders (65). Therefore, approaches that target molecular chaperones may be beneficial in protein conformational diseases.

In the present study, we report for the first time the effect of the sHsp αB-crystallin (αBc) in a full-length mHtt model, the BACHD mouse. Expression of αBc in astrocytes improved the motor (RotaRod and Balance Beam) and cognitive performance (Water-T-maze) of the BACHD mice, as well as neuropathological features associated with HD. Overall, our data indicate that modulating the levels of αBc protect against the progression of HD.

We hypothesize that αBc has an important modulatory role during HD since the ability to effectively initiate the heat shock response (HSR), and other homeostatic cellular pathways (e.g., apoptosis, oxidative stress) in which αBc functions, are compromised during HD disease progression (66). We should also take into account, as a chaperone with multi-functional capabilities, αBc may alleviate stress by promoting ubiquitin/proteasomal degradation of corrupt proteins (67, 68) preventing apoptosis (69–72) or by stabilizing intermediate filaments and the cytoskeleton integrity (73, 74).

The most obvious candidate mechanism for chaperone-mediated rescue of HD neurotoxicity is inhibiting or reversing Htt aggregate (fibrils/polymers) formation. Although mHtt is expressed in glial cells, the neuronal population contains most of mHtt aggregates (4, 75). Our results indicate that αBc modulates mHtt levels and the features of IBs in a typical chaperone manner. Interestingly, however, the effect of this chaperone is via overexpressing αBc in astrocytes. Overexpression of chaperones may reduce large IBs by preventing oligomer formation, and oligomeric precursors may be the most toxic species (6, 76, 77). As with most Hsps, sHps can also be important for protein stability and protein turnover. Evidence suggests that affinity of αBc for its chaperone substrates is modulated by its chaperone oligomerization status and the functional structure of αBc is a dimer, which results

from interactions of β-strands in the α-crystallin domain (78, 79). Since the binding capacity can reach one substrate protein per sHsp subunit, big chaperone oligomer structures (via sHsp oligomerized complexes) are major contributors to the chaperoning capacity of the cell. It remains unclear how the decision to refold or degrade a misfolded protein is made. Some small sHsps (αBc and Hsp27) interact directly or indirectly with the proteasome and form part of ubiquitin ligase complexes (αBc and HspB10) that are involved in the proteasomal degradation of certain proteins in a quite selective manner under stress conditions (80). Thus, αBc could regulate mHtt protein levels by stabilizing mHtt in IBs or by promoting misfolded mHtt refolding with the cooperative help of other chaperone complexes, namely the Hsp70/Hsp40 machinery, as well as targeting it for proteosomal degradation.

But how could astrocytic αBc mediate this effect on neuronal aggregation and mhtt levels? αBc is secreted in exosomes under a variety of stress-related conditions (81). One possible mechanism of modulating neuronal IBs could be through αBc-mediated extracellular signaling from astrocytes to neurons. There is emerging evidence that astrocyte-derived exosomes carry neuroprotective cargo and could contribute to neuronal survival (82). Exosomes may execute their functions by distinct modes of action: (1) internalization by target cells and cargo retrieval, (2) binding to the cell surface and triggering second messenger pathways, and (3) release of components into the extracellular matrix. However, their interaction as well as their protein content with target cells is not well understood at a mechanistic level (82). A study using retinal pigment epithelial (RPE) cells (83) showed that an increased uptake of exogenous αBc and protection from oxidative stress and apoptosis by inhibition of caspase-3 and PARP activation were observed in stressed RPE cultures. In this manner, we speculate that exosomes containing αBc could protect both glia and neuronal population in BACHD from mhtt-derived toxicity, as activation of caspase-3 and oxidative stress. Future studies will be necessary to test this hypothesis.

In our BACHD model, we additionally observed that astrocytic αBc overexpression resulted in protection of medium spiny neurons in the striatum, as well as cortical neurons. This rescue effect of astrocytic αBc on neurons further suggests that αBc confers neuroprotection in a non-cell-autonomous manner. The vast range of astrocytic functions, such as maintaining homeostasis at the synapse, regulating neuronal signaling, protecting neurons from oxidative damage, and glutamate uptake, may have wide-ranging implications

for the pathogenesis of protein aggregation disorders (84, 85). HD, PD, spinocerebellar ataxia and ALS all demonstrate non-cell-autonomous pathology in which glial expression of mutant proteins has a toxic effect on vulnerable neurons, suggesting this may be a common feature of neurodegenerative disorders (86). In addition, a marked decreased expression of both glutamate transporters, GLAST and GLT-1, and of glutamate uptake, in a HD mouse model, were associated with neuronal dysfunction as observed by a reduction of the DARPP-32 and NR2B expression (31). Also, viral delivery of potassium channels (Kir4.) to striatal astrocytes restored Kir4.1 function, normalized extracellular K(+), ameliorated aspects of MSN dysfunction, prolonged survival and attenuated some motor phenotypes in R6/2 mice (32). These studies together may suggest astrocytes and ion channels and astrocytic-mediated transport as therapeutic targets. Interestingly, αBc over- expression was shown to maintain astrocyte functions such as glutamate uptake in Alexander Disease mouse model (26) however we could not observe the same result in the BACHD mice. Further studies will be necessary to test αBc over- expression in astrocytic-mediated ion transport and ion channels expression in HD.

Co-culture of neurons with astrocytes from WT or BACHD mice identified mutant astrocytes as a source of adverse non-cell autonomous effects on neuron energy metabolism possibly by increasing oxidative stress (33). Therefore, BACHD astrocytes may fail to provide adequate metabolic support to neurons. As αBc overexpression in astrocytes is sufficient to protect BACHD neurons in our study, it is possible that αBc is helping to restore metabolic support in astrocytes (e.g., antioxidant protection and glucose uptake) in DTg mice, protecting the neighboring neuronal population from mHtt-derived toxicity. Also, the chaperoning ability of αBc could be functioning to restore dysfunctional proteostasis in a general manner in astrocytes, leading to improvement in astrocyte health and astrocyte-to-neuron signaling. Overall, our studies indicate that astrocyte-mediated neuronal protection could be an important component of a therapeutic strategy for HD and other degenerative disorders with glial involvement.

In summary, our findings show that elevation of αBc in astrocytes may protect vulnerable neurons from mHtt toxicity, which could lead to improvements in motor behavior and cognition, as well as protecting against neuropathological deficits during BACHD disease progression. Our data are consistent with the possibility that metabolic deficiency in HD

astrocytes plays a significant role in disease progression. Restoration of this deficiency by chaperones, such as αBc, may represent a potential mechanism of neuroprotection. Although the precise mechanism by which αBc overexpression alleviates neurodegeneration in BACHD is not fully understood, future studies will help to unravel the function of αBc in complex interactions with mHtt and potential other stressor targets in HD.

3.5. References

1. Landles,C. and Bates,G.P. (2004) Huntingtin and the molecular pathogenesis of Huntington's disease. Fourth in molecular medicine review series. *EMBO Rep.*, **5**, 958–63.
2. Finkbeiner,S. (2011) Huntington ' s Disease. *Cold Spring Harb. Perspect. Biol.*, **3**, 1–24.
3. Gil,J.M. and Rego,A.C. (2008) Mechanisms of neurodegeneration in Huntington's disease. *Eur. J. Neurosci.*, **27**, 2803–20.
4. Vonsattel, Jean Paul,D.M. (1998) Hungtington's disease. *J. Neuropathol. Exp. Neurol.*
5. Lindquist,S. (1986) THE HEAT-SHOCK RESPONSE. *Ann. Rev. Biochem.*, **55**, 1151–91.
6. Muchowski,P.J. and Wacker,J.L. (2005) Modulation of neurodegeneration by molecular chaperones. *Nat. Rev. Neurosci.*, **6**, 11–22.
7. Wyttenbach,A. (2004) Role of Heat Shock Proteins During Polyglutamine Neurodegeneration. *J. Mol. Neurosci.*, **23**, 69–95.
8. Wyttenbach,A., Carmichael,J., Swartz,J., Furlong,R.A., Narain,Y., Rankin,J. and Rubinsztein,D.C. (2000) Effects of heat shock, heat shock protein 40 (HDJ-2), and proteasome inhibition on protein aggregation in cellular models of Huntington's disease. *Proc. Natl. Acad. Sci. U. S. A.*, **97**, 2898–2903.
9. Vos,M.J., Zijlstra,M.P., Kanon,B., van Waarde-Verhagen,M. a W.H., Brunt,E.R.P., Oosterveld-Hut,H.M.J., Carra,S., Sibon,O.C.M. and Kampinga,H.H. (2010) HSPB7 is the most potent polyQ aggregation suppressor within the HSPB family of molecular chaperones. *Hum. Mol. Genet.*, **19**, 4677–93.
10. Warrick,J.M., Chan,H.Y., Gray-Board,G.L., Chai,Y., Paulson,H.L. and Bonini,N.M. (1999) Suppression of polyglutamine-mediated neurodegeneration in Drosophila by the molecular chaperone HSP70. *Nat. Genet.*, **23**, 425–8.
11. Garrido,C., Paul,C., Seigneuric,R. and Kampinga,H.H. (2012) The small heat shock proteins family: the long forgotten chaperones. *Int. J. Biochem. Cell Biol.*, **44**, 1588–92.
12. Hayes,D., Napoli,V., Mazurkie,A., Stafford,W.F. and Graceffa,P. (2009) Phosphorylation dependence of Hsp27 multimeric size and molecular chaperone function. *J. Biol. Chem.*, **284**, 18801–18807.
13. Robertson,A.L., Headey,S.J., Saunders,H.M., Ecroyd,H., Scanlon,M.J., Carver,J. a and Bottomley,S.P. (2010) Small heat-shock proteins interact with a flanking domain to suppress polyglutamine aggregation. *Proc. Natl. Acad. Sci. U. S. A.*, **107**, 10424–9.
14. Carver,J.A., Rekas,A., Thorn,D.C. and Wilson,M.R. (2003) Review Article Small Heat-shock Proteins and Clusterin : Intra- and Extracellular Molecular Chaperones with a Common Mechanism of Action and Function ? *IUBMB Life*, **55**, 661–668.
15. Ecroyd,H. and Carver,J. a (2009) Crystallin proteins and amyloid fibrils. *Cell. Mol. Life Sci.*, **66**, 62–81.
16. Westerheide,S.D. and Morimoto,R.I. (2005) Heat shock response modulators as therapeutic tools for diseases of protein conformation. *J. Biol. Chem.*, **280**, 33097–100.
17. Muchowski,P.J., Schaffar,G., Sittler, a, Wanker,E.E., Hayer-Hartl,M.K. and Hartl,F.U. (2000) Hsp70 and hsp40 chaperones can inhibit self-assembly of polyglutamine proteins into amyloid-like fibrils. *Proc. Natl. Acad. Sci. U. S. A.*, **97**, 7841–6.
18. Satyal,S.H., Schmidt,E., Kitagawa,K., Sondheimer,N., Lindquist,S., Kramer,J.M. and Morimoto,R.I. (2000) Polyglutamine aggregates alter protein folding homeostasis in Caenorhabditis elegans. *Proc. Natl. Acad. Sci. U. S. A.*, **97**, 5750–5.
19. Jana,N.R., Tanaka,M., Wang,G.H. and Nukina,N. (2000) Polyglutamine length-dependent interaction of Hsp40 and Hsp70 family chaperones with truncated N-terminal huntingtin: their role in suppression of

aggregation and cellular toxicity. *Hum. Mol. Genet.*, **9**, 2009–2018.
20. Hay,D.G., Sathasivam,K., Tobaben,S., Stahl,B., Marber,M., Mestril,R., Mahal,A., Smith,D.L., Woodman,B. and Bates,G.P. (2004) Progressive decrease in chaperone protein levels in a mouse model of Huntington's disease and induction of stress proteins as a therapeutic approach. *Hum. Mol. Genet.*, **13**, 1389–1405.
21. Horwitz,J. (2003) Alpha-crystallin. *Exp. Eye Res.*, **76**, 145–153.
22. Rekas,A., Adda,C.G., Andrew Aquilina,J., Barnham,K.J., Sunde,M., Galatis,D., Williamson,N. a, Masters,C.L., Anders,R.F., Robinson,C. V, *et al.* (2004) Interaction of the molecular chaperone alphaB-crystallin with alpha-synuclein: effects on amyloid fibril formation and chaperone activity. *J. Mol. Biol.*, **340**, 1167–83.
23. Waudby,C. a., Knowles,T.P.J., Devlin,G.L., Skepper,J.N., Ecroyd,H., Carver,J. a., Welland,M.E., Christodoulou,J., Dobson,C.M. and Meehan,S. (2010) The interaction of αB-crystallin with mature α-synuclein amyloid fibrils inhibits their elongation. *Biophys. J.*, **98**, 843–851.
24. Hochberg,G.K. a, Ecroyd,H., Liu,C., Cox,D., Cascio,D., Sawaya,M.R., Collier,M.P., Stroud,J., Carver,J. a, Baldwin,A.J., *et al.* (2014) The structured core domain of αB-crystallin can prevent amyloid fibrillation and associated toxicity. *Proc. Natl. Acad. Sci. U. S. A.*, **111**, E1562-70.
25. Wang,J., Xu,G., Li,H., Gonzales,V., Fromholt,D., Karch,C., Copeland,N.G., Jenkins,N. a. and Borchelt,D.R. (2005) Somatodendritic accumulation of misfolded SOD1-L126Z in motor neurons mediates degeneration: αB-crystallin modulates aggregation. *Hum. Mol. Genet.*, **14**, 2335–2347.
26. Hagemann,T.L., Boelens,W.C., Wawrousek,E.F. and Messing,A. (2009) Suppression of GFAP toxicity by alphaB-crystallin in mouse models of Alexander disease. *Hum. Mol. Genet.*, **18**, 1190–9.
27. Muchowski,P.J., Ramsden,R., Nguyen,Q., Arnett,E.E., Greiling,T.M., Anderson,S.K. and Clark,J.I. (2008) Noninvasive measurement of protein aggregation by mutant huntingtin fragments or alpha-synuclein in the lens. *J. Biol. Chem.*, **283**, 6330–6.
28. Tue,N.T., Shimaji,K., Tanaka,N. and Yamaguchi,M. (2012) Effect of alphaB-crystallin on protein aggregation in drosophila. *J. Biomed. Biotechnol.*, **2012**.
29. Zabel,C. (2002) Alterations in the Mouse and Human Proteome Caused by Huntington's Disease. *Mol. Cell. Proteomics*, **1**, 366–375.
30. Ehrlich,M.E. (2012) Huntington's disease and the striatal medium spiny neuron: cell-autonomous and non-cell-autonomous mechanisms of disease. *Neurotherapeutics*, **9**, 270–84.
31. Faideau,M., Kim,J., Cormier,K., Gilmore,R., Welch,M., Auregan,G., Dufour,N., Guillermier,M., Brouillet,E., Hantraye,P., *et al.* (2010) In vivo expression of polyglutamine-expanded huntingtin by mouse striatal astrocytes impairs glutamate transport: A correlation with Huntington's disease subjects. *Hum. Mol. Genet.*, **19**, 3053–3067.
32. Tong,X., Ao,Y., Faas,G.C., Nwaobi,S.E., Xu,J., Haustein,M.D., Anderson,M. a, Mody,I., Olsen,M.L., Sofroniew,M. V, *et al.* (2014) Astrocyte Kir4.1 ion channel deficits contribute to neuronal dysfunction in Huntington's disease model mice. *Nat. Neurosci.*, **17**, 694–703.
33. Boussicault,L., Hérard,A.-S., Calingasan,N., Petit,F., Malgorn,C., Merienne,N., Jan,C., Gaillard,M.-C., Lerchundi,R., Barros,L.F., *et al.* (2014) Impaired brain energy metabolism in the BACHD mouse model of Huntington's disease: critical role of astrocyte-neuron interactions. *J. Cereb. Blood Flow Metab.*, **23**, 1–11.
34. Gray,M., Shirasaki,D.I., Cepeda,C., André,V.M., Wilburn,B., Lu,X.-H., Tao,J., Yamazaki,I., Li,S.-H., Sun,Y.E., *et al.* (2008) Full-length human mutant huntingtin with a stable polyglutamine repeat can elicit progressive and selective neuropathogenesis in BACHD mice. *J. Neurosci.*, **28**, 6182–95.
35. Hagemann,T.L., Boelens,W.C., Wawrousek,E.F. and Messing,A. (2009) Suppression of GFAP toxicity by aB-crystallin in mouse models of Alexander disease. **18**, 1190–1199.
36. Lister,R.G. (1987) The use of a plus-maze to measure anxiety in the mouse. *Psychopharmacology (Berl).*, **92**, 180–185.
37. Larkin, Paul B., Muchowski,P.J. (2012) Genetic Deficiency of Complement Component 3 Does Not Alter Disease Progression in a Mouse Model of Huntington's Disease. *J. Huntingtons. Dis.*, **29**, 997–1003.
38. Bouchard,J., Truong,J., Bouchard,K., Dunkelberger,D., Desrayaud,S., Moussaoui,S., Tabrizi,S.J., Stella,N. and Muchowski,P.J. (2012) Cannabinoid receptor 2 signaling in peripheral immune cells modulates disease onset and severity in mouse models of Huntington's disease. *J. Neurosci.*, **32**, 18259–68.
39. Van Raamsdonk,J.M., Pearson,J., Slow,E.J., Hossain,S.M., Leavitt,B.R. and Hayden,M.R. (2005) Cognitive dysfunction precedes neuropathology and motor abnormalities in the YAC128 mouse model of Huntington's disease. *J. Neurosci.*, **25**, 4169–80.
40. Taketo,M., Schroeder, a C., Mobraaten,L.E., Gunning,K.B., Hanten,G., Fox,R.R., Roderick,T.H., Stewart,C.L., Lilly,F. and Hansen,C.T. (1991) FVB/N: an inbred mouse strain preferable for transgenic

analyses. *Proc. Natl. Acad. Sci. U. S. A.*, **88**, 2065–2069.
41. Osmand,A.P., Berthelier,V. and Wetzel,R. (2006) Imaging polyglutamine deposits in brain tissue. *Methods Enzymol.*, **412**, 106–22.
42. Wellner,P.D. (1993) Adaptive thresholding for the DigitalDesk. *Eur. Tech. Rep.*, **110**, 1–17.
43. Samsi,S., Lozanski,G., Shana'ah,A., Krishanmurthy,A.K. and Gurcan,M.N. (2010) Detection of follicles from IHC-stained slides of follicular lymphoma using iterative watershed. *IEEE Trans Biomed Eng*, **57**, 2609–2612.
44. Slow,E.J., van Raamsdonk,J., Rogers,D., Coleman,S.H., Graham,R.K., Deng,Y., Oh,R., Bissada,N., Hossain,S.M., Yang,Y.Z., *et al.* (2003) Selective striatal neuronal loss in a YAC128 mouse model of Huntington disease. *Hum. Mol. Genet.*, **12**, 1555–1567.
45. Menalled,L., El-Khodor,B.F., Patry,M., Suárez-Fariñas,M., Orenstein,S.J., Zahasky,B., Leahy,C., Wheeler,V., Yang,X.W., MacDonald,M., *et al.* (2009) Systematic behavioral evaluation of Huntington's disease transgenic and knock-in mouse models. *Neurobiol. Dis.*, **35**, 319–36.
46. Kwan,W., Träger,U., Davalos,D., Chou,A., Bouchard,J., Andre,R., Miller,A., Weiss,A., Giorgini,F., Cheah,C., *et al.* (2012) Mutant huntingtin impairs immune cell migration in Huntington disease. *J. Clin. Invest.*, **122**.
47. Crook,Z.R. and Housman,D. (2011) Huntington's disease: can mice lead the way to treatment? *Neuron*, **69**, 423–35.
48. Abada,Y.-S.K., Nguyen,H.P., Ellenbroek,B. and Schreiber,R. (2013) Reversal learning and associative memory impairments in a BACHD rat model for Huntington disease. *PLoS One*, **8**, e71633.
49. Paulsen,J.S., Langbehn,D.R., Stout,J.C., Aylward,E., Ross,C.A., Nance,M., Guttman,M., Johnson,S., MacDonald,M., Beglinger,L.J., *et al.* (2008) Detection of Huntington's disease decades before diagnosis: the Predict-HD study. *J. Neurol. Neurosurg. Psychiatry*, **79**, 874–880.
50. Paulsen,J.S., Ready,R.E., Hamilton,J.M., Mega,M.S. and Cummings,J.L. (2001) Neuropsychiatric aspects of Huntington ' s disease. *J Neurol Neurosurg Psychiatry*, **5**, 310–314.
51. Hahn-Barma,V., Deweer,B., Durr,A., Dode,C., Feingold,J., Pillon,B., Agid,Y., Brice,A. and Dubois,B. (1998) Are cognitive changes the first symptoms of Huntington's disease? A study of gene carriers. *J. Neurol. Neurosurg. Psychiatry*, **64**, 172–177.
52. Lawrence,A.D., Sahakian,B.J., Hodges,J.R., Rosser,A.E., Lange,K.W. and Robbins,T.W. (1996) Executive and mnemonic functions in early Huntington's disease. *Brain*, **119**, 1633–1645.
53. Lawrence,A.D., Hodges,J.R., Rosser,A.E., Kershaw,A., Ffrench-Constant,C., Rubinsztein,D.C., Robbins,T.W. and Sahakian,B.J. (1998) Evidence for specific cognitive deficits in preclinical Huntington's disease. *Brain*, **121**, 1329–1341.
54. Lawrence,A.D., Sahakian,B.J. and Robbins,T.W. (1998) Cognitive functions and corticostriatal circuits: Insights from Huntington's disease. *Trends Cogn. Sci.*, **2**, 379–388.
55. Snowden,J.S., Craufurd,D., Thompson,J. and Neary,D. (2002) Psychomotor, executive, and memory function in preclinical Huntington's disease. *J. Clin. Exp. Neuropsychol.*, **24**, 133–145.
56. Thompson,J.C., Ph,D., Harris,J., Sc,B., Sollom,A.C., Stopford,C.L., Howard,E., Snowden,J.S., Craufurd,D. and Sc,M. (2012) Longitudinal Evaluation of Neuropsychiatric Symptoms in Huntington ' s Disease. *J Neuropsychiatry Clin Neurosci*.
57. Snowden,J.S., Gibbons,Z.C., Blackshaw,A., Doubleday,E., Thompson,J., Craufurd,D., Foster,J., Happé,F. and Neary,D. (2003) Social cognition in frontotemporal dementia and Huntington's disease. *Neuropsychologia*, **41**, 688–701.
58. Pouladi,M. a, Stanek,L.M., Xie,Y., Franciosi,S., Southwell,A.L., Deng,Y., Butland,S., Zhang,W., Cheng,S.H., Shihabuddin,L.S., *et al.* (2012) Marked differences in neurochemistry and aggregates despite similar behavioural and neuropathological features of Huntington disease in the full-length BACHD and YAC128 mice. *Hum. Mol. Genet.*, **21**, 2219–32.
59. Miller,J., Arrasate,M., Brooks,E., Libeu,C.P., Legleiter,J., Hatters,D., Curtis,J., Cheung,K., Krishnan,P., Mitra,S., *et al.* (2012) Identifying polyglutamine protein species in situ that best predict neurodegeneration. *Nat. Chem. Biol.*, **8**, 318–318.
60. Miller,J., Arrasate,M., Shaby,B.A., Mitra,S., Masliah,E. and Finkbeiner,S. (2010) Quantitative relationships between huntingtin levels, polyglutamine length, inclusion body formation, and neuronal death provide novel insight into huntington's disease molecular pathogenesis. *J. Neurosci.*, **30**, 10541–10550.
61. Gu,X., Greiner,E.R., Mishra,R., Kodali,R., Osmand,A., Finkbeiner,S., Steffan,J.S., Thompson,L.M., Wetzel,R. and Yang,X.W. (2009) Serines 13 and 16 Are Critical Determinants of Full-Length Human Mutant Huntingtin Induced Disease Pathogenesis in HD Mice. *Neuron*, **64**, 828–840.

62. Gourfinkel-An,I., Vila,M., Faucheux,B., Duyckaerts,C., Viallet,F., Hauw,J.J., Brice,A., Agid,Y. and Hirsch,E.C. (2002) Metabolic changes in the basal ganglia of patients with Huntington's disease: An in situ hybridization study of cytochrome oxidase subunit I mRNA. *J. Neurochem.*, **80**, 466–476.
63. Herndon,E.S., Hladik,C.L., Shang,P., Burns,D.K., Raisanen,J. and White,C.L. (2009) Neuroanatomic profile of polyglutamine immunoreactivity in Huntington disease brains. *J. Neuropathol. Exp. Neurol.*, **68**, 250–261.
64. Ouimet,C.C., Langley-Gullion,K.C. and Greengard,P. (1998) Quantitative immunocytochemistry of DARPP-32-expressing neurons in the rat caudatoputamen. *Brain Res.*, **808**, 8–12.
65. Labbadia,J. and Morimoto,R.I. (2013) Huntington's disease: Underlying molecular mechanisms and emerging concepts. *Trends Biochem. Sci.*, **38**, 378–385.
66. Arrigo,A.P., Simon,S., Gibert,B., Kretz-Remy,C., Nivon,M., Czekalla,A., Guillet,D., Moulin,M., Diaz-Latoud,C. and Vicart,P. (2007) Hsp27 (HspB1) and αB-crystallin (HspB5) as therapeutic targets. *FEBS Lett.*, **581**, 3665–3674.
67. den Engelsman,J., Keijsers,V., de Jong,W.W. and Boelens,W.C. (2003) The small heat-shock protein alpha B-crystallin promotes FBX4-dependent ubiquitination. *J. Biol. Chem.*, **278**, 4699–704.
68. Lin,D.I., Barbash,O., Kumar,K.G.S., Weber,J.D., Harper,J.W., Klein-Szanto,A.J.P., Rustgi,A., Fuchs,S.Y. and Diehl,J.A. (2006) Phosphorylation-Dependent Ubiquitination of Cyclin D1 by the SCFFBX4-αB Crystallin Complex. *Mol. Cell*, **24**, 355–366.
69. Kamradt,M.C., Lu,M., Werner,M.E., Kwan,T., Chen,F., Strohecker,A., Oshita,S., Wilkinson,J.C., Yu,C., Oliver,P.G., *et al.* (2005) The small heat shock protein aB-crystallin is a novel inhibitor of TRAIL-induced apoptosis that suppresses the activation of caspase-3. *J. Biol. Chem.*, **280**, 11059–66.
70. Mao,Y.-W., Liu,J.-P., Xiang,H. and Li,D.W.-C. (2004) Human alphaA- and alphaB-crystallins bind to Bax and Bcl-X(S) to sequester their translocation during staurosporine-induced apoptosis. *Cell Death Differ.*, **11**, 512–526.
71. Kamradt,M.C., Chen,F., Sam,S. and Cryns,V.L. (2002) The small heat shock protein aB-crystallin negatively regulates apoptosis during myogenic differentiation by inhibiting caspase-3 activation. *J. Biol. Chem.*, **277**, 38731–38736.
72. Kamradt,M.C., Chen,F. and Cryns,V.L. (2001) The Small Heat Shock Protein aB-Crystallin Negatively Regulates Cytochrome c- and Caspase-8-dependent Activation of Caspase-3 by Inhibiting Its Autoproteolytic Maturation. *J. Biol. Chem.*, **276**, 16059–16063.
73. Ghosh,J.G., Shenoy,A.K. and Clark,J.I. (2007) Interactions between important regulatory proteins and human alphaB crystallin. *Biochemistry*, **46**, 6308–6317.
74. Ghosh,J.G., Houck,S.A. and Clark,J.I. (2007) Interactive Domains in the Molecular Chaperone Human aB Crystallin Modulate Microtubule Assembly and Disassembly. *PLoS One*, **2**.
75. DiFiglia,M., Sapp,E., Chase,K.O., Davies,S.W., Bates,G.P., Vonsattel,J.P. and Aronin,N. (1997) Aggregation of huntingtin in neuronal intranuclear inclusions and dystrophic neurites in brain. *Science*, **277**, 1990–1993.
76. Arrasate,M., Mitra,S., Schweitzer,E.S., Segal,M.R. and Finkbeiner,S. (2004) Inclusion body formation reduces levels of mutant huntingtin and the risk of neuronal death. *Nature*, **431**, 805–10.
77. Takahashi,T. and Mihara,H. (2008) Peptide and protein mimetics inhibiting amyloid ??-peptide aggregation. *Acc. Chem. Res.*, **41**, 1309–1318.
78. Quraishe,S., Asuni, a, Boelens,W.C., O'Connor,V. and Wyttenbach, a (2008) Expression of the small heat shock protein family in the mouse CNS: differential anatomical and biochemical compartmentalization. *Neuroscience*, **153**, 483–91.
79. Quraishe,S. (2010) The sHsp expression signature in the brain and modulation in models of chronic neurodegeneration.
80. Lanneau,D., de Thonel,A., Maurel,S., Didelot,C. and Garrido,C. (2007) Apoptosis versus cell differentiation: role of heat shock proteins HSP90, HSP70 and HSP27. *Prion*, **1**, 53–60.
81. Kore,R. a. and Abraham,E.C. (2014) Inflammatory cytokines, interleukin-1 beta and tumor necrosis factor-alpha, upregulated in glioblastoma multiforme, raise the levels of CRYAB in exosomes secreted by U373 glioma cells. *Biochem. Biophys. Res. Commun.*, **453**, 326–331.
82. Frühbeis,C., Fröhlich,D. and Krämer-Albers,E.M. (2012) Emerging roles of exosomes in neuron-glia communication. *Front. Physiol.*, **3 APR**, 1–7.
83. Sreekumar,P.G., Kannan,R., Kitamura,M., Spee,C., Barron,E., Ryan,S.J. and Hinton,D.R. (2010) αB crystallin is apically secreted within exosomes by polarized human retinal pigment epithelium and provides neuroprotection to adjacent cells. *PLoS One*, **5**.

84. Chan,C.S. and Surmeier,D.J. (2014) Astrocytes go awry in Huntington's disease. *Nat. Neurosci.*, **17**, 641–2.
85. Zhang,Y. and Barres,B. a. (2010) Astrocyte heterogeneity: An underappreciated topic in neurobiology. *Curr. Opin. Neurobiol.*, **20**, 588–594.
86. Lobsiger,C.S. and Cleveland,D.W. (2007) Glial cells as intrinsic components of non-cell-autonomous neurodegenerative disease. *Nat. Neurosci.*, **10**, 1355–1360.

3.6. Supplemental Data

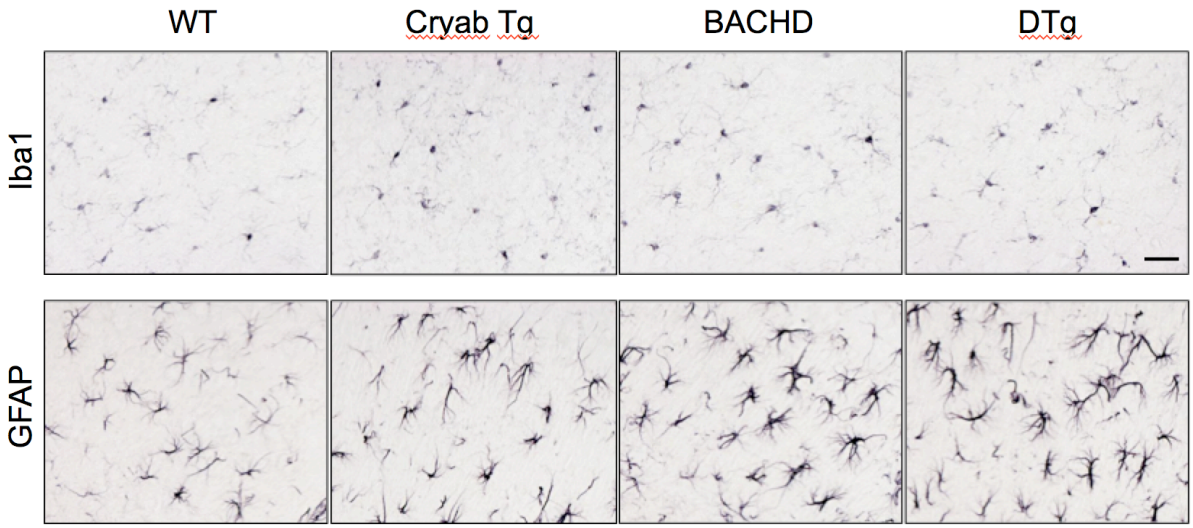

Supplementary Figure S1 – BACHD mice brains do not present microgliosis and astrogliosis.
Representative staining of microglia Iba1-positive cells and GFAP-positive cells in WT (n=5), Cryab Tg (n=5), BACHD (n=8), DTg (n=7).
Representative light micrographs of Iba1 (top panel) and of GFAP (bottom panel) immunostaining. Despite some minimal astrogliosis found in the BACHD and DTg groups, no obvious and significant differences in inflammation - microgliosis (Iba1) or astrogliosis (GFAP) – were found between the 4 different mice groups.
Each field is 600 x 600 µm, and the scale bar represents 20 µm.

For striatal and cortical counts:

MatLab Script for Image Analyses

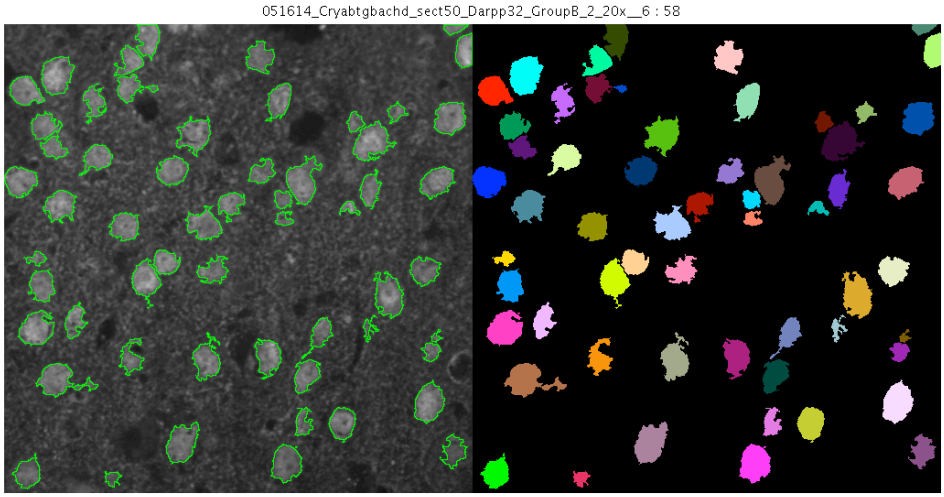

Supplementary Figure S2. Example of the files obtained from our cell counting analyses using a Matlab script. On the left panel, we have the result for number of cells outlined in green. In the right panel of the figure we are showing the individual cells that were extracted. Different colors show different cells. The color feature helps reviewing and manual curating the final counts of cells. (e.g, removing noise from the image).

Supplemental Tables

Table S1. Cohen's *d* and effect-size correlation, r_{YI} for Figure 4 - αBc overexpression decreases soluble levels of mHtt in BACHD mice.
Values (mean ± SD): WT (0.02 ± 0.009), Cryab Tg (0.03 ± 0.01), BACHD (1.2 ± 0.04), DTg (0.89 ± 0.12).

Groups	Cohen's d	Effect size r
WT vs Cryab Tg	-1.53	-0.60
WT vs BACHD	-38.29	-0.99
WT vs DTg	-8.98	-0.97
Cryab Tg vs BACHD	-37.14	-0.99
Cryab Tg vs DTg	-8.79	-0.98
BACHD vs DTg	3.02	-0.83

Table S2. Cohen's *d* and effect-size correlation, r_{YI} for Figure 4 - αBc overexpression reduces the size of S830 inclusion bodies in BACHD mice.
Values (mean ± SD): BACHD (236.3 ± 53.52), DTg (79.71 ± 16.51)

Groups	Cohen's d	Effect size r
BACHD vs DTg	3.95	0.89

Table S3. Cohen's *d* and effect-size correlation, r_{YI} for Figure 4 - αBc overexpression rescues the number of DARPP-32+ cells in the striatum of the DTg mice.
Values (mean ± SD): WT (48.14 ± 6.26), Cryab Tg (46.19 ± 6.81), BACHD (42.10 ± 10.76), DTg (47.27 ± 7.21)

Groups	Cohen's d	Effect size r
WT vs Cryab Tg	0.29	0.15
WT vs BACHD	0.69	0.32
WT vs DTg	0.13	0.06
Cryab Tg vs BACHD	0.45	0.22
Cryab Tg vs DTg	-0.15	-0.08
BACHD vs DTg	-0.56	-0.27

Table S4. Cohen's *d* and effect-size correlation, r_{YI} for Figure 4 - αBc over-expression rescues the number of NeuN+ cells in the cortex of the DTg mice.
Values (mean ± SD): WT (93.27 ± 9.27), Cryab Tg (90.52 ± 9.91), BACHD (75.79 ± 13.24), DTg (89.71 ± 8.48)

Groups	Cohen's d	Effect size r
WT vs Cryab Tg	0.28	0.13
WT vs BACHD	1.37	0.56
WT vs DTg	0.39	0.19
Cryab Tg vs BACHD	1.15	0.49
Cryab Tg vs DTg	0.09	0.04
BACHD vs DTg	-1.13	-0.49

Table S5. Cohen's *d* and effect-size correlation, r_{YI} for Figure 4 - αBc over-expression rescues the number of NeuN+ cells in the striatum of the DTg mice.
Values (mean ± SD): WT (69.74 ± 6.74), Cryab Tg (70.32 ± 6.72), BACHD (61.82 ± 12.7), DTg (69.84 ± 11.41)

Groups	Cohen's d	Effect size r
WT vs Cryab Tg	-0.09	-0.04
WT vs BACHD	0.78	0.36
WT vs DTg	-0.01	-0.01
Cryab Tg vs BACHD	0.84	0.39
Cryab Tg vs DTg	0.05	0.02
BACHD vs DTg	-0.65	-0.31

Chapter 4.

Cell non-autonomous potential antioxidant effects of αB-crystallin in HD

4.1. Introduction

The mechanism by which mHtt causes neuronal dysfunction and degeneration in HD is still not fully understood. Nevertheless, among other essential cellular pathways such as apoptosis, oxidative stress, inflammation, mitochondrial and metabolic dysfunction, have been shown to play important roles in the pathogenesis of HD (1, 2).

Oxidative stress is one of several dysfunctional mechanisms described in HD (3) (1), which may result from impaired mitochondrial function, due to interactions with mHtt (4) and imbalanced redox homeostasis. Altered oxidative stress have been observed in both central and peripheral samples of HD patients (5) and in some animal models of the disease (6). In addition, a study in primary cell culture models from BACHD mice showed that mHtt does not directly affect metabolic activity in a cell autonomous manner (7). In fact, co-culture of neurons with astrocytes from WT or BACHD mice identified mutant astrocytes as a source of adverse non-cell autonomous effects on neuron energy metabolism possibly by increasing oxidative stress. These results suggest that astrocyte-to-neuron signaling is involved in early metabolic alterations in HD (7). These data are in agreement with our findings in Chapter 3 that show the protective effect of astrocytic overexpression of αBc in the BACHD mouse model may occur through a cell non-autonomous manner (8).

αBc is a pleiotropic protein, and in addition to chaperone activity, αBc performs multiple other functions: prevents oxidative stress-induced cell death (9–12), protects from GFAP toxicity and glutamate excitotoxicity (13), inhibits inflammation (14–17), prevents disruption of cytoskeletal assembly (18), protects against hydrogen peroxide (H_2O_2) damage (19) by inhibiting caspase-3 activation.

Here, we explored the cytoprotective role of αBc against various stresses such as oxidative stress and modulation of cell death and mHtt-induced downstream pathways in the BACHD mouse model.

To better understand whether astrocytic αBc overexpression and astrocyte–neuron interactions modulate neuropathological deficits in BACHD, we used caspase-3 expression and activity as an apoptotic marker, measured carbonyl content as a measurement for oxidative stress, and other HD pathological markers, in brain tissue from our mice cohort as well as primary neurons and astrocytes cultures from the same cohort. Our results suggest that BACHD do not exhibit strong phenotypes of caspase-3 activation or increased levels of carbonylated proteins. However, we observed a protective trend of

astrocytic αBc in BACHD mice. Our data suggests that αBc antioxidant properties may play a role in our BACHD model in a cell non-autonomous manner.

4.2. Materials and Methods

Cell culture

Primary astrocytes

Highly purified astrocytes cultures were prepared from 1- or 2-day-old pups from WT, Cryab Tg, BACHD and DTg mice of either sex as previously described (20). Briefly, forebrains were removed aseptically from the skulls, the meninges were carefully excised under a dissecting microscope and the neocortex was dissected free of brainstem, thalamus, striatum, and hippocampus. The cells were dissociated by passage through needles of decreasing gauge size three times with a 5-ml syringe. The cells were seeded on six-well plates in Dulbecco's Modified Eagle's medium (DMEM Life Technologies) containing 5.5 mM glucose and supplemented with 10% fetal bovine serum, 2 mM L-glutamine (Gibco, Life Technologies) and antibiotics (Penicillin-Streptomycin, Gibco, Life Technologies) in a final volume of 2 ml/well and incubated at 37 °C in an atmosphere containing 5% CO_2/95% air. The culture medium was renewed 3 to 4 days after seeding and subsequently three times per week. Cultures were used between 19 to 21 DIV.

Neuron–Astrocyte Cell-Insert Coculture

Astrocyte cultures were prepared as described above. After 10 days in vitro, and 1 week before neuronal culture preparation, astrocytes were treated with trypsin and seeded on cell culture inserts (35-3102, Falcon) with 1 mm pores. Primary culture of cortical neurons was made from embryonic days 18-19 (E18-19) mouse embryos. Timed pregnant females from our BACHD and Cryab Tg cohort mice were sacrified with isoflurane and embryos quickly removed and dissected on cooled Hank's balanced sodium salts without Ca^{2+} and Mg^{2+}. Cortices were isolated and incubated for 15min at 37ºC in 0.3mg/ml DNase I (Sigma-Aldrich). Tissues were mechanically dissociated with P1000 and P200 pipettes. Cells were finally concentrated by centrifugation (20ºC, 10minutes, 1,000g) and resuspended in serum-free Neurobasal medium supplemented with 2% B27 supplement (Invitrogen, Carlsbad, CA, USA), 1% antibiotic–antifungal mixture (Invitrogen) and 0.5mM L-glutamine (Sigma-Aldrich). Cells were plated at a density of $2x10^5$ cells/cm2 in 12- or 24-well plates coated with 50mg/ml of poly-D-lysine (Sigma Aldrich). Astrocytes

inserts were placed onto neurons 2 days after neurons seeding. Cultures were used for experiment 13 days after neuron seeding.

Genotyping

Mouse-tail DNA was analyzed by PCR to determine the genotypes. The BACHD transgene was identified as described in the section 3.2 Material and Methods, Chapter 3. The Cryab transgene was identified as described (21).

Quantitative real-time PCR (QPCR)

Mice were anesthetized with Avertin (tribromoethanol, 250 mg per kg) and perfused transcardially with 0.9% saline, and brains were removed. RNA was harvested from frozen mice striatum and cortex (striatum was microdissected as described (22) with an RNeasy Mini kit (Qiagen, USA), according to the manufacturer's instructions. RNA was immediately reverse transcribed to cDNA with Multiscribe™ reverse transcriptase (Applied Biosystems, USA) and stored at −20°C. For HD associated gene expression studies and quantification of caspase-3 mRNA, quantitative real-time PCR (QPCR) was performed using FAST SYBR Green Mastermix (Applied Biosystems, USA) as provided by the manufacturer and thermal cycling was performed using an ABI Prism 7900 HT Sequence Detector (Applied Biosystems, USA) with the following program: UNG activation (50 °C for 2 min), initial denaturation (95 °C for 10 min), and then 40 cycles of denaturation (95 °C for 15 seconds) then annealing and extension (60 °C for 1 min), followed by a disassociation stage for melting curve analysis. Analysis of fluorescence data from genes of interest and from the control gene ATP synthase subunit 5b (Atp5b) (23), was performed using the online analysis tool QPCR (24). Amplification efficiency was calculated for each primer pair using serially diluted standards. This efficiency was used to convert threshold cycle (number of PCR cycles required to reach an arbitrary threshold fluorescence value) into relative gene expression using the efficiency corrected delta Ct method as described (25). For each sample, expression of the gene of interest was normalized to the control gene Atp5b. All data are expressed as a fold change compared to WT mice, and all primers are listed in Table 1. Primers were designed using the online Roche Universal Probe Library Assay Design Center (Roche Applied Science, USA) or the online tool Primer-BLAST (NCBI). Primer specificity was evaluated using Primer-BLAST (NCBI) and melting curve analysis.

Protein extraction

Mice were anesthetized with Avertin (tribromoethanol, 250 mg per kg) and perfused transcardially with 0.9% saline. Brains were removed, micro-dissected in ice-cold PBS and immediately. Frozen mice striatum and cortex were homogenized in ice-cold standard RIPA buffer (150 mM NaCl, 1% NP-40, 0.1% sodium dodecyl sulfate, 0.5% sodium deoxycholate, 50 mM Tris, pH 7.4) supplemented with complete protease inhibitors (Roche Applied Science) and spun at 14,000 × g for 30 min at 4 °C.

Western blotting

Proteins (10–20 μg/well) from brain tissue and primary cultures were separated on a 4–12% NuPAGE Bis-Tris gel (Life Technologies) and transferred onto nitrocellulose membranes, which were incubated for 1 h in 5% bovine serum albumin (Sigma-Aldrich) diluted in Tris-buffered saline containing 0.05% Tween (BSA-TBST). Immunoblots were probed and incubated overnight at 4 °C in rabbit anti-αB-crystallin (1:1,000, Stressgen), or anti-B-tubulin (Abcam, ab6046, 1:20,000) antibodies diluted in BSA-TBST. Appropriate IRDye secondary antibodies (LI-COR Biosci) were used at a 1:20,000 dilution. Images were captured with the Odyssey CLx (LI-COR Biosci).

Caspase-3 activity assay

Caspase-3 activity was determined by colorimetric assay (R&D Systems, Minneapolis, MN), according to the manufacturer's instructions. In brief, we tested brain tissue (striatum and cortex) as well primary neurons and astrocytes. As we did not observed caspase-3 upregulation in BACHD mice, we later induced apoptosis by adding 300 mM H_2O_2 to primary cultures for 1 h. Cells were then harvested and aliquots of 2.5x 10^6 cells were used for caspase-3 activity assays. Cell lysates were incubated in the presence or absence of 50 ml DEVD-pNA for 1 h at 37ºC, and absorbance was measured at 405 nm using a micro-plate reader. Not induced and induced cells without substrate served as background controls. In addition, induced cells were incubated with DEVD-DHO, an inhibitor of caspase-3, to correlate protease activity and signal detection.

Protein carbonyl content assay

We measured protein carbonyl groups as biomarkers of oxidative stress (26).

Protein carbonyls were measured from tissue and primary cell homogenates using 2,4-dinitrophenylhydrazine (DNPH) derivatization, according to the manufacturer's directions (Protein Carbonyl Assay Kit, cat#ab126287; Abcam).

Briefly, we tested brain tissue (striatum and cortex) as well primary neurons and astrocytes. 100 µl of sample containing approximately 0.5-2 mg protein per assay, including a reagent background control by using 100 µl of dH_2O alone were added to 100 µl and incubated for 10 min. TCA and acetone were added for washing steps to remove the nucleic acids that could interfere in the reaction. After the washing steps, 200 µl of Guaninine solution was added and samples were sonicated briefly and protein was re-solubilized easily. After a very brief spin, 100 µl of each sample was transferred to a 96-well plate. OD was measured at 375 nm in a micro-plate reader.

4.3. Results

4.3.1. BACHD mice do not induce upregulation of Caspase-3 and BACHD astrocytes overexpressing αBc are more resistant to H_2O_2-induced toxicity

In vitro cell studies showed that αBc confers protection against apoptosis through the regulation of caspase-3, a proapoptotic factor (19). In addition, αBc was also shown to sequester the p53 tumor suppressor, thus preventing apoptosis (27).

Caspase-3 expression is upregulated in brains of a mouse model of HD, R6/2 mice (28), and a recent study has also reported the same effect in hearts of aged BACHD (29). Thus, caspase-3 upregulation may play a role in HD progression. We next wanted to determine whether BACHD mice brain displayed increase of caspase-3 levels, and if αBc over-expression could have a protective effect in our DTg mouse brains when compared to BACHD.

Reverse transcriptase–quantitative polymerase chain (RT-qPCR) reaction was performed on cortical and striatal samples from brain lysates of the Cryab Tg crossed with BACHD that we studied in Chapter 3.

Surprisingly, the levels of caspase-3 were not significantly upregulated in both cortex and striatum of BACHD brain lysates when compared to the control littermates WT (Fig. 1A). This suggests that aged brains of BACHD mice do not present transcriptional upregulation of caspase-3 in the most sensitive brain regions of HD. We have also

analyzed the protein levels, but did not find cleaved caspase-3 in blots of brain lysates from our mice cohort (data not shown).

To rule out that there could be differences in caspase-3 activity, we then measured caspase-3 activity using a common colorimetric assay. We have used brain lysates from striatum and cortex, as well as primary astrocytes and neurons from our mice cohort, to determine if the stage of the disease (primary cells vs aged brains) could be having a role on caspase-3 expression and/or activity (Fig. 1B,C). Our results showed no caspase-3 activity induction in both striatum and cortex of BACHD aged brains (Fig 1B), and in primary neurons and astrocytes (Fig. 1C) from the mice cohort. These results suggest that full-length mHtt in aged BACHD and also in primary cultures (neurons and astrocytes) does not directly or indirectly modify levels and activity of caspase-3.

Oxidative stress is mediated by increases in reactive oxygen species (ROS) including superoxide (O_2^-), hydrogen peroxide (H_2O_2), hydroxyl radical (OH^-), and reactive nitrogen species such as peroxynitrite ($ONOO^-$). We then decided to directly insult the primary cultures of neurons and astrocytes with H_2O_2 to induce oxidative stress in these cells as shown previously (19), and determine if αBc could exert a protective effect against H_2O_2 – induced toxicity, as previously observed in studies in cell lines (9, 19). We next wanted to demonstrate that our Cryab Tg and DTg primary astrocytes were over-expressing αBc. We observed a 6-7 fold upregulation of αBc in both Cryab Tg and DTg when compared to WT and BACHD (Fig1 D,E). In contrast, neuronal population of both αBc transgenics did not show upregulation of αBc (data not shown) supporting that any protective effect of αBc, driven by a GFAP promoter, is a cell non-autonomous effect. After inducing primary neurons and astrocytes with 300 uM of H_2O_2, caspase-3 activity increased in both cell types. Primary neurons and astrocytes are sensitive to the toxicity induced by H_2O_2 resulting in caspase-3 activity upregulation ~5 fold for neurons and ~4 in astrocytes, when compared to no treatment conditions for each genotype (Fig.1F). Despite responding to the toxic stimulus caused by H_2O_2, the different genotypes, expression of mHtt and/or αBc, in primary neurons did not play a role in this response. In contrast, in astrocytes, the αBc transgenics were more resistant to the toxic effect of H_2O_2 treatment and showed a significant decrease on caspase-3 activity when compared to WT and BACHD, respectively (Fig. 1F). DTg astrocytes showed a partial rescue against H_2O_2 damage suggesting endogenous mHtt expression in DTg astrocytes decreased their antioxidant effect when compared to Cryab Tg. These results support the potential

antioxidant role of astrocytic αBc against H_2O_2 – induced toxicity as previously reported (19).

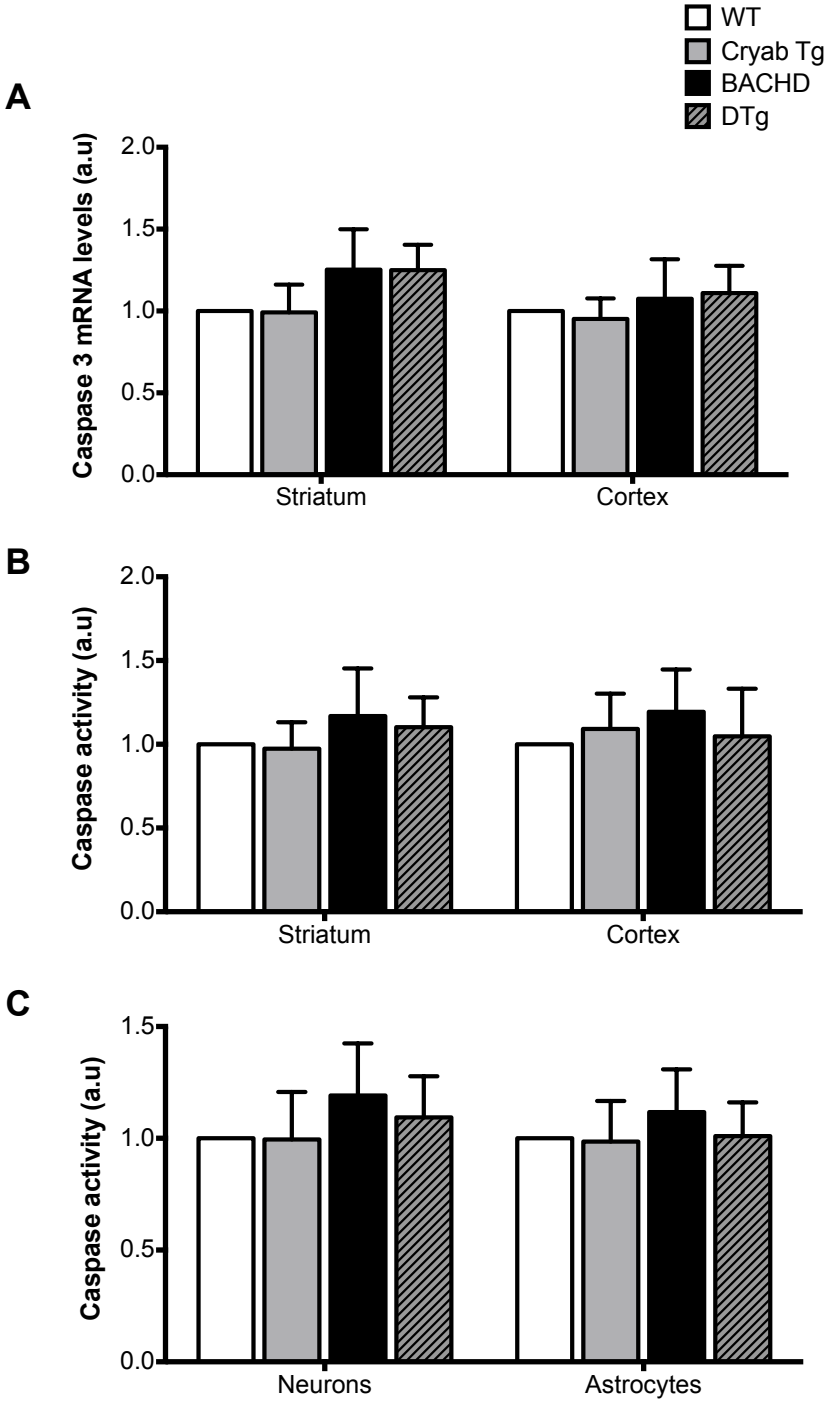

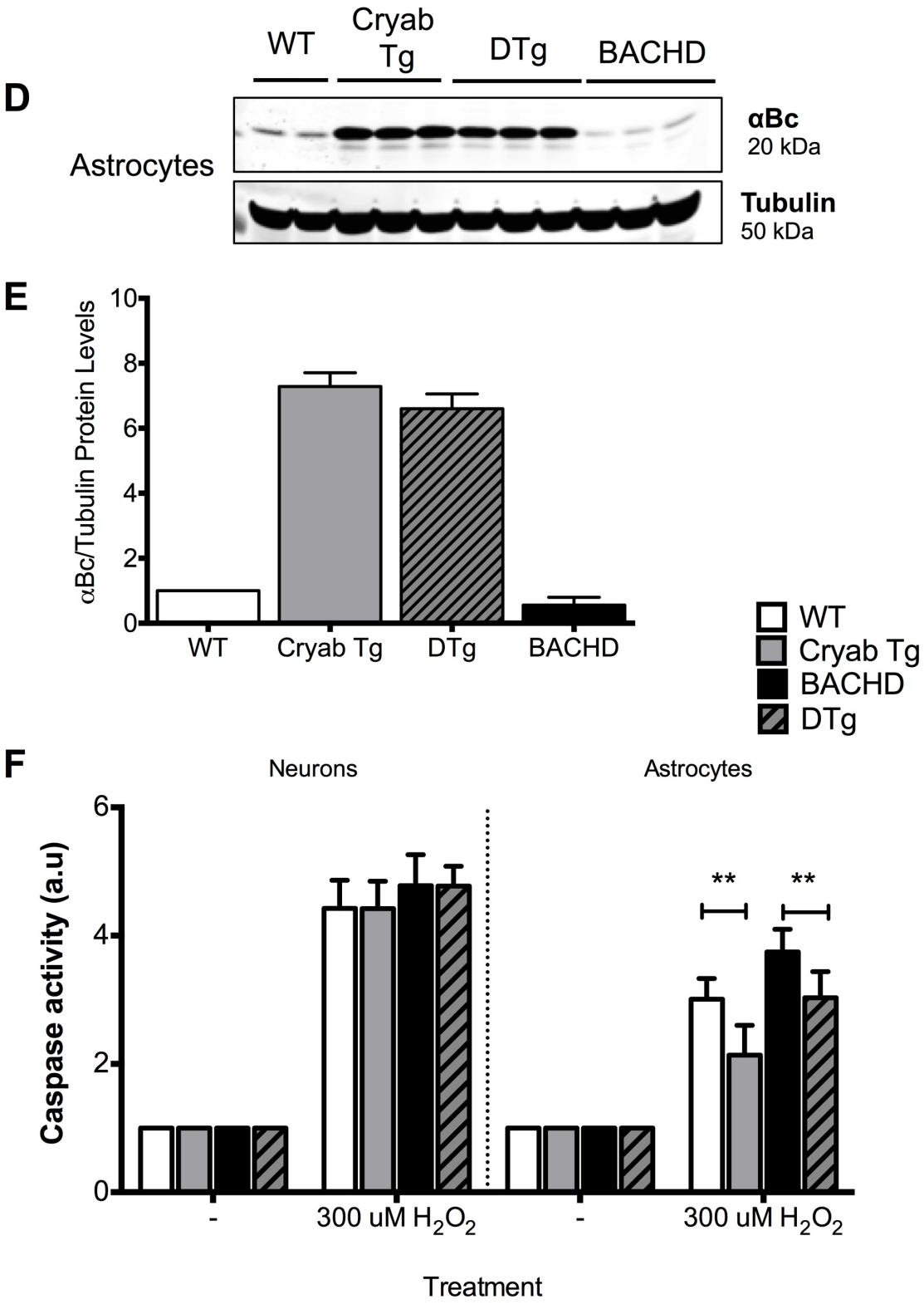

Figure 1. BACHD mice do not have upregulation of caspase-3 and BACHD astrocytes over-expressing αBc are more resistant to H_2O_2 induced toxicity.

Caspase-3 expression was evaluated by QPCR (A) and caspase-3 activities using a colometric assay (B,C and F) in striatum and cortex of 13 month-old brains of WT, Cryab Tg, BACHD and DTg (n=6 per genotype), as well as neurons and astrocytes primary cultures of these mice (n=5 embryos/pups). (A) Caspase-3 mRNA is not upregulated in BACHD mice. Caspase-3 mRNA

expression was not statistically significant different among the different genotypes (when normalized to WT). (B) Caspase-3 activity was also not induced in striatum and cortex of any group of our mice cohort. (C) Despite a trend for an increase of caspase-3 activity in BACHD astrocytes, no statistical difference was observed in both neurons and astrocytes from WT, Cryab Tg, BACHD and DTg (when normalized to WT). Caspase-3 activity was not different among the different genotypes. (C, D) Western Blot and quantification of showing 6/7 fold over-expression in αBc protein levels in astrocytes of Cryab Tg and DTg, which is expression is driven by a GFAP promoter. (F) Since expression of mHtt on BACHD was not enough induce caspase-3 activity, oxidative stress was induced on primary neurons and astrocytes by H_2O_2, treatment mHtt. Both primary neurons and astrocytes were sensitive to the toxic insult, but astrocytes were significantly more resistant to stress than neurons. αBc over –expression transgenics (Cryab Tg and DTg) exhibited an antioxidant and protective effect when compared to WT and BACHD. DTg astrocytes were more resistant than BACHD astrocytes when exposed to H_2O_2, treatment.
Data represent Means±SD. Two –way nova analysis were performed followed by multiple comparison by Tukey post-hoc tests. Statistical significance was achieved when $p< 0.05$.

4.3.2. BACHD astrocytes affect neuronal carbonyl content by a non-cell autonomous mechanism

Oxidative stress and damage occurs in cells, animal models and tissues from HD patients (2, 5, 6). Carbonyl groups are initiated into proteins by oxidative reactions of nitrogen oxides or by metal-catalysed oxidation in the tissue. These are an important and immediate biomarker of oxidative stress (30, 31). The DNP hydrazones (DNPH) tagging of protein carbonyls has been a common measure of oxidative stress (30). A recent study reported that BACHD astrocytes increased the expression of carbonyl residues in both WT and BACHD neurons. These results suggest that mutant astrocytes may be the source of adverse non-cell autonomous effects on neuron dysfunction and death (7). To further investigate the potential of αBc to modulate oxidative stress *in vivo*, we used a protein carbonyl content assay. We wanted to determine first, whether protein carbonylation levels were altered in BACHD brains when compared with WT at 13 months; and second, whether this could be attenuated by astrocytic αBc over-expression (Fig. 2A). Presence of carbonyl groups, marker for oxidative stress (26), was measured in the 13 months brain regions, striatum and cortex, of WT,Cryab Tg, BACHD and DTg. Expression of mHtt in both striatum and cortex of BACHD and DTg mice failed to induce upregulation of carbonyl protein content. (Fig. 2A). We then performed the same experiment on primary neurons and astrocytes from our mice cohort (Fig 2B). Despite a trend for an increase of carbonyl content, especially in BACHD astrocytes, we did not detect statistically significant difference on both neurons and astrocytes from WT, Cryab Tg, BACHD and DTg (when normalized to WT). Interestingly, a recent study (7) using neuron-astrocyte

co-culture system has reported that BACHD astrocytes are the source of oxidative stress (ROS and carbonyl groups formation) in both WT and BACHD neurons. This study suggested a cell non-autonomous adverse effect from mHtt expressed astrocytes in neuronal populations that are more prone to cell death (7, 32).

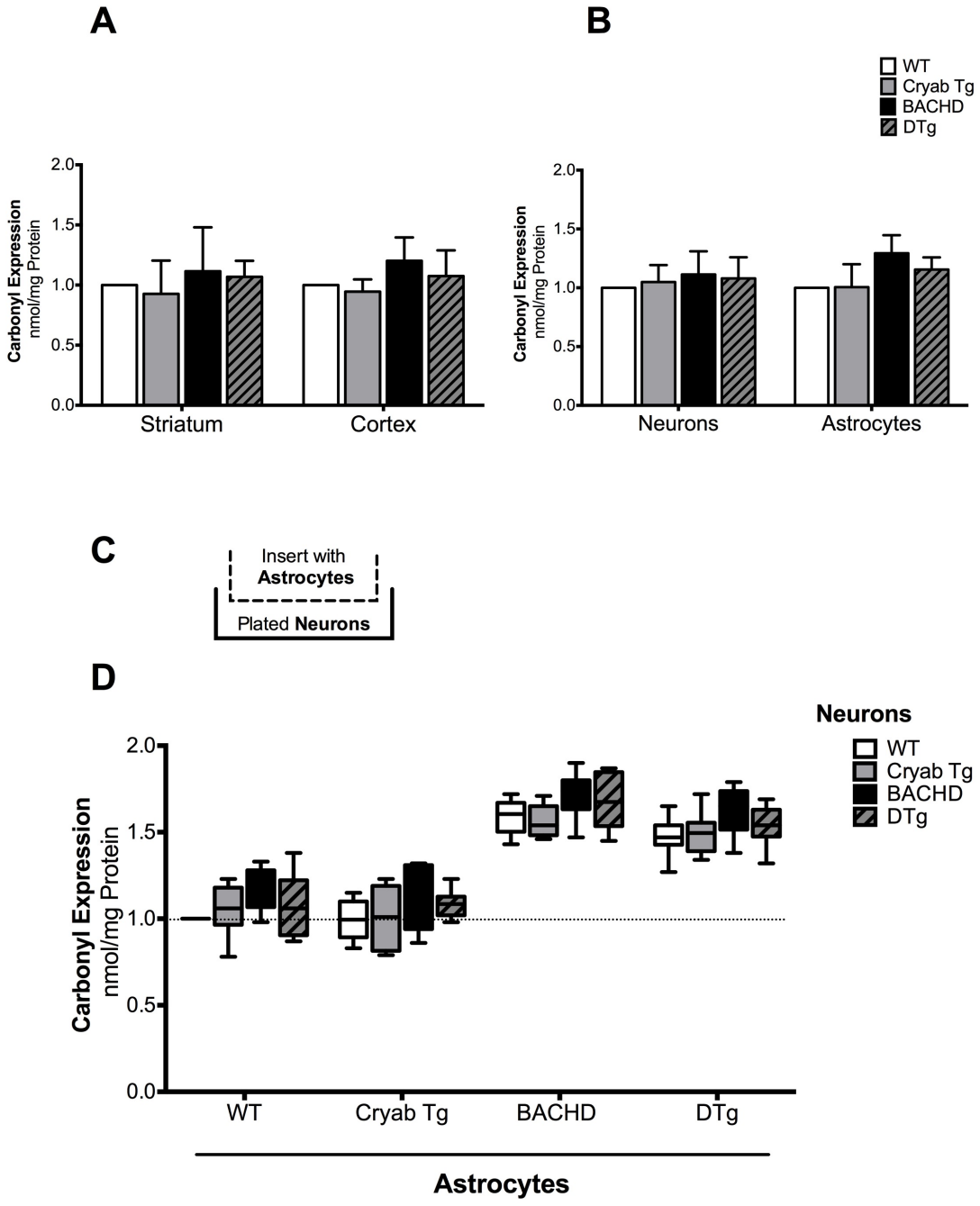

Figure 2. BACHD astrocytes affect neuronal carbonyl content by a non-cell autonomous mechanism. (A) BACHD brains do not induce upregulation of carbonyl protein content. Presence of carbonyl groups, marker for oxidative stress, was measured in the 13 mo brain regions, striatum and cortex, of WT,Cryab Tg, BACHD and DTg (n=6 per genotype). Carbonyl expression was not statistically significant different among the different genotypes. (when normalized to WT). (B) Same assay was then measured in neuronal and astrocytic primary cultures obtained from same

mice cohort (n=5 different embryos/pups). Despite a trend for an increase of carbonyl content in BACHD astrocytes, no statistical significant difference was observed in both neurons and astrocytes from WT, Cryab Tg, BACHD and DTg (when normalized to WT). Carbonyl expression was not different among the different genotypes. (C) Diagram for Co-Culture experiments. (D) BACHD and DTg astrocytes affected neuronal carbonyl content by a non-cell autonomous mechanism. αBc overexpression did not confer a protective effect against carbonyl groups formation and hence oxidative damage was present in neuronal population exposed to both BACHD and DTg astrocytes. Data represent Means±SD. Two –way nova analysis were performed followed by multiple comparison by Tukey post-hoc tests. Statistical significance was achieved when $p< 0.05$.

We decided to test this system (Fig. 2C) in our model, to evaluate whether BACHD astrocytes could induce neuronal toxicity through carbonyl formation, and whether αBc astrocytic over-expression could rescue the toxic effects (Fig 2D). As observed before, BACHD astrocytes were able to significantly affect neuronal carbonyl content in WT, Cryab, BACHD and DTg populations, by a non-cell autonomous mechanism. However, αBc overexpression did not confer protective effect against carbonyl groups formation and therefore oxidative stress induced by carbonyl content expression was present in all neuronal populations exposed to both BACHD and DTg astrocytes (Fig. 2D).

4.3.3. The levels of HD pathology-related markers is not altered in the brains of BACHD mice

To gain a broader understanding of the neuropathological status, as well as transcriptional dysregulation present in HD (33–35), we used QPCR and western-blot to quantify mRNA and protein levels, respectively, of HD related genes in cortex and striatum from 13 month old WT, Cryab Tg, BACHD and DTg mice. We chose genes shown to be involved in diverse pathomechanisms in HD, and that have shown to be modulated by αBc or other sHsps, that share identical properties to αBc.

We observed few significant differences in gene expression in BACHD mice (Table 2). Of note that brain derived neurotrophic factor (BDNF) downregulation is a robust feature on human HD brain samples (34, 36) and in multiple mouse models of HD (37–39) , was not significantly downregulated in BACHD mice. Generally, the large-scale upregulation or down-regulation of HD-related genes that is observed in human HD brains is not paralleled in late-stage BACHD brains.

Table 1. HD-related genes tested in αBc overexpressing animals.

Function/Markers	QPCR	WB	αBc OE effect
Chaperones (HSR)			
Hsp70	n.s	n.s	
Hsp40	n.s	n.s	
Hsp27	n.s	n.s	
Apoptosis / Oxidative stress			
p53	n.s	n.s	
Caspase-3	a trend in BACHD	n.s	Protective effect against H_2O_2
iNOS	n.s	n.s	
Excitotoxicity			
Glut1 (EEAT2)	n.s		
Neurotrophic factor			
BDNF	n.s	Not detected	
Neurotransmitters Receptors			
DR1, DR2	n.s		
Autophagy			
LC3	n.s	n.s	
Inflammation			
IL-1B; IL-2; IL-6; IL-12	n.s	-	

HSR – Heat Shock Response

4.4. Discussion

Damage to a specific set of key partner cells as well as to vulnerable neurons may account for the selective susceptibility of neuronal subtypes in many human neurodegenerative diseases, including Huntington's disease (HD), Parkinson's disease (PD), prion disease, the spinal cerebellar ataxias (SCAs), and Alzheimer's disease (AD).

We recently showed that overexpression of the sHsps αBc was shown to suppress mHtt-mediated neurotoxicity and behavioral abnormalities in the BACHD mouse model of HD (8). Expression of αBc was driven through a GFAP promoter, therefore overexpression of this sHsp was targeted in astrocytes (13). Besides neurons, growing evidence demonstrated that the expression of mHtt in glial cells, namely in astrocytes can contribute to the pathogenesis of HD (32, 40). Therefore we decided to investigate at a deeper level the cell non-autonomous effect of αBc over-expression in the BACHD mice observed in Chapter 3.

Our data suggests that BACHD astrocytes may be the source of adverse cell non-autonomous effects on neuronal toxicity caused by mHtt aggregation, oxidative stress, and cellular dysfunction. Astrocytic αBc may alleviate neuronal death by not only preventing mHtt misfolding and downstream toxic events as a chaperone, but presenting an antioxidant role and alleviating neurons from oxidative stress, apoptosis cascades and excitotoxicity events.

We hypothesize that astrocytic αBc has an important modulatory role during HD since the ability to effectively initiate the heat shock response (HSR), and other homeostatic cellular pathways (e.g., apoptosis, oxidative stress) in which αBc functions, are compromised during HD disease progression (41). We should also take into account, as a chaperone with multi-functional capabilities, αBc may alleviate stress by promoting ubiquitin/proteasomal degradation of corrupt proteins (42, 43) preventing apoptosis (9, 11, 12, 44) or by stabilizing intermediate filaments and the cytoskeleton integrity (45, 46).

As the presence of mHtt in BACHD did not compromise the transcription of the major genes and protein levels known to be involved in the HD pathobiology, we investigated other mechanisms that could be involved.

The most obvious candidate mechanism for chaperone-mediated rescue of HD neurotoxicity is inhibiting or reversing Htt aggregate (fibrils/polymers) formation. Although mHtt is expressed in glial cells, the neuronal population contains most of mHtt aggregates (47, 48). Our results from Chapter 3 indicate that αBc modulates mHtt levels and the features of IBs in a typical chaperone manner. Overexpression of chaperones may reduce large IBs by preventing oligomer formation, and oligomeric precursors may be the most toxic species (49–51). As with most Hsps, sHps can also be important for protein stability and protein turnover. Evidence suggests that affinity of αBc for its chaperone substrates is modulated by its chaperone oligomerization status and the functional

structure of αBc is a dimer, which results from interactions of β-strands in the α-crystallin domain (52, 53).

Another hypothesis also suggests that BACHD astrocytes may fail to provide adequate metabolic support to neurons, in particular lactate. Lactate, released by astrocytes, has been shown to sustain glutamatergic neurotransmission and synaptic plasticity (54, 55). Although we did not measure extracellular lactate and the expression of the monocarboxylate transporters responsible for lactate fluxes across cells in our model, this hypothesis deserves further examination particularly in the context of increased oxidative stress.

Other possibility is related to chronic inflammation, which involves glia and is known to accelerate disease progression in HD. Indeed, αBc is critical for DRD2-mediated modulation of innate immune response in astrocytes (56) . This study has shown that astrocytic DRD2 activation normally suppresses neuro-inflammation in the central nervous system through a αBc -dependent mechanism, and provides a new strategy for targeting the astrocyte- mediated innate immune. Although we did not directly test this hypothesis, we performed QPCR for a variety of cytokines (Table 1) and immunostaining of microglia using Iba-1 antibody and the astrocytic GFAP in the brain of 13-month old BACHD and did not find any cytokine transcriptional dysregulation and activated microglia or activated astrocytes (surrogate markers of neuroinflammation – microgliosis and astrogliosis (Chapter 3, sup Fig1.), indicating no significant inflammation in these mice. In addition, we suggest that BACHD astrocytes have a reduced antioxidant potential leading to an increased oxidative stress in neurons. We indeed provided evidence that oxidative stress is increased in BACHD mice and is induced *in vitro* in neurons when co-cultured with BACHD astrocytes. However, astrocytic αBc overexpression is suggested to confer antioxidant protection, especially against H_2O_2 insults, consistent with previous studies that described the anti-apoptotic effect of αBc mediated via the disruption of the proteolytic activation of caspase-3 (11). By directly binding to procaspase-3, αBc inhibits the pro-apoptotic proteins, bcl-X(S), Bax and p53 by preventing their translocations from cytosol into mitochondria during apoptosis (12, 27). However, we failed to detect these effects in p53 and caspase-3 expression and activity in our BACHD mouse model system (Table 1). We observed few significant differences in gene expression in BACHD mice (Table 1). Of note that brain derived neurotrophic factor (BDNF) downregulation is a robust feature on human HD brain samples (34, 36) and in multiple mouse models of HD

(37–39) , was not significantly downregulated in BACHD mice. Generally, the large-scale upregulation of HD-related genes that is observed in human HD brains is not paralleled in late-stage BACHD brains. However, our data do not establish a mechanism by which overexpression of αBc in astrocytes is likely to play a critical function in the modulation of mHtt and oxidative stress in the context of BACHD mice. These findings open up new avenues in the investigation of Hsps and sHsps overexpression in astrocytes and their potential protective role in neurons through a cell non-autonomous manner in HD and other proteinopathies.

4.5. References

1. Firdaus,W.J.J., Wyttenbach,A., Diaz-Latoud,C., Currie,R.W. and Arrigo,A.-P. (2006) Analysis of oxidative events induced by expanded polyglutamine huntingtin exon 1 that are differentially restored by expression of heat shock proteins or treatment with an antioxidant. *FEBS J.*, **273**, 3076–93.
2. Jonson,I., Ougland,R., Klungland,A. and Larsen,E. (2013) Oxidative stress causes DNA triplet expansion in Huntington's disease mouse embryonic stem cells. *Stem Cell Res.*, **11**, 1264–71.
3. Browne,S.E., Ferrante,R.J. and Beal,M.F. (1999) Oxidative stress in Huntington's disease. *Brain Pathol.*, **9**, 147–63.
4. Panov,A. V, Gutekunst,C.A., Leavitt,B.R., Hayden,M.R., Burke,J.R., Strittmatter,W.J. and Greenamyre,J.T. (2002) Early mitochondrial calcium defects in Huntington's disease are a direct effect of polyglutamines. *Nat Neurosci*, **5**, 731–736.
5. Sorolla,M.A., Reverter-Branchat,G., Tamarit,J., Ferrer,I., Ros,J. and Cabiscol,E. (2008) Proteomic and oxidative stress analysis in human brain samples of Huntington disease. *Free Radic. Biol. Med.*, **45**, 667–78.
6. Chen,C. (2011) Mitochondrial dysfunction, metabolic deficits, and increased oxidative stress in Huntington's disease. *Chang Gung Med. J.*, **34**, 135–52.
7. Boussicault,L., Hérard,A.-S., Calingasan,N., Petit,F., Malgorn,C., Merienne,N., Jan,C., Gaillard,M.-C., Lerchundi,R., Barros,L.F., *et al.* (2014) Impaired brain energy metabolism in the BACHD mouse model of Huntington's disease: critical role of astrocyte-neuron interactions. *J. Cereb. Blood Flow Metab.*, **23**, 1–11.
8. Oliveira,A.O., Osmand,A., Outeiro,T.F., Muchowski,P.J. and Finkbeiner,S. (2016) αB-Crystallin overexpression in astrocytes modulates the phenotype of the BACHD mouse model of Huntington's disease. *Hum. Mol. Genet.*, 10.1093/hmg/ddw028.
9. Kamradt,M.C., Chen,F., Sam,S. and Cryns,V.L. (2002) The small heat shock protein aB-crystallin negatively regulates apoptosis during myogenic differentiation by inhibiting caspase-3 activation. *J. Biol. Chem.*, **277**, 38731–38736.
10. Kamradt,M.C., Lu,M., Werner,M.E., Kwan,T., Chen,F., Strohecker,A., Oshita,S., Wilkinson,J.C., Yu,C., Oliver,P.G., *et al.* (2005) The Small Heat Shock Protein aB-crystallin Is a Novel Inhibitor of TRAIL-induced Apoptosis That Suppresses the Activation of Caspase-3 *. **280**, 11059–11066.
11. Kamradt,M.C., Chen,F. and Cryns,V.L. (2001) The Small Heat Shock Protein aB-Crystallin Negatively Regulates Cytochrome c- and Caspase-8-dependent Activation of Caspase-3 by Inhibiting Its Autoproteolytic Maturation. *J. Biol. Chem.*, **276**, 16059–16063.
12. Mao,Y.-W., Liu,J.-P., Xiang,H. and Li,D.W.-C. (2004) Human alphaA- and alphaB-crystallins bind to Bax and Bcl-X(S) to sequester their translocation during staurosporine-induced apoptosis. *Cell Death Differ.*, **11**, 512–526.
13. Hagemann,T.L., Boelens,W.C., Wawrousek,E.F. and Messing,A. (2009) Suppression of GFAP toxicity by alphaB-crystallin in mouse models of Alexander disease. *Hum. Mol. Genet.*, **18**, 1190–9.
14. Masilamoni, J.G., Jesudason, E.P., Bharathi, S.N., Jayakumar,R. (2005) The protective effect of

alpha-crystallin against acute inflammation in mice. *Biochim Biophys Acta 2005*, **1740**, 411–20.
15. Masilamoni, J.G., Jesudason, E.P., Baben, B., et al. (2006) Molecular chaperone alpha-crystallin prevents detrimental effects of neuroinflammation. *Biochim Biophys Acta*, **1762**, 284– 93.
16. Ousman, S.S., Tomooka, B.H., van Noort, J.M., et al. Protective and therapeutic role for alphaB-crystallin in autoimmune demyelination. 2007; : *Nature*, **448**, 474–9.
17. Arac, A., Brownell, S.E., Rothbard, J.B., et al. (2011) Systemic augmentation of alphaB-crystallin provides therapeutic benefit twelve hours post-stroke onset via immune modulation. *Proc Natl Acad Sci*, **108**, 13287–92.
18. Elliott,J.L., Der Perng,M., Prescott,A.R., Jansen,K. a, Koenderink,G.H. and Quinlan,R. a (2013) The specificity of the interaction between αB-crystallin and desmin filaments and its impact on filament aggregation and cell viability. *Philos. Trans. R. Soc. Lond. B. Biol. Sci.*, **368**, 20120375.
19. Shin,J.-H., Kim,S.-W., Lim,C.-M., Jeong,J.-Y., Piao,C.-S. and Lee,J.-K. (2009) aB-crystallin suppresses oxidative stress-induced astrocyte apoptosis by inhibiting caspase-3 activation. *Neurosci. Res.*, **64**, 355–61.
20. Vega, C., Pellerin, L., Dantzer, R., Magistretti,P.J. (2002) Long-term modulation of glucose utilization by IL-1 alpha and TNF-alpha in astrocytes: Na+ pump activity as a potential target via distinct signaling mechanisms. *Glia*, **39**, 10–18.
21. Hagemann,T.L., Boelens,W.C., Wawrousek,E.F. and Messing,A. (2009) Suppression of GFAP toxicity by aB-crystallin in mouse models of Alexander disease. **18**, 1190–1199.
22. Chiu, K., Lau, W.M., Lau, H.T., So, K-F., Chang,R.-C. (2007) Micro-dissection of rat brain for RNA or protein extraction from specific brain region. *J Vis Exp.*, **7**, 269.
23. Benn, C.L., Fox, H., Bates, G.P. (2008) Optimisation of region-specific reference gene selection and relative gene expression analysis methods for pre-clinical trials of Huntington's disease. *Mol Neurodegener.*, **3**, 17.
24. Pabinger, S., Thallinger, G.G., Snajder, R., Eichhorn, H., Rader, R., Trajanoski ,Z. (2009) QPCR: Application for real-time PCR data management and analysis. *BMC Bioinformatics.*, **10**, 268–269.
25. Bookout, A.L., Cummins, C.L., Mangelsdorf, D.J., Pesola, J.M., Kramer ,M.F. (2006) High-Throughput Real- Time Quantitative Reverse Transcription PCR. : *Curr. Protoc. Mol. Biol.*
26. Dalle-Donne,I., Rossi,R., Giustarini,D., Milzani,A. and Colombo,R. (2003) Protein carbonyl groups as biomarkers of oxidative stress. *Clin. Chim. Acta*, **329**, 23–38.
27. Liu,S., Li,J., Tao,Y. and Xiao,X. (2007) Small heat shock protein alphaB-crystallin binds to p53 to sequester its translocation to mitochondria during hydrogen peroxide-induced apoptosis. *Biochem. Biophys. Res. Commun.*, **354**, 109–14.
28. Chen, M., Ona, V.O., Li, M., Ferrante, R.J., Fink, K.B., Zhu, S., Bian, J., Guo, L., Farrell, L.A., Hersch, S.M., Hobbs, W., Vonsattel, J.P., Cha, J.H., Friedlander,R.M. (2000) Minocycline inhibits caspase-1 and caspase-3 expression and delays mortality in a transgenic mouse model of Huntington disease. *Nat. Med.*, **6**, 797–801.
29. Schroeder, A. M., Wang, H. B., Park, S., Jordan, M. C., Gao, F., Coppola, G., Colwell,C.S. (2016) Cardiac Dysfunction in the BACHD Mouse Model of Huntington's Disease. *PLoS One*, **11**, e0147269.
30. Zourlidou,A., Gidalevitz,T., Kristiansen,M., Landles,C., Woodman,B., Wells,D.J., Latchman,D.S., de Belleroche,J., Tabrizi,S.J., Morimoto,R.I., *et al.* (2007) Hsp27 overexpression in the R6/2 mouse model of Huntington's disease: chronic neurodegeneration does not induce Hsp27 activation. *Hum. Mol. Genet.*, **16**, 1078–90.
31. Firdaus,W.J.J., Wyttenbach,A., Giuliano,P., Kretz-Remy,C., Currie,R.W. and Arrigo,A.-P. (2006) Huntingtin inclusion bodies are iron-dependent centers of oxidative events. *FEBS J.*, **273**, 5428–41.
32. Hsiao,H.-Y. and Chern,Y. (2010) Targeting Glial Cells to Elucidate the Pathogenesis of Huntington's Disease. *Mol. Neurobiol.*, **41**, 248–255.
33. Labbadia,J. and Morimoto,R.I. (2013) Huntington's disease: Underlying molecular mechanisms and emerging concepts. *Trends Biochem. Sci.*, **38**, 378–385.
34. Zuccato,C., Valenza,M. and Cattaneo,E. (2010) Molecular Mechanisms and Potential Therapeutical Targets in Huntington ' s Disease. *Physiol. Rev*, 10.1152/physrev.00041.2009.
35. Gil,J.M. and Rego,A.C. (2008) Mechanisms of neurodegeneration in Huntington's disease. *Eur. J. Neurosci.*, **27**, 2803–20.
36. Landles,C. and Bates,G.P. (2004) Huntingtin and the molecular pathogenesis of Huntington's

disease. Fourth in molecular medicine review series. *EMBO Rep.*, **5**, 958–63.
37. Zuccato, C., Ciammola, A., Rigamonti, D., Leavitt, B.R., Goffredo, D., Conti, L., MacDonald, M.E., Friedlander, R.M., Silani, V., Hayden, M.R., Timmusk, T., Sipione, S., Cattaneo,E. (2001) Loss of huntingtin-mediated BDNF gene transcription in Huntington's disease. *Science (80-.).*, **293**, 493–498.
38. Luthi-Carter, R., Hanson, S.A., Strand, A.D., Bergstrom, D.A., Chun, W., Peters, N.L., Woods, A.M., Chan, E.Y., Kooperberg, C., Krainc, D., Young, A.B., Tapscott, S.J., Olson,J.M. (2002) Dysregulation of gene expression in the R6/2 model of polyglutamine disease: parallel changes in muscle and brain. *Hum. Mol. Genet.*, **11**, 1911–1926.
39. Luthi-Carter, R., Strand, A., Peters, N.L., Solano, S.M., Hollingsworth, Z.R., Menon, A.S., Frey, A.S., Spektor, B.S., Penney, E.B., Schilling, G., Ross, C.A., Borchelt, D.R., Tapscott, S.J., Young, A.B., Cha, J.H., Olson,J.M. (2000) Decreased expression of striatal signaling genes in a mouse model of Huntington's disease. *Hum. Mol. Genet.*, **9**, 1259–1271.
40. Lobsiger,C.S. and Cleveland,D.W. (2007) Glial cells as intrinsic components of non-cell-autonomous neurodegenerative disease. *Nat. Neurosci.*, **10**, 1355–1360.
41. Arrigo,A.P., Simon,S., Gibert,B., Kretz-Remy,C., Nivon,M., Czekalla,A., Guillet,D., Moulin,M., Diaz-Latoud,C. and Vicart,P. (2007) Hsp27 (HspB1) and αB-crystallin (HspB5) as therapeutic targets. *FEBS Lett.*, **581**, 3665–3674.
42. den Engelsman,J., Keijsers,V., de Jong,W.W. and Boelens,W.C. (2003) The small heat-shock protein alpha B-crystallin promotes FBX4-dependent ubiquitination. *J. Biol. Chem.*, **278**, 4699–704.
43. Lin,D.I., Barbash,O., Kumar,K.G.S., Weber,J.D., Harper,J.W., Klein-Szanto,A.J.P., Rustgi,A., Fuchs,S.Y. and Diehl,J.A. (2006) Phosphorylation-Dependent Ubiquitination of Cyclin D1 by the SCFFBX4-αB Crystallin Complex. *Mol. Cell*, **24**, 355–366.
44. Kamradt,M.C., Lu,M., Werner,M.E., Kwan,T., Chen,F., Strohecker,A., Oshita,S., Wilkinson,J.C., Yu,C., Oliver,P.G., *et al.* (2005) The small heat shock protein aB-crystallin is a novel inhibitor of TRAIL-induced apoptosis that suppresses the activation of caspase-3. *J. Biol. Chem.*, **280**, 11059–66.
45. Ghosh,J.G., Shenoy,A.K. and Clark,J.I. (2007) Interactions between important regulatory proteins and human alphaB crystallin. *Biochemistry*, **46**, 6308–6317.
46. Ghosh,J.G., Houck,S.A. and Clark,J.I. (2007) Interactive Domains in the Molecular Chaperone Human aB Crystallin Modulate Microtubule Assembly and Disassembly. *PLoS One*, **2**.
47. DiFiglia,M., Sapp,E., Chase,K.O., Davies,S.W., Bates,G.P., Vonsattel,J.P. and Aronin,N. (1997) Aggregation of huntingtin in neuronal intranuclear inclusions and dystrophic neurites in brain. *Science*, **277**, 1990–1993.
48. Vonsattel, Jean Paul,D.M. (1998) Hungtington's disease. *J. Neuropathol. Exp. Neurol.*
49. Arrasate,M., Mitra,S., Schweitzer,E.S., Segal,M.R. and Finkbeiner,S. (2004) Inclusion body formation reduces levels of mutant huntingtin and the risk of neuronal death. *Nature*, **431**, 805–10.
50. Muchowski,P.J. and Wacker,J.L. (2005) Modulation of neurodegeneration by molecular chaperones. *Nat. Rev. Neurosci.*, **6**, 11–22.
51. Takahashi,T. and Mihara,H. (2008) Peptide and protein mimetics inhibiting amyloid ??-peptide aggregation. *Acc. Chem. Res.*, **41**, 1309–1318.
52. Quraishe,S., Asuni, a, Boelens,W.C., O'Connor,V. and Wyttenbach, a (2008) Expression of the small heat shock protein family in the mouse CNS: differential anatomical and biochemical compartmentalization. *Neuroscience*, **153**, 483–91.
53. Quraishe,S. (2010) The sHsp expression signature in the brain and modulation in models of chronic neurodegeneration.
54. Lee,W., Reyes,R.C., Gottipati,M.K., Lewis,K., Lesort,M., Parpura,V. and Gray,M. (2013) Enhanced Ca2+-dependent glutamate release from astrocytes of the BACHD Huntington's disease mouse model. *Neurobiol. Dis.*, **58**, 192–199.
55. Nambron,R., Silajdžić,E., Kalliolia,E., Ottolenghi,C., Hindmarsh,P., Hill,N.R., Costelloe,S.J., Martin,N.G., Positano,V., Watt,H.C., *et al.* (2016) A Metabolic Study of Huntington's Disease. *PLoS One*, **11**, e0146480.
56. Shao,W., Zhang,S., Tang,M., Zhang,X., Zhou,Z., Yin,Y., Zhou,Q., Huang,Y., Liu,Y., Wawrousek,E., *et al.* (2013) Suppression of neuroinflammation by astrocytic dopamine D2 receptors via αB-crystallin. *Nature*, **494**, 90–4

Chapter 5.

Genetic deficiency of αB-crystallin does not aggravate the disease progression of the BACHD mouse model of HD

5.1. Introduction

Accumulation of misfolded and aggregated proteins is a pathological hallmark of several neurological disorders (1). Members of the sHsp family, whose expression is regulated by the heat shock transcription factor 1 (HSF1), are known to constitute a line of defense to protect cells from the deleterious effects caused by toxicity associated with misfolded proteins (2). In addition, sHsps are pleiotropic proteins, i.e., they can protect cells from a variety of environmental conditions such as oxidative stress, heat, apoptosis, inflammation and by other degradation mechanisms (2, 3). Therefore, their importance in proteinopathies should be further understood. sHsps share a conserved α-crystallin domain of 80–100 amino acids at their C-terminus whereas their N-terminal regions are highly variable in sequence and length (4). The sHsps form dynamic oligomeric structures ranging from 9–50 subunits associating as either homo- or hetero-multimeric complexes (5). It has been proposed that the ATP-independent sHsps help in refolding of denatured proteins by holding them in a reactivation-competent state and target them to subsequent refolding or degradation with the help of ATP-dependent chaperones like Hsp70 and Hsp40 (6, 7). The human and mouse genomes contain for 10 genes for sHsps differing between 45 and 85% in sequence (8, 9). Point mutations in human sHsps lead to several aggregation diseases (4) – for example, mutations in αA-crystallin leads to cataract (10), mutations in αBc leads to desmin-related myopathy (11–14), missense mutations in HSP27 is associated with Charcot-Marie-Tooth disease (15, 16). Induction of αBc has been noted in Alexander's disease (17), Creutzfeldt-Jacob disease (18), Parkinson's disease and taupathies (19) and in Alzheimer's disease (11, 20, 21). In contrast with findings in other protein aggregation diseases of the CNS, elevation of αBc and other sHsps have not been observed in the poly-Q diseases (2). Studies in the R6/2 (22) and BACHD (23) mice models of HD found reduced overall levels of αBc at the end of the disease course.

In addition, expression of a mHtt fragment in mice lacking αBc, markedly accelerated the onset and severity of aggregation, demonstrating that the endogenous chaperone activity of αBc suppresses aggregation *in vivo*. Moreover, studies using a mouse model deficient in αBc crossed with an AD transgenic mouse model has shown that lack of αBc increases behavioral impairment in AD disease progression (24, 25). Our previous studies (Chapter 3),

have shown that elevating αBc could protect from behavioral and neuropathological deficits in BACHD mice (23). Thus, we hypothesized that endogenous αBc protects cells against mHtt toxicity and play a role in HD disease progression. To note, that targeted deletion of αBc also disrupted the adjacent gene, HspB2, due to the proximity of the promoter sequences (26). Similar to αBc, HspB2 is expressed in skeletal and cardiac muscles where it is often localized to the Z lines and has also been shown to associate with and activate myotonic dystrophy protein kinase (20). Importantly HspB2 is not expressed in the brain and is not presently known to be involved in protein aggregation prevention (4, 26). Also, mice knocked-out for αBc and HspB2 are viable suggesting that it is either non-essential or redundant during development. Older knockout mice consistently lost weight and body fat and subsequently developed severe spine curvature (kyphosis) and skeletal muscle degeneration (26). Therefore, we decided to test for the first time the impact of αBc (and HspB2) deletion in HD in the BACHD mice. For this purpose, we crossed αBc/HspB2 deficient ($CRYAB^{-/-}HSPB2^{-/-}$) mice with the BACHD mouse model of HD, previously used in our studies. Transgenic and non-transgenic mice in chaperone-sufficient or deficient backgrounds were examined for representative behavioral paradigms for motor and cognitive functions: motor and locomotor activity was evaluated by rotarod and balance beam, spatial orientation and locomotion was monitored by open field test and anxious behavior was evaluated on elevated plus maze. Unexpectedly, αBc/HspB2 deficiency did not increase the severity of the BACHD disease progression. Instead, αBc/HspB2 modulated the body weight on BACHD mice and this effect play a role on the behavioral readouts. Our data suggests and highlights that all chaperones have many cellular functions and when chronically overexpressed or deleted, may have deleterious as well as beneficial consequences on metabolism and other essential physiological functions, causing the protein networks to further adjust to neutralize potentially damaging effects. Further studies should pursue unique and single deletions of αBc and other sHsps to clarify novel potential roles of these proteins in the context of neurological disorders.

5.2. Materials and Methods

Animals and breeding strategy

Animal experiments were approved by the Institutional Animal Care and Use Committee of the University of California, San Francisco. Mice were housed, bred and maintained in compliance with National Institutes of Health guidelines. BACHD (BACHD ^{tg}) mice in C56Bl/6J background were obtained from Dr. William Yang (University of California, Los Angeles) and one breeding pair of CRYAB$^{-/-}$/HSPB2$^{-/-}$ (or αBc/HspB2 deficient) mice in C56Bl/6J background (26) were gifted kindly by Dr. John Clark, (University of Washington, Seattle) MD. Both lines were maintained by breeding to wild-type (WT) 129Sv animals from the Jackson Laboratory (Bar Harbor, ME). To test if deletion αBc/HspB2 could modulate HD progression, we crossed the αBc/HspB2 mice to BACHD mice. Progeny from this breeding resulted CRYAB$^{+/-}$/HSPB2$^{+/-}$, mice with equal numbers of non-transgenic and transgenic. The CRYAB$^{+/-}$/HSPB2$^{+/-}$ transgenic mice were crossed with CRYAB$^{+/-}$/HSPB2$^{+/-}$ littermates to generate (i) CRYAB$^{+/+}$/HSPB2$^{+/+}$, BACHD Tg $^{0/0}$ (hereafter referred to as WT); (ii) CRYAB$^{+/+}$/HSPB2$^{+/+}$, BACHD Tg$^{+/0}$ (hereafter referred to as BACHD); (iii) CRYAB$^{-/-}$ /HSPB2$^{-/-}$, BACHD Tg$^{0/0}$ (hereafter referred to as KO) and (iv) CRYAB$^{-/-}$/HSPB2$^{-/}$-, BACHD Tg$^{+/0}$ (hereafter referred to as BACHD-KO) in addition to parental genotypes CRYAB$^{+/-}$ /HSPB2$^{+/-}$, BACHD Tg$^{0/0}$ (hereafter referred to as HET) and CRYAB$^{+/-}$/HSPB2$^{+/-}$, BACHD Tg$^{+/0}$, (hereafter referred to as BACHD-HET). All groups of mice were mice and were used for behavioral studies and HD-associated biochemical studies.

Genotyping

Genotypes of the mice were confirmed by PCR of tail genomic DNA using appropriate primers as described in Brady et al (26) for KO mice genotyping and in Gray et al (27). The use of littermates for all genotypes minimizes the effect of out-crossing the mice. The genetic variations between the two parental mouse strains are expected to affect all six experimental genotypes identically.

Behavioral assays

For all behavior experiments, experimenters were blinded to genotype. Experimental readouts were analyzed at 3, 7, 10 and 13 months for rotarod and balance beam to evaluate HD phenotype progression. All cages contained at least one mouse from each genotype, and mice were given environmental enrichment. Mice were subject to a 12-h light/dark cycle. Behavioral analysis of WT, HET, KO, BACHD, BACHD-HET and BACHD-KO, were done blind to genotype.

Elevated plus maze, Open Field, Rotarod and Balance Beam were performed as previously described (Chapter 3, Materials and Methods Section – Behavioral Assays), for the 3, 7, 10 and 13 times points.

5.3. Results

5.3.1. Abnormal genotype distribution in BACHD combined with αBc/HspB2 deficient mice.

We have previously observed (Chapter 3, Fig. 1) that αBc protein levels decreased in a time-dependent manner in BACHD brains. Therefore, we hypothetized that the overproduced mHtt in BACHD could affect proteostasis not only by increased demand for chaperone function but also because of its reduced expression. In this mouse model, we speculated that if αBc could protect the mice from mHtt-mediated neuronal dysfunction, then in its absence these deficits should manifest at an earlier age. It was demonstrated that the BACHD mice showed more robust behavioral around 6 months of age (27). Since the mice deficient for αBc/HspB2 showed debilitating phenotypes about 9-10 months of age (26), we decided to investigate the behavioral phenotypes of WT (n=20), HET (n=20), KO (n=27) BACHD (n=20), BACHD-HET (n=20), and BACHD-KO (n=12).

The observed offspring genotypes were compared, and we noticed abnormal genotype distribution: the group of BACHD-KO genotype had significantly fewer mice than expected. Comparatively with all the other genotypes that had numbers according to the expected Mendelian ratios, above 25 % for WT, BACHD, and KO groups, and above 50% for HET and BACHD-HET groups, we were surprised to have only 12 individuals in the BACHD-KO

group that corresponded to only 10% of total offspring. Currently, association with embryonic development or birth defects has not been reported for BACHD or the KO mice, and our numbers confirm this information. However, in our studies, the synergistic cross combination of BACHD with KO mice αBc/HspB2 resulted in fewer animals and therefore this genetic combination may have affected embryonic development or birth of these mice.

5.3.2. αBc/HspB2 deficiency does not impair behavioral deficits in BACHD mice

After noticing an abnormal genotype distribution in our mice cohort, we premised that αBc/HspB2 deficiency would worsen and accelerate the BACHD deficits. To confirm αBc was efficiently deleted, we performed QPCR to evaluate αBc in our mice cohort (Fig. 1A). It was demonstrated that the BACHD mice showed behavioral changes as early as 2-3 months of age (27, 28). Since the mice deficient for αBc/HspB2 showed debilitating phenotypes about 9-10 months of age (24, 26), we decided to investigate the behavioral phenotypes of our mice groups (above described) at 3, 7, 10, 13 months of age corresponding to early-, mid- and late-stages of the disease, respectively. The rotarod and balance beam assays are tests of motor coordination, while the open field test affords insight into general activity levels and anxiety related behavior. These tests were designed to examine the effect αBc/HspB2 deficiency on motor and coordination defects in BACHD mice.

Rotarod performance is a sensitive indicator of balance and motor coordination, which has been repeatedly shown to decline in mouse models of HD.

During testing for each time, latency to fall from the apparatus was measured, and we observed as in Chapter 3, and impairment of motor coordination performing the test in the BACHD mice. This behavioral deficit in BACHD was consistently significant from early to late stage of the disease, 3 month to 13 months, respectively (Fig. 1B). Unexpectedly, deletion of αBc/HspB2 on the KO mice ameliorated their rotarod performance when compared to WT mice, from 3 to 13 months of age. The same effect was observed on the combined HD transgene and chaperone deficiency group of mice, BACHD-KO, in which deletion αBc/HspB2 was shown to improve motor ability in the rotarod in the BACHD mice, especially at 13 months of age (Fig. 1B).

Balance Beam is commonly used to test refined balance and motor tasks. Time to cross the beam was also evaluated in this group of mice. Consistent with previous results, we could find a BACHD phenotype on the time to cross the beam, being significant after the 10 months time point (Fig. 1C). Genetic deletion of αBc/HspB2 did not worsen the BACHD phenotype at any time point (Fig. 1C) and similar to what we found on the Rotarod, at 13 months of age it showed a tendency to improve time to cross the beam on the BACHD-KO group (Fig. 1C).

Open field test is one of the most common tests to monitor general motor activity, exploratory behavior and elevated plus maze measures of anxiety (29, 30). Normal behavior in mice is to seek the protection of the periphery rather than the vulnerability of the center in the open field, and to stay longer periods in the closed arms in the elevated plus maze. Mice were individually placed in an open arena equipped with infrared photobeams to monitor mice behavior for 15 minutes without the experimenter being present in the room. First of all, WT and KO groups behaved similarly in terms of rearing (data not shown), and total movement indicating that loss of αBc/HspB2 alone had negligible effect on locomotion at this age group (Fig 1D). Age associated muscle degeneration reported in the KO mice was not manifested in terms of locomotion defects at this age group as all parameters counts of KO group of animals was comparable to WT. Similarly, the BACHD group was comparable to WT suggesting that the expression of mutant mHtt in mice did not significantly affect locomotion by itself during Open Field (Fig. 1D) and it did not affect anxiety levels in the elevated plus maze (data not shown). When the BACHD transgene expression was combined with αBc/HspB2 deficiency in the BACHD-KO group, the effect did not worsen the behavioral activity of the BACHD or the KO groups in total activity (Fig 1D).

As expected, we observed that BACHD and BACHD-HET and BACHD-KO mice gain significantly more weight (an average of 20–30%) than their littermate's controls, between 3 and 7 months until 13 months of age (Fig. 1E). However, after 9-10 months of age, when αBc/HspB2 deficient mice (KO) has been indicated to have a more robust phenotype, we observe a strong weight loss on the BACHD-KO mice, suggesting that chaperone deficiency may play a role at metabolic functions in BACHD mice. Since weight can affect motor performance, we examined the relationship of weight and rotarod and balance beam performance in BACHD mice. We found that the rotarod and balance beam performance in

this cohort of BACHD and BACHD-KO mice at 7, 10 and 13 months was significantly correlated with body weight (Fig 1G). Therefore, the improvement seen in the KO when compared to WT (Fig 1F) and in BACHD-KO when compared to BACHD may be explained by weight differences or the effect of weight on motor performance. Thus, we conclude that αBc/HspB2 deletion affects BACHD motor performance by altering their body weight and most likely metabolic functions.

These results suggest a stronger implication of body weight on motor behavioral analyses and the need to perform correlation analyses during the performance of these tests.

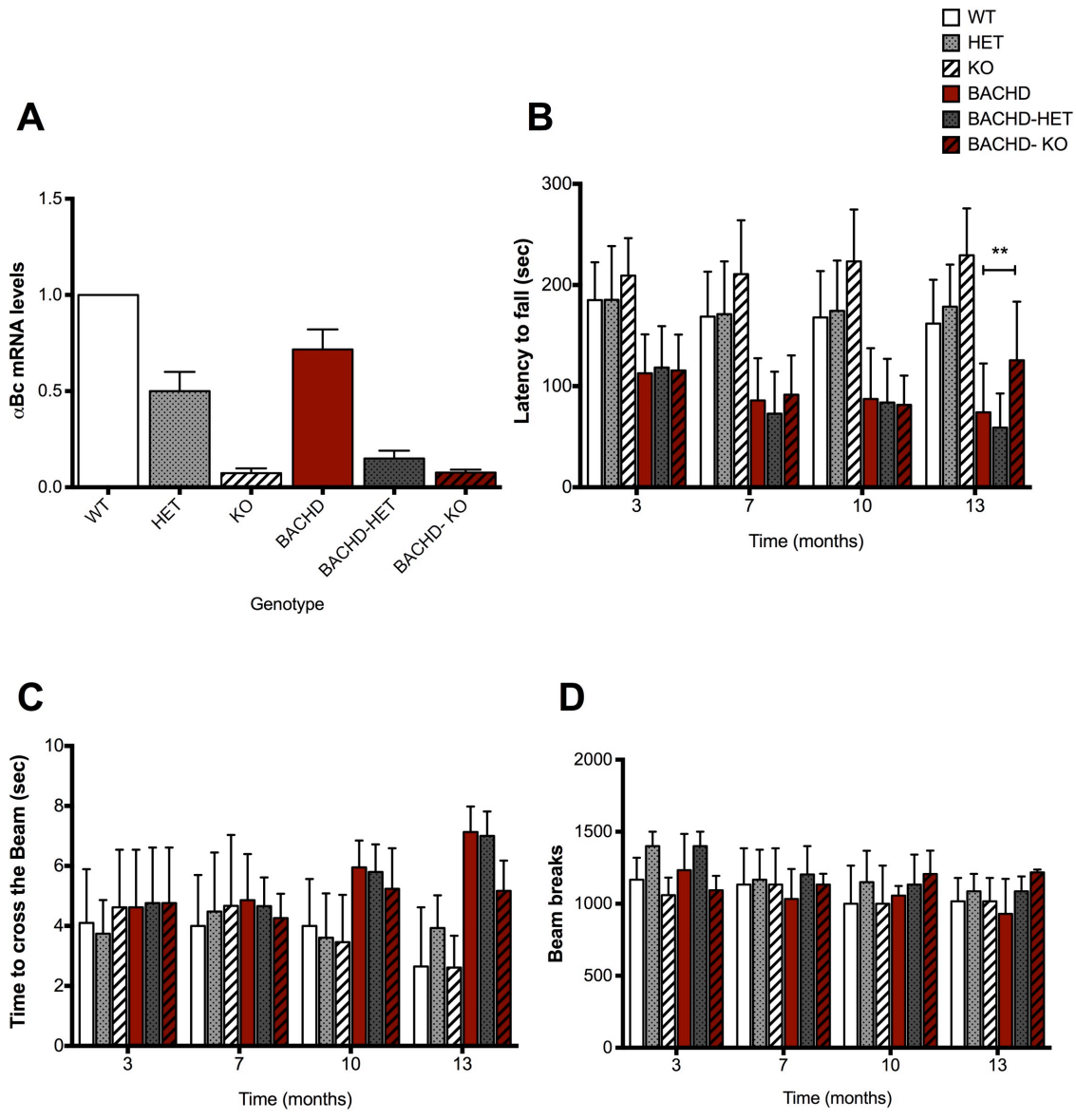

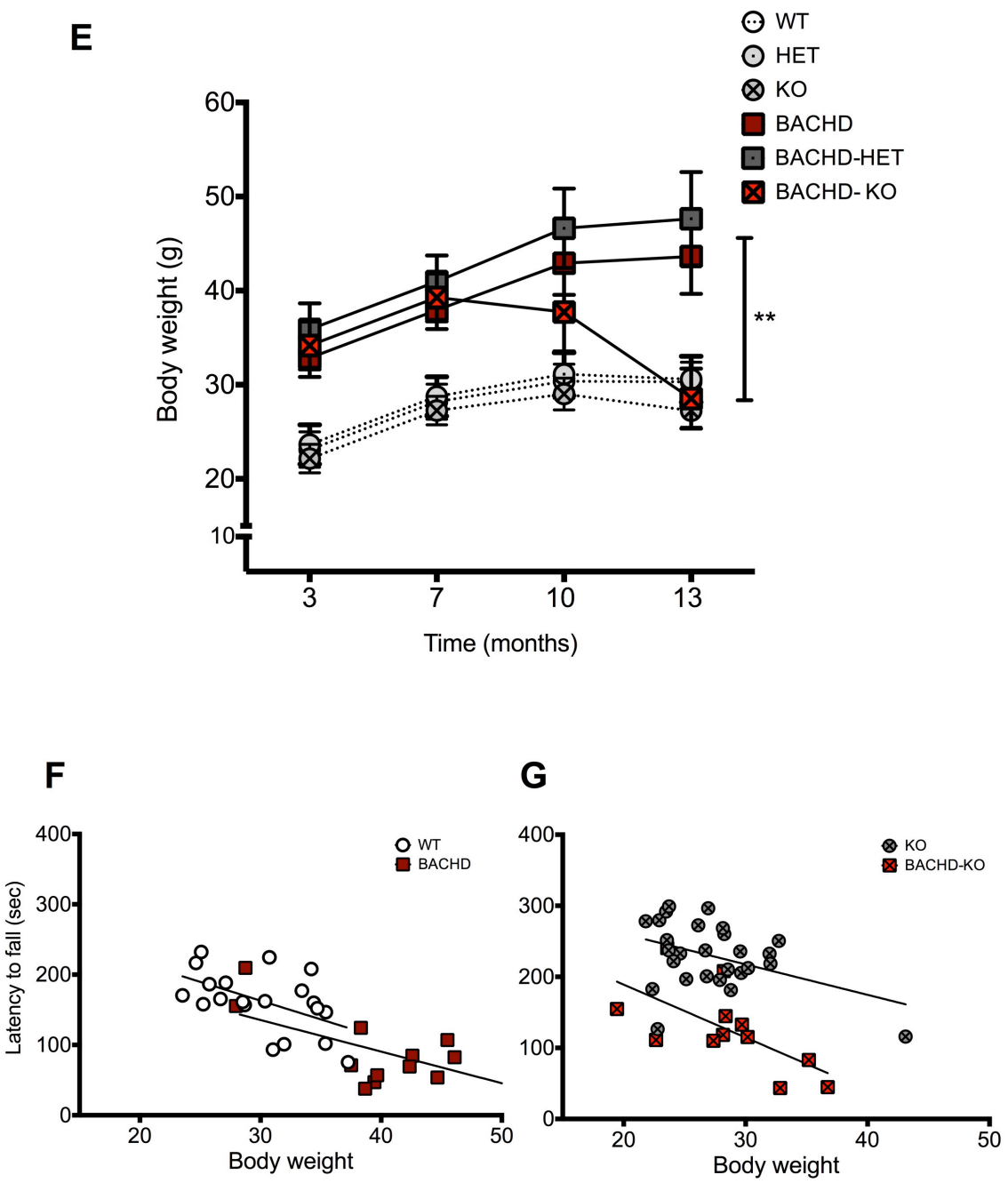

Figure 1. **αBc/HspB2 genetic deletion does not influence behavioral phenotypes in BACHD mice.** Behavioral readouts of disease progression were measured at 3, 7, 10 and 13 months of age using rotarod, balance beam and open fieldtesting. Data at each time point were tested for statistically significant differences using two-way ANOVA followed by Tukey post-hoc tests. At 3 months of age, group sizes were as follows WT (n=20), HET (n=20), KO (n=27) BACHD (n=20), BACHD-HET (n=20), and BACHD-KO (n=12). Error bars represent SD. * = p <0.05 or **= <0.01 for main p effect of the BACHD by two-way ANOVA.

A) αBc mRNA protein levels in brains from 3 month old mice. As expected, we could verify downregulation of αBc (CRYAB gene) in brain from αBc /HspB2−/− mice. **B**) Rotarod. BACHD mice

fall off an accelerating rotarod sooner than WT littermates, but this is surprisingly not aggravated by αBc KO genotype. Instead, KO mice perform significantly better than WT at rotarod at every time point. The BACHD-KO group also performs better than the BACHD group at 13 months. **C**) Balance Beam. BACHD mice are slower to cross an elevated balance beam than WT littermates at 13 months of age, but this is not affected by αBc KO genotype (no significant effect of αBc KO genotype at any age) and there is no significant interaction between the two factors. **D**) Open field. BACHD do not present a phenotype on the open field movement evaluation when compared to WT littermates, and there is no additional effect by αBc KO genotype (no significant effect of αBc KO genotype at any age). **E**) Body Weight BACHD. KO genotype does not influence WT body weight, but it does significantly impact BACHD body weight after the 10 to 13 month time points. The correlation between body weight and rotarod and balance beam performance in BACHD (n=20) and BACHD-KO mice (n=12) was examined. Correlations graphs with comparisons for WT and KO and for BACHD and BACHD-KO. F**)** Body weight correlation with latency to fall in rotarod at 13 months, WT and KO were significantly different, G**)** Body weight correlation with latency to fall in rotarod at 13 months, BACHD and BACHD-KO were significantly different.
Our data indicate that the rotarod and balance beam BACHD and BACHD-KO mice motor performance is correlated with their body weight loss at 7, 10 and months. Therefore, the improvement seen in the KO compared to WT mice, and BACHD-KO compared to the BACHD may be explained by weight differences or the effect of weight on motor performance. Data were analyzed by using the nonparametric Spearman correlation coefficient.

5.3.3. αBc/HspB2 deficiency does not alter HD related genes

Despite finding a that αBc/HspB2 deficiency was responsible to decrease the BACHD body weight phenotype, especially after 10 months, we wanted to confirm that besides playing a role on metabolic functions in the BACHD mice, we could study whether this chaperone genetic ablation, could be related to any HD related genes. We repeated the same procedure described above in Chapter 3, and looked at known and well established HD genes. We used QPCR to quantify mRNA levels of some genes in brains from 13-month-old KO mice. We did not find any alteration caused by αBc/HspB2 deficiency in common HD genes as DARPP-32, Dopamine receptors, other sHsps (Hsp70, Hsp27, and Hsp90), caspase-3 and p53. Unfortunetaly, we did not analyze any potential HD associated-metabolic markers in our study. However based on our results here, we hypothesized that αBc/HspB2 deletion may play an important role in metabolic function overall. Studying αBc/HspB2 genetic ablation in

lipid and bone markers, glucose homeostasis, peripheral hormones that are know to affect energy homeostasis in Huntington's disease (31), could be a useful approach to study HD metabolic impairment and its modulation by sHsps.

5.4. Discussion

Here, we performed an extensive study of the effect of the small Hsps αBc/HspB2 genetic deletion on the BACHD mouse model. We focused on behavioral and motor analyses, including rotarod, balance beam and open field. In contrast to many previous studies, our results did not show aggravated BACHD motor deficits by the knocking down αBc/HspB2. Unexpectedly, we observed that αBc/HspB2 deficient mice (KO) could have a better motor performance on rotarod due to a direct effect on BACHD weight loss. Alternatively, the failure of two sHsps genetic deletion to be detrimental in the context of HD could reflect the requirement for a finely balanced concerted action of several chaperone systems, along with the ability to up- or down-regulate their levels in response to specific cellular requirements. A better strategy might be to target the regulators of the stress-induced chaperone response, thereby coordinately inducing many chaperones with distinct and complimentary cytoprotective functions. Together with our results from Chapter 3, we hypothesize that constitutive or transient overexpression of individual sHsps may be more successful in ameliorating disease phenotypes. Although, all Hsps have many cellular functions and when chronically deleted or overexpressed, may have deleterious as well as beneficial consequences and cause the protein networks to further adjust to neutralize potentially damaging. It is possible that αBc/HspB2 deficiency alters disease progression in other studies and other disease like its has been shown in AD (32) but not in ours because αBc/HspB2 deficiency has

multiple positive and negative effects that offset each other in BACHD mice. Further studies will be needed to address how to modulate the chaperone network in order to alleviate the devastating symptoms of HD and other neurological disorders. Regardless of the mechanisms governing expression and modulation of sHsp activity, the discrepancy between large scale upregulation in HD patients of certain genes and biomarkers and few alterations in the BACHD mice system highlights the need to use multiple animal models of disease in order to explore disease mechanisms. Here, we have shown that removing αBc/HspB2 does not worsen disease-associated behavioral changes in the full-length HD mouse model - BACHD.

5.5. References

1. Muchowski,P.J. and Wacker,J.L. (2005) Modulation of neurodegeneration by molecular chaperones. *Nat. Rev. Neurosci.*, **6**, 11–22.
2. Brownell,S.E., Becker,R.A. and Steinman,L. (2012) The protective and therapeutic function of small heat shock proteins in neurological diseases. *Front. Immunol.*, **3**, 1–10.
3. Lindquist,S. (1986) THE HEAT-SHOCK RESPONSE. *Ann. Rev. Biochem.*, **55**, 1151–91.
4. Clark,J.I. and Muchowski,P.J. (2000) Small heat-shock proteins and their potential role in human disease. *Curr. Opin. Struct. Biol.*, **10**, 52–9.
5. Horwitz,J. (1992) Alpha-crystallin can function as a molecular chaperone. *Proc. Natl. Acad. Sci. U. S. A.*, **89**, 10449–53.
6. Basha,E., O'Neill,H. and Vierling,E. (2012) Small heat shock proteins and α-crystallins: dynamic proteins with flexible functions. *Trends Biochem. Sci.*, **37**, 106–17.
7. Ecroyd,H. and Carver,J.A. (2009) Review Crystallin proteins and amyloid fibrils. **66**, 62–81.
8. Kampinga,H.H., Hageman,J., Vos,M.J., Kubota,H., Tanguay,R.M., Bruford,E.A., Cheetham,M.E., Chen,B. and Hightower,L.E. (2009) Guidelines for the nomenclature of the human heat shock proteins. *Cell Stress Chaperones*, **14**, 105–111.
9. Taylor,R.P. and Benjamin,I.J. (2005) Small heat shock proteins: a new classification scheme in mammals. *J Mol Cell Cardiol*, **38**, 433–444.
10. Litt,M., Kramer,P., LaMorticella,D.M., Murphey,W., Lovrien,E.W. and Weleber,R.G. (1998) Autosomal dominant congenital cataract associated with a missense mutation in the human alpha crystallin gene CRYAA. *Hum. Mol. Genet.*, **7**, 471–474.
11. Stege,G.J., Renkawek,K., Overkamp,P.S., Verschuure,P., van Rijk, a F., Reijnen-Aalbers, a, Boelens,W.C., Bosman,G.J. and de Jong,W.W. (1999) The molecular chaperone alphaB-crystallin enhances amyloid beta neurotoxicity. *Biochem. Biophys. Res. Commun.*, **262**, 152–156.
12. Wanschit,J., Nakano,S., Goudeau,B., Str□□□bel,T., Rinner,W., Wimmer,G., Resch,H., Jaksch,M., Akiguchi,I., Vicart,P., *et al.* (2002) Myofibrillar (desmin-related) myopathy: clinico-pathological spectrum in 3 cases and review of the literature. *Clin Neuropathol*, **21**, 220–231.
13. Li,H., Li,C., Lu,Q., Su,T., Ke,T., Li,D.W.-C., Yuan,M., Liu,J., Ren,X., Zhang,Z., *et al.* (2008) Cataract mutation P20S of alphaB-crystallin impairs chaperone activity of alphaA-crystallin and induces apoptosis of human lens epithelial cells. *Biochim. Biophys. Acta*, **1782**, 303–9.

14. Bova,M.P., Yaron,O., Huang,Q., Ding,L., Haley,D. a, Stewart,P.L. and Horwitz,J. (1999) Mutation R120G in alphaB-crystallin, which is linked to a desmin-related myopathy, results in an irregular structure and defective chaperone-like function. *Proc. Natl. Acad. Sci. U. S. A.*, **96**, 6137–6142.
15. Evgrafov,O. V, Mersiyanova,I., Irobi,J., Van Den Bosch,L., Dierick,I., Leung,C.L., Schagina,O., Verpoorten,N., Van Impe,K., Fedotov,V., *et al.* (2004) Mutant small heat-shock protein 27 causes axonal Charcot-Marie-Tooth disease and distal hereditary motor neuropathy. *Nat. Genet.*, **36**, 602–606.
16. Almeida-souza,L., Asselbergh,B., Ydewalle,C., Moonens,K., Goethals,S., Winter,V. De, Azmi,A., Irobi,J., Timmermans,J., Gevaert,K., *et al.* (2011) Small Heat-Shock Protein HSPB1 Mutants Stabilize Microtubules in Charcot-Marie-Tooth Neuropathy. **31**, 15320–15328.
17. Hagemann,T.L., Boelens,W.C., Wawrousek,E.F. and Messing,A. (2009) Suppression of GFAP toxicity by alphaB-crystallin in mouse models of Alexander disease. *Hum. Mol. Genet.*, **18**, 1190–9.
18. Renkawek,K., de Jong,W.W., Merck,K.B., Frenken,C.W., van Workum,F.P. and Bosman,G.J. (1992) alpha B-crystallin is present in reactive glia in Creutzfeldt-Jakob disease. *Acta Neuropathol*, **83**, 324–327.
19. Dabir,D. V, Trojanowski,J.Q., Richter-Landsberg,C., Lee,V.M.-Y. and Forman,M.S. (2004) Expression of the small heat-shock protein alphaB-crystallin in tauopathies with glial pathology. *Am. J. Pathol.*, **164**, 155–166.
20. Wilhelmus,M.M.M., Otte-Höller,I., Wesseling,P., De Waal,R.M.W., Boelens,W.C. and Verbeek,M.M. (2006) Specific association of small heat shock proteins with the pathological hallmarks of Alzheimer's disease brains. *Neuropathol. Appl. Neurobiol.*, **32**, 119–130.
21. Shinohara,H., Inaguma,Y., Goto,S., Inagaki,T. and Kato,K. (1993) aB crystallin and HSP28 are enhanced in the cerebral cortex of patients with Alzheimer's disease. *J. Neurol. Sci.*, **119**, 203–208.
22. Zabel,C. (2002) Alterations in the Mouse and Human Proteome Caused by Huntington's Disease. *Mol. Cell. Proteomics*, **1**, 366–375.
23. Oliveira,A.O., Osmand,A., Outeiro,T.F., Muchowski,P.J. and Finkbeiner,S. (2016) αB-Crystallin overexpression in astrocytes modulates the phenotype of the BACHD mouse model of Huntington's disease. *Hum. Mol. Genet.*, 10.1093/hmg/ddw028.
24. Ojha,J., Karmegam,R. V, Masilamoni,J.G., Terry,A. V and Cashikar,A.G. (2011) Behavioral defects in chaperone-deficient Alzheimer's disease model mice. *PLoS One*, **6**, e16550.
25. Ojha,J., Karmegam,R. V, Jeyaraj,G.M., Jr,A.V.T. and Anil,G. Enhancement of protein misfolding in chaperone-deficient mice causes behavioral defects Center for Molecular Chaperones and Radiobiology , Medical College of Georgia , Augusta , GA Department of Pharmacology and Toxicology , Medical College of Georgia , A.
26. Brady,J.P., Garland,D.L., Green,D.E., Tamm,E.R., Giblin,F.J. and Wawrousek,E.F. (2001) AlphaB-crystallin in lens development and muscle integrity: a gene knockout approach. *Invest. Ophthalmol. Vis. Sci.*, **42**, 2924–34.
27. Gray,M., Shirasaki,D.I., Cepeda,C., André,V.M., Wilburn,B., Lu,X.-H., Tao,J., Yamazaki,I., Li,S.-H., Sun,Y.E., *et al.* (2008) Full-length human mutant huntingtin with a stable polyglutamine repeat can elicit progressive and selective neuropathogenesis in BACHD mice. *J. Neurosci.*, **28**, 6182–95.
28. Pouladi,M. a, Stanek,L.M., Xie,Y., Franciosi,S., Southwell,A.L., Deng,Y., Butland,S., Zhang,W., Cheng,S.H., Shihabuddin,L.S., *et al.* (2012) Marked differences in neurochemistry and aggregates despite similar behavioural and neuropathological features of Huntington disease in the full-length BACHD and YAC128 mice. *Hum. Mol. Genet.*, **21**, 2219–32.
29. Wilson,R.C., Vacek,T., Lanier,D.L. and Dewsbury,D.A. (1976) Open-field behavior in muroid rodents. *Behav. Biol.*, **17**, 495–506.
30. Lister,R.G. (1987) The use of a plus-maze to measure anxiety in the mouse. *Psychopharmacology*

(Berl)., **92**, 180–185.
31. Nambron,R., Silajdžić,E., Kalliolia,E., Ottolenghi,C., Hindmarsh,P., Hill,N.R., Costelloe,S.J., Martin,N.G., Positano,V., Watt,H.C., *et al.* (2016) A Metabolic Study of Huntington's Disease. *PLoS One*, **11**, e0146480.
32. Ojha,J., Karmegam,R. V, Masilamoni,J.G., Jr,A.V.T. and Cashikar,A.G. (2011) Behavioral Defects in Chaperone-Deficient Alzheimer ' s Disease Model Mice. **6**.

Chapter 6.

General Discussion and Conclusions

6. General Discussion and Conclusions

Huntington's disease (HD) is a fatal, devastating and progressive neurodegenerative disorder for which only minor symptomatic treatments are available. A better understanding of the pathology, and identification of biomarkers will facilitate the development of disease-modifying treatments. HD is, in principal, a privilledged model disease for development of biomarkers because it is an autosomal-dominant disease with complete penetrance, caused by a single gene mutation, in which the neurodegenerative process can be assessed many years before onset of signs and symptoms of manifest disease. Therefore, approaches that target molecular chaperones may be beneficial in protein misfolding diseases.

In Chapter 3, we report for the first time the effect of the sHsp αBc in a full-length mHtt model, the BACHD mouse. Expression of αBc in astrocytes improved the motor (Rotarod and Balance Beam) and cognitive performance (Water-T-maze) of the BACHD mice, as well as neuropathological features associated with HD. Overall, our data indicate that modulating the levels of αBc protect against the progression of HD. Taken into account our results, the most obvious candidate mechanism for chaperone-mediated rescue of HD neurotoxicity is inhibiting or reversing htt aggregate (fibrils/polymers) formation. Although mHtt is expressed in glial cells, it is primarily in neuronal cells that Htt inclusions are found (1, 2). Our results indicate that αBc modulates mhtt levels and the features of IBs in a typical chaperone manner. Interestingly, however, the effect of this chaperone is via overexpressing αBc in astrocytes. Overexpression of chaperones may reduce large IBs by preventing oligomer formation, and oligomeric precursors may be the most toxic species to the cell (3–5). As with most Hsps, sHps can also be important for protein stability and protein turnover. Evidence suggests that affinity of αBc for its chaperone substrates is modulated by its chaperone oligomerization status and the functional structure of αBc is a dimer, which results from interactions of β-strands in the α-crystallin domain (6, 7). Since the binding capacity can reach one substrate protein per sHsp subunit, big chaperone oligomer structures (via sHsp oligomerized complexes) are major contributors to the chaperoning capacity of the cell. It remains unclear how the decision to refold or degrade a misfolded protein is made. Some sHsps (αBc and Hsp27)

interact directly or indirectly with the proteasome and form part of ubiquitin ligase complexes (αBc and HspB10) that are involved in the proteasomal degradation of certain proteins in a quite selective manner under stress conditions (8). Thus, αBc could regulate mHtt protein levels by stabilizing mHtt in IBs or by promoting misfolded mhtt refolding with the cooperative help of other chaperone complexes, namely the Hsp70/Hsp40 machinery, as well as targeting it for proteosomal degradation.

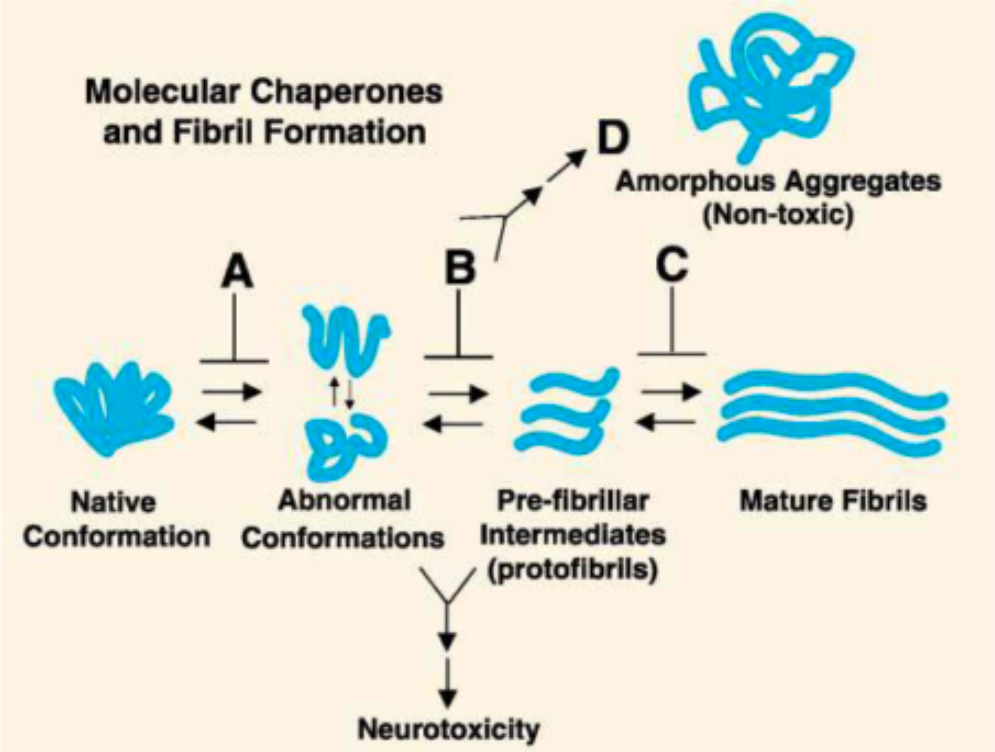

Figure 1. A model for chaperone-mediated suppression of neurotoxicity. Fibril formation is a multi step process involving a number of intermediate structures that are thought to mediate neurotoxicity. Chaperone proteins may prevent neurotoxicity by preventing the conversion of native proteins to abnormal toxic conformations (A), by preventing the formation of pre-fibrillar intermediates (B), by preventing the conversion to mature fibrils (C), and/or by facilitating the conversion of toxic intermediates to non-toxic amorphous aggregates (D). (4)

We hypothesize that αBc has an important modulatory role in HD since the ability to effectively initiate the heat shock response, and other homeostatic cellular pathways (e.g., apoptosis, oxidative stress) in which αBc functions, are compromised during HD disease progression (9). We should also take into account, as a chaperone with multi-functional capabilities, αBc may alleviate stress by promoting the proteasomal

degradation of corrupt proteins (10, 11), by stabilizing intermediate filaments and the cytoskeleton integrity (12, 13) or preventing apoptosis (14–17). In Chapter 4 we tested the hypothesis that BACHD astrocytes have a reduced antioxidant potential leading to an increased oxidative stress in neurons, and overexpression of αBc can rescue this effect and protect neurons from those deleterious effects. Our data shows a trend towards an increase of caspase-3 activity and protein carbonyl groups in primary cell cultures of BACHD. Oxidative stress is mediated by increases in ROS including superoxide (O_2^-), hydrogen peroxide (H_2O_2), hydroxyl radical (OH^-), and reactive nitrogen species such as peroxynitrite ($ONOO^-$) (18). Indeed, we provided evidence that αBc overexpression could protect astrocytes from H_2O_2 –induced oxidative stress is increased. Mitochondria dysfunction may be a source of ROS overproduction in neurons and it is a common feature found in HD (19, 20). By directly binding to procaspase-3, αBc inhibits the pro-apoptotic proteins, bcl-X(S), Bax and p53 by preventing their translocations from cytosol into mitochondria during apoptosis (15, 21). However, we failed to detect these effects in p53 and caspase-3 expression and activity in our BACHD mouse brains (Chapter 4 – Table 1).

Evidence of enhanced oxidative stress in HD brains includes an accumulation of lipofuscin, 8-OH-dG, and carbonyl formation (22). However, although oxidative damage is well described in HD, little is known about the specific protein targets of this damage. The major carbonylated proteins in both striatum and cortex from human HD samples are those involved in mitochondrial energy pathways and glucose metabolism in accordance with the impaired energy metabolism described in HD. Despite not testing for expression of 8-OH-dG in our mice model, we did observe a trend for levels of carbonylation in our BACHD mice, but αBc overexpression did not significantly rescue this effect.

We also observed in general that the large-scale upregulation of HD-related genes that is observed in human HD brains is not paralleled in late-stage BACHD brains. Regardless of the mechanisms governing the protective effects of αBc expression, the discrepancy between large scale complement upregulation in HD patients and few alterations in the complement system in BACHD mice highlights the need to use multiple animal models of disease in order to explore disease mechanisms. Specifically, future studies of the sHsps overexpression in HD should consider other animal models besides

the BACHD mouse model in the hope that they more accurately reflect the status of human HD patients.

Although our data do not establish a mechanism by which overexpression of αBc in astrocytes is likely to play a critical function in the modulation of mHtt and oxidative stress in the context of BACHD mice, these findings open up new avenues in the investigation of Hsps over-expression in astrocytes and their potential protective role in neurons through a non-cell autonomous manner in HD and other proteinopathies.

In Chapter 5, we tested the impact of αBc deletion in the BACHD mice model. An enormous caveat to this study using the αBc deficient mice: these mice also lack the sHsp HspB2 due to their promoter proximity (23). HspB2 is not thought to be inducible, so the levels of HspB2 are typically not elevated in neurological disorders (7). Mice lacking both αBc and HspB2 showed a decrease of the BACHD body weight phenotype, confirming the role of sHsps in metabolic changes as previously discussed. The decrease on body weight was correlated with better performance in our behavior paradigms such as rotarod and balance beam. Though, αBc/HspB2 mice have worse disease (24), which supports the idea that sHsps are serving protective roles whether that is due to αBc or HspB2. An additional point to consider is whether the phenotype observed in αBc/HspB2 deficient mice is due to the lack of the sHSPs or the altered levels of another molecule that is dependent on normal sHsp function. If isogenic mouse strains are not used as controls, then it is possible that polymorphisms in other genes could be the cause of differences seen between the WT and αBc/HspB2 deficient mice.

How sHsps , especially αBc, are neuroprotective is still a subject of debate.

6.1. Non–cell autonomous pathology in HD

Growing evidence shows that HD and other neurodegenerative diseases (ALS, AD, PD) result from the convergence of damage developed within multiple cell types, including within neighboring non-neuronal supporting cells, which is crucial to neuronal dysfunction.

We have analysed αBc expression in astrocytes, but we did not test these conditions in other glial cells, namely oligodendrocytes, that are also known to express sHsps (7, 25) and to contribute to in HD progression (26). In fact, previous MRI studies

have detected abnormalities in both gray and white matter starting in premanifest stages of HD (27). Recently, structural and molecular myelination deficits were found to occur prior to neuronal loss in the YAC128 and BACHD (29) and knock-in (28) models of HD. These findings indicate that white matter deficits in HD are an early phenotype associated with cell-intrinsic effects of mHtt on myelin-related transcripts in oligodendrocytes, and raise the possibility that white matter abnormalities may be an early contributing factor to the pathogenesis of HD. Thus, testing *in vitro* and *in vivo* overexpression of sHsps in oligodendrocytes could provide novel potential therapeutic targets for HD and other neurodegenerative diseases.

6.2. Prion-like spreading of mHtt pathology in HD

Several reports have provided evidence that large Htt-containing inclusions are not correlated with cytotoxicity (30) and might even be protective (3). However, as discussed above, many aggregated precursors to inclusions are present, including individual oligomeric and amyloid fibrils, that are too small to be visualized by light microscopy and that were therefore undetectable in many of these studies, including ours. Although tracking the various oligomeric and aggregated forms of Htt that are below the size of an inclusion in either mouse models or patients in vivo is not possible at the present time, the observation of inclusions in a specific cell type provides evidence that self-association has progressed through a series of smaller aggregated species to an amyloid fibril end point (31, 32). Inclusions form in a wide range of peripheral tissues in mouse models that carry highly expanded CAG repeats (33). These inclusions occur predominantly in cells that have entered mitotic arrest, which suggests that cell division acts to delay the pathogenetic process. The acceleration of aggregation through seeding suggests the possibility of a prion-like mechanism of cell-to-cell transmission (34) and trans-neuronal propagation of mHtt might be an important and underestimated contributor to the pathophysiology of HD. Interestingly, αBc is secreted in exosomes under a variety of stress-related conditions (35). One possible mechanism of modulating neuronal IBs and its percursor species could be through αBc-mediated extracellular signaling from astrocytes to neurons.

There is emerging evidence that astrocyte-derived exosomes carry neuroprotective cargo and could contribute to neuronal survival (36). Exosomes may execute their functions by distinct modes of action: (1) internalization by target cells and cargo retrieval, (2) binding to the cell surface and triggering second messenger pathways, and (3) release of components into the extracellular matrix. However, their interaction as well as their protein content with target cells is not well understood at a mechanistic level (36). A study using retinal pigment epithelial (RPE) cells (37) showed that an increased uptake of exogenous αBc and protection from oxidative stress and apoptosis by inhibition of caspase-3 and PARP activation were observed in stressed RPE cultures. In this manner, we speculate that exosomes containing αBc could protect both glia and neuronal population in BACHD from mhtt-derived toxicity, as activation of caspase-3 and oxidative stress. Future and critical experiments need to be designed to address the extent to which secreted αBc may modulates mHtt prion-like aggregate propagation and its contribution to disease progression in HD.

6.3. Final Remarks

The results obtained in this thesis, provide several insights into the complex role of the pleiotropic sHsp, αBc, in HD-related mechanisms and also other neurodegenerative disorders. Although there are currently no effective disease-modifying therapies, therapeutic strategies involving overexpression of chaperones and other protein quality control mechanisms are under investigation. Therefore, our study will help to open new research venues, crucial for obtaining a more comprehensive level of understanding the interplay between Hsps and their multiple functions on neurological disorders. Ultimately, the knowledge reported here will help targetting important molecules, cellular mechanisms and pathways for therapeutic intervention in HD and in other diseases of protein misfolding.

6.4. References

1. DiFiglia,M., Sapp,E., Chase,K.O., Davies,S.W., Bates,G.P., Vonsattel,J.P. and Aronin,N. (1997) Aggregation of huntingtin in neuronal intranuclear inclusions and dystrophic neurites in brain. *Science*, **277**, 1990–1993.
2. Vonsattel, Jean Paul,D.M. (1998) Hungtington's disease. *J. Neuropathol. Exp. Neurol.*
3. Arrasate,M., Mitra,S., Schweitzer,E.S., Segal,M.R. and Finkbeiner,S. (2004) Inclusion body formation reduces levels of mutant huntingtin and the risk of neuronal death. *Nature*, **431**, 805–10.
4. Muchowski,P.J. and Wacker,J.L. (2005) Modulation of neurodegeneration by molecular chaperones. *Nat. Rev. Neurosci.*, **6**, 11–22.
5. Takahashi,T. and Mihara,H. (2008) Peptide and protein mimetics inhibiting amyloid ??-peptide aggregation. *Acc. Chem. Res.*, **41**, 1309–1318.
6. Quraishe,S., Asuni, a, Boelens,W.C., O'Connor,V. and Wyttenbach, a (2008) Expression of the small heat shock protein family in the mouse CNS: differential anatomical and biochemical compartmentalization. *Neuroscience*, **153**, 483–91.
7. Quraishe,S. (2010) The sHsp expression signature in the brain and modulation in models of chronic neurodegeneration.
8. Lanneau,D., de Thonel,A., Maurel,S., Didelot,C. and Garrido,C. (2007) Apoptosis versus cell differentiation: role of heat shock proteins HSP90, HSP70 and HSP27. *Prion*, **1**, 53–60.
9. Arrigo,A.P., Simon,S., Gibert,B., Kretz-Remy,C., Nivon,M., Czekalla,A., Guillet,D., Moulin,M., Diaz-Latoud,C. and Vicart,P. (2007) Hsp27 (HspB1) and αB-crystallin (HspB5) as therapeutic targets. *FEBS Lett.*, **581**, 3665–3674.
10. den Engelsman,J., Keijsers,V., de Jong,W.W. and Boelens,W.C. (2003) The small heat-shock protein alpha B-crystallin promotes FBX4-dependent ubiquitination. *J. Biol. Chem.*, **278**, 4699–704.
11. Lin,D.I., Barbash,O., Kumar,K.G.S., Weber,J.D., Harper,J.W., Klein-Szanto,A.J.P., Rustgi,A., Fuchs,S.Y. and Diehl,J.A. (2006) Phosphorylation-Dependent Ubiquitination of Cyclin D1 by the SCFFBX4-αB Crystallin Complex. *Mol. Cell*, **24**, 355–366.
12. Ghosh,J.G., Shenoy,A.K. and Clark,J.I. (2007) Interactions between important regulatory proteins and human alphaB crystallin. *Biochemistry*, **46**, 6308–6317.
13. Ghosh,J.G., Houck,S.A. and Clark,J.I. (2007) Interactive Domains in the Molecular Chaperone Human ??B Crystallin Modulate Microtubule Assembly and Disassembly. *PLoS One*, **2**.
14. Kamradt,M.C., Lu,M., Werner,M.E., Kwan,T., Chen,F., Strohecker,A., Oshita,S., Wilkinson,J.C., Yu,C., Oliver,P.G., *et al.* (2005) The small heat shock protein aB-crystallin is a novel inhibitor of TRAIL-induced apoptosis that suppresses the activation of caspase-3. *J. Biol. Chem.*, **280**, 11059–66.
15. Mao,Y.-W., Liu,J.-P., Xiang,H. and Li,D.W.-C. (2004) Human alphaA- and alphaB-crystallins bind to Bax and Bcl-X(S) to sequester their translocation during staurosporine-induced apoptosis. *Cell Death Differ.*, **11**, 512–526.
16. Kamradt,M.C., Chen,F., Sam,S. and Cryns,V.L. (2002) The small heat shock protein aB-crystallin negatively regulates apoptosis during myogenic differentiation by inhibiting caspase-3 activation. *J. Biol. Chem.*, **277**, 38731–38736.
17. Kamradt,M.C., Chen,F. and Cryns,V.L. (2001) The Small Heat Shock Protein aB-Crystallin Negatively Regulates Cytochrome c- and Caspase-8-dependent Activation of Caspase-3 by Inhibiting Its Autoproteolytic Maturation. *J. Biol. Chem.*, **276**, 16059–16063.
18. Browne,S.E., Ferrante,R.J. and Beal,M.F. (1999) Oxidative stress in Huntington's disease. *Brain Pathol.*, **9**, 147–63.

19. Chen,C. (2011) Mitochondrial dysfunction, metabolic deficits, and increased oxidative stress in Huntington's disease. *Chang Gung Med. J.*, **34**, 135–52.
20. Panov,A. V, Gutekunst,C.A., Leavitt,B.R., Hayden,M.R., Burke,J.R., Strittmatter,W.J. and Greenamyre,J.T. (2002) Early mitochondrial calcium defects in Huntington's disease are a direct effect of polyglutamines. *Nat Neurosci*, **5**, 731–736.
21. Liu,S., Li,J., Tao,Y. and Xiao,X. (2007) Small heat shock protein alphaB-crystallin binds to p53 to sequester its translocation to mitochondria during hydrogen peroxide-induced apoptosis. *Biochem. Biophys. Res. Commun.*, **354**, 109–14.
22. Browne,S.E. and Beal,M.F. (2006) Oxidative damage in Huntington's disease pathogenesis. *Antioxid Redox Signal*, **8**, 2061–2073.
23. Brady,J.P., Garland,D.L., Green,D.E., Tamm,E.R., Giblin,F.J. and Wawrousek,E.F. (2001) AlphaB-crystallin in lens development and muscle integrity: a gene knockout approach. *Invest. Ophthalmol. Vis. Sci.*, **42**, 2924–34.
24. Ojha,J., Karmegam,R. V, Masilamoni,J.G., Terry,A. V and Cashikar,A.G. (2011) Behavioral defects in chaperone-deficient Alzheimer's disease model mice. *PLoS One*, **6**, e16550.
25. Bajramovic,J.J., Lassmann,H. and van Noort,J.M. (1997) Expression of alphaB-crystallin in glia cells during lesional development in multiple sclerosis. *J Neuroimmunol*, **78**, 143–151.
26. Huang,B., Wei,W., Wang,G., Gaertig,M.A., Feng,Y., Wang,W., Li,X.-J. and Li,S. (2015) Mutant Huntingtin Downregulates Myelin Regulatory Factor-Mediated Myelin Gene Expression and Affects Mature Oligodendrocytes. *Neuron*, **85**, 1212–1226.
27. Nambron,R., Silajdžić,E., Kalliolia,E., Ottolenghi,C., Hindmarsh,P., Hill,N.R., Costelloe,S.J., Martin,N.G., Positano,V., Watt,H.C., *et al.* (2016) A Metabolic Study of Huntington's Disease. *PLoS One*, **11**, e0146480.
28. Jin,J., Peng,Q., Hou,Z., Jiang,M., Wang,X., Langseth,A.J., Tao,M., Barker,P.B., Mori,S., Bergles,D.E., *et al.* (2015) Early white matter abnormalities, progressive brain pathology and motor deficits in a novel knock-in mouse model of Huntington's disease. *Hum. Mol. Genet.*, **24**, 2508–2527.
29. Teo,R.T.Y., Hong,X., Yu-Taeger,L., Huang,Y., Tan,L.J., Xie,Y., To,X.V., Guo,L., Rajendran,R., Novati,A., *et al.* (2016) Structural and molecular myelination deficits occur prior to neuronal loss in the YAC128 and BACHD models of Huntington disease. *Hum. Mol. Genet.*, 10.1093/hmg/ddw122.
30. Saudou, F., Finkbeiner, S., Devys, D., Greenberg,M.E. (1998) Huntingtin acts in the nucleus to induce apoptosis but death does not correlate with the formation of intranuclear inclusions. *Cell*, **95**, 55–66.
31. Miller,J., Arrasate,M., Shaby,B.A., Mitra,S., Masliah,E. and Finkbeiner,S. (2010) Quantitative relationships between huntingtin levels, polyglutamine length, inclusion body formation, and neuronal death provide novel insight into huntington's disease molecular pathogenesis. *J. Neurosci.*, **30**, 10541–10550.
32. Hoffner,G. and Djian,P. (2014) Monomeric, oligomeric and polymeric proteins in huntington disease and other diseases of polyglutamine expansion. *Brain Sci.*, **4**, 91–122.
33. Ehrnhoefer,D.E., Butland,S.L., Pouladi,M. a. and Hayden,M.R. (2009) Mouse models of Huntington disease: variations on a theme. *Dis. Model. Mech.*, **2**, 123–129.
34. Frost, B. & Diamond,M.I. (2010) Prion-like mechanisms in neurodegenerative diseases. *Nat. Rev. Neurosci.*, **11**, 155–159.
35. Kore,R. a. and Abraham,E.C. (2014) Inflammatory cytokines, interleukin-1 beta and tumor necrosis factor-alpha, upregulated in glioblastoma multiforme, raise the levels of CRYAB in exosomes secreted by U373 glioma cells. *Biochem. Biophys. Res. Commun.*, **453**, 326–331.
36. Frühbeis,C., Fröhlich,D. and Krämer-Albers,E.M. (2012) Emerging roles of exosomes in neuron-glia communication. *Front. Physiol.*, **3 APR**, 1–7.
37. Sreekumar,P.G., Kannan,R., Kitamura,M., Spee,C., Barron,E., Ryan,S.J. and Hinton,D.R. (2010) αB crystallin is apically secreted within exosomes by polarized human retinal

pigment epithelium and provides neuroprotection to adjacent cells. *PLoS One*, **5**.

Chapter 7.

Appendix

7.1. αB-crystallin overexpression does not increase life span in the R6/2 mouse model of Huntington's disease

The early onset of behavioral symptoms, robust and severe HD-like phenotypes and brain neurodegeneration make the exon-1 fragment model R6/2 mice an attractive model for the study of presymptomatic therapies. During the time of my PhD project, I have tried to test in parallel the overexpression of αBc in the modulation of the disease in both full-length mHtt model – BACHD and in the exon-1 fragment model R6/2 mice of HD, to have be able to expect robust results in two distinct HD models for the distinct behavioral paradigms. However, the R6/2 mice breeding results were more difficult than expected, and even using ovarian-transplanted R6/2 mice, my ratios of the 4 genotypes were very low to perform behavioral analyses. Therefore, with the single good cohort I could obtain from R6/2 and Cryab Tg mice crossing towards the end of my studies, I have decided to perform survival analyses to test the potential protective rescue effect of αBc overexpression in the severe and short life-span of the R6/2 mice (Figure A1).

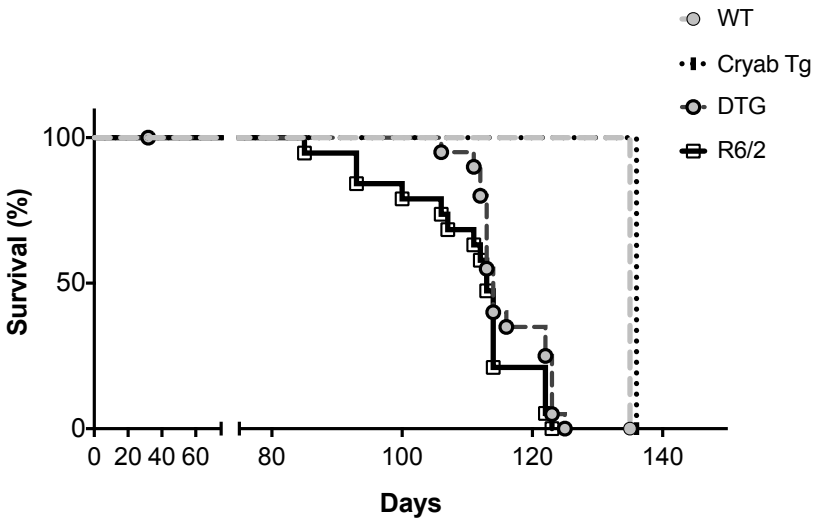

Figure A1. αB-crystallin overexpression does not increase life span in the R6/2 mouse model of Huntington's disease
Kaplan-Meier survival curve for the indicated genotypes WT (n=24), Cryab Tg (n=26), R6/2 (n=18), DTg (n=21), demonstrates that the astrocytic overexpression of αBc does not significantly impact the survival of R6/2 mice (log rank Mantel-Cox test: p = 0.2893)

αBc astrocytic overexpression does not increase life span in the R6/2 mouse model of Huntington's disease. The Cryab Tg did not change the WT phenotype - normal life - span, thus both WT and Cryab Tg Despite the fact of observing encouraging results in the initial phase, where R6/2 start dying earlier (83-84 days) than the DTg littermates that

started 20 days later (106-108 days) (Fig. A1), the Kaplan-Meier survival curves were not significantly different between R6/2 and DTg, according to the of Mantel-Cox test (Fig. A1).

We concluded then, that despite the R6/2 model being an extremely attractive model for therapeutic targets' testing, to be able to study the progression of HD disease and to evaluate modest but significant improvement of astrocytic αBc, this model may be to severe, and therefore the full-length BACHD model was more suitable for our aims during this PhD project.

7.2. Published paper:

A. Osório Oliveira, A. Osmand, T.F. Outeiro, P.J. Muchowski, S. Finkbeiner "αB-crystallin overexpression in astrocytes modulates the phenotype of the BACHD mouse model of Huntington's disease", Human Molecular Genetics (2016); 1-13